UNIVERSIDADE ESTADUAL DE CAMPINAS
FACULDADE DE ENGENHARIA MECÂNICA

Fábio Menegatti de Melo

On the use of particle impact dampers to control vertical impact-induced vibration: An experimental investigation

Uso de absorvedores por efeito de impacto multi-particulados no controle de vibrações verticais impacto-induzidas: estudo experimental

CAMPINAS
2018

Fábio Menegatti de Melo

On the use of particle impact dampers to control vertical impact-induced vibration: An experimental investigation

Uso de absorvedores por efeito de impacto multi-particulados no controle de vibrações verticais impacto-induzidas: estudo experimental

A Thesis submitted to the School of Mechanical Engineering of the University of Campinas in partial fulfillment of the requirements for the degree of Doctor of Philosophy in Mechanical Engineering, area of Solid Mechanics and Mechanical Design.

Tese de Doutorado apresentada à Faculdade de Engenharia Mecânica da Universidade Estadual de Campinas como parte dos requisitos exigidos para obtenção do título de Doutor em Engenharia Mecânica, na Área de Mecânica dos Sólidos e Projeto Mecânico.

Orientador: Prof. Dr. Milton Dias Junior

ESTE EXEMPLAR CORRESPONDE À VERSÃO FINAL DA TESE DEFENDIDA PELO ALUNO Fábio Menegatti de Melo E ORIENTADA PELO Prof. Dr. Milton Dias Junior.

_____

Prof. Dr. Milton Dias Junior

CAMPINAS
2018

Agência(s) de fomento e nº(s) de processo(s): CAPES; CNPq, 205203/2014-0
ORCID: https://orcid.org/0000-0002-5812-9187

Ficha catalográfica
Universidade Estadual de Campinas
Biblioteca da Área de Engenharia e Arquitetura
Rose Meire da Silva - CRB 8/5974

Melo, Fábio Menegatti de, 1988-
M491u On the use of particle impact dampers to control vertical impact-induced vibration : an experimental investigation / Fábio Menegatti de Melo. – Campinas, SP : [s.n.], 2018.

Orientador: Milton Dias Junior.
Tese (doutorado) – Universidade Estadual de Campinas, Faculdade de Engenharia Mecânica.

1. Vibração. 2. Controle de ruído. I. Dias Junior, Milton, 1961-. II. Universidade Estadual de Campinas. Faculdade de Engenharia Mecânica. III. Título.

Informações para Biblioteca Digital

Título em outro idioma: Uso de absorvedores por efeito de impacto multi-particulados no controle de vibrações verticais impacto-induzidas : estudo experimental
Palavras-chave em inglês:
Vibration
Noise control
Área de concentração: Mecânica dos Sólidos e Projeto Mecânico
Titulação: Doutor em Engenharia Mecânica
Banca examinadora:
Milton Dias Junior [Orientador]
Robson Pederiva
Alberto Luiz Serpa
Valder Steffen Junior
Arcanjo Lenzi
Data de defesa: 31-01-2018
Programa de Pós-Graduação: Engenharia Mecânica

UNIVERSIDADE ESTADUAL DE CAMPINAS
FACULDADE DE ENGENHARIA MECÂNICA
COMISSÃO DE PÓS-GRADUAÇÃO EM ENGENHARIA MECÂNICA
DEPARTAMENTO DE SISTEMAS INTEGRADOS

TESE DE DOUTORADO

On the use of particle impact dampers to control vertical impact-induced vibration: An experimental investigation

Uso de absorvedores por efeito de impacto multi-particulados no controle de vibrações verticais impacto-induzidas: estudo experimental

Autor: Fábio Menegatti de Melo
Orientador: Prof. Dr. Milton Dias Junior

A Banca Examinadora composta pelos membros abaixo aprovou esta Tese:

Prof. Dr. Milton Dias Junior
DSI / FEM / UNICAMP

Prof. Dr. Robson Pederiva
DSI / FEM / UNICAMP

Prof. Dr. Alberto Luiz Serpa
DMC / FEM / UNICAMP

Prof. Dr. Valder Steffen Junior
UFU / Uberlândia

Prof. Dr. Arcanjo Lenzi
UFSC / Florianópolis

A Ata da defesa com as respectivas assinaturas dos membros encontra-se no processo de vida acadêmica do aluno.

Campinas, 31 de janeiro de 2018.

This Thesis is dedicated to my mother Cleunice (in memoriam) *and my father Wilson*

Acknowledgments

I would like to express my gratitude to all those who directly or indirectly supported me during the conclusion of this Thesis. This includes the kind support of my advisor Dr. Milton Dias Jr. and the valuable help provided by Dr. Kenneth Cunefare, from Georgia Institute of Technology (Georgia Tech). I thank my parents and brothers, friends, colleagues and my girlfriend Thaís for their love and patience. I also have to acknowledge the support from The Hunnicuts, my host family in Atlanta, who witnessed all the afflictions and joys of living abroad.

Now, let me also write some words in Portuguese...

Quero reforçar aqui meu agradecimento por todo apoio dado pelos meus pais Wilson e Cleunice até a conclusão de mais esta etapa. Certamente sem o apoio deles e dos meus irmãos Filipe e Fernando, que também trilharam esse mesmo caminho sinuoso da academia e hoje são Doutores*, grande parte do que eu consegui até o momento não teria se concretizado. Agradeço aqui também os meus quatro avós José Carlos, Clarice, Waldemar e Ruth, por também fazerem parte da minha formação como pessoa.*

O Doutorado foi um período de muitas experiências que mudaram a minha vida e que vou levar eternamente comigo. Nesse período pude viver diversos momentos, como a oportunidade única de morar no exterior (e isso inclui todo o pacote de vivências, aprendizados, sensações e emoções associados), mas também vivenciar algo que nenhum de nós espera acontecer tão cedo: a perda da própria Mãe. Minha mãe sempre fez de tudo por nós e nunca mediu esforços para que tivéssemos uma boa educação e uma boa formação moral. Espero que ela se sinta orgulhosa pelo que deixou!

Nesses quatro anos e meio, enquanto eu me preocupava em montar minha bancada e fazer as medições necessárias, meus dois Avôs também se foram. Um período pra lidar com a perda, inclusive, do Kim, que esteve conosco nesses últimos 12 anos.

O Doutorado também foi época de deixar o orgulho de lado e buscar ajuda profissional para as minhas aflições e ansiedades. Termino esse período me conhecendo mais e melhor do que entrei!

Quero aproveitar esse espaço e agradecer aqui:

- *Minha namorada Thaís principalmente pela extrema paciência e por ser bem mais realista que eu;*
- *Meu orientador Prof. Milton (*Miltão*) pela amizade, pelos ensinamentos técnicos e pela preocupação com o bem estar e convívio dentro do grupo;*

- *Meus amigos com os quais tive contato mais próximo durante essa fase: Fernando, Alexandre, Henrique, Gustavo, Martin e Daniel Schmidt;*
- *Todos os amigos do LDEM e, em especial, o Vinícius e Hugo, que sempre estão presentes com suas opiniões e conhecimento;*
- *Os colegas de corredor, especialmente Marcos e Clodoaldo pelas conversas sobre nossos trabalhos e sobre assuntos aleatórios;*
- *O Prof. Dr. Kenneth Cunefare, da Georgia Tech, pela atitude solícita em me receber em seu laboratório e pela postura sempre positiva ao me auxiliar na interpretação dos dados;*
- *O Dr. Ricardo Ugliara pela ajuda fundamental com o LabVIEW;*
- *Os técnicos da oficina do DSI – Maurício, Mauro e Ferreira – que são fundamentais pra toda pesquisa desenvolvida ali;*
- *Os demais funcionários da Faculdade de Engenharia Mecânica da UNICAMP;*
- *À banca pelos comentários e sugestões*
- *O financiamento proporcionado pela Capes, CNPq (205203/2014-0) e pela Funcamp.*

"The only thing that disturbs me when writing is the complete silence. There must have some noise around; there must have life around, otherwise I can't produce much."

"A única coisa que me atrapalha para escrever é o silêncio total. Tem que ter um barulho qualquer, tem que ter vida em volta senão não rende tanto."

Jô Soares, Brazilian talk show host, humorist, and author

"Believe me: any loneliness is smaller than that felt when you lose your mother..."

"Creiam-me: nunca se está tão só como quando se perde nossa mãe..."

Leandro Karnal, Brazilian History professor

Resumo

Absorvedores por efeito de impacto multi-particulados (uma tradução livre do termo em inglês *particle impact dampers*, ou *PIDs*) são dispositivos que vêm sendo pesquisados e aplicados como alternativa aos métodos comumente usados no controle passivo de vibração e ruído. Embora uma grande quantidade de trabalhos vêm sendo conduzidos de forma a entender o comportamento dinâmico dessa categoria de absorvedores, ainda existe espaço para novos estudos. Grande parte da literatura é focada na análise da resposta livre e forçada (harmônica) de PIDs quando acoplados tanto em sistemas de um grau de liberdade (GL) quanto de múltiplos GLs. Além disso, dentre os trabalhos encontrados, parte deles se propõe a caracterizar o amortecimento proporcionado por tais absorvedores utilizando alguns indicadores de dissipação. Nesse sentido, propõe-se neste trabalho: 1) Analisar e comparar dois desses indicadores que caracterizam a dissipação de PIDs; 2) Analisar o comportamento desses absorvedores quando sujeitos à excitação vertical impacto-induzida.

Palavras-chave: vibração; controle de ruído; controle passivo; absorvedores por efeito de impacto multi-particulados; excitação impacto-induzida.

Abstract

Particle impact dampers (*PIDs*) are devices that have been explored as an alternative to the conventional methods employed in the passive control of noise and vibration. Although a great deal of articles has been conducted in order to understand the dynamic behavior of these dampers, there are still some new possibilities of study to be conducted. Many studies found in the literature are focused on the analysis of free and harmonically forced response of PIDs attached to SDOF or MDOF systems. Moreover, many of the performed works are concentrated on the characterization of damping by using and/or proposing dissipation parameters. Based on that, this Thesis has two main objectives: 1) It is of particular interest to analyze and compare two of such dissipation parameters; 2) Additionally, it is proposed the use of PIDs in structures that are subject to vertical impact-induced excitations.

Keywords: vibration; noise control; passive control; particle impact dampers; impact-induced excitation.

List of Figures

List of Tables

List of Abbreviations and Acronyms

The items in this list are sorted in order of appearance. Their definitions are valid for every chapter.

Chapter 1

N&V - Noise and vibration
TMD - Tuned mass damper
DVA - Dynamic vibration absorber
RCS - Resonant circuit shunted
PID - Particle impact damper
HAVS - Hand-arm vibration syndrome
NIHL - Noise-induced hearing loss
PAIR - *Perda auditiva induzida pelo ruído*

Chapter 2

ID - Impact damper
SDOF - Single Degree of Freedom
SPID - Single-Particle Impact Damper
MPID - Multi-Particle Impact Damper
PD - Particle damper
NOPD - Non-obstructive particle damper
SID - Shot impact damper
CID - Conventional impact damper
FPID - Fine particle impact damper
F - Number of particle layers
Γ - Dimensionless acceleration
a - Acceleration
A - Displacement
ω - Excitation frequency measured in [rad/s]
g - Gravitational acceleration ($9.81 m/s^2$)
d_p - Diameter of a single particle
h - Height of the cylinder that circumscribes the particle bed
N_p - Total number of particles
N_{p1} - Number of particles in one layer, the very bottom for example

Δ - Dimensionless displacement
L - Gap clearance
DEM - Discrete Element Method
MDOF - Multiple Degree of Freedom
Ψ - Dissipation parameter proposed by Friend and Kinra (2000)
E_k - Kinetic energy
FRF - Frequency Response Function
DPE - Dissipated Power Efficiency
P_{diss} - Dissipated power
P_{total} - Total power available
n - Number of periods
T - Period
t - Time
$F(t)$ - Measured force
$v(t)$ - Velocity signal (integrated from the measured acceleration $a(t)$)
m_{bed} Total mass of particle bed
$\dot{var}$ - First time derivative of a given variable var
m_α - Generalized mass
k_α - Generalized stiffness
M - Mass matrix in a given finite element model
i, j - Degrees of freedom of a given finite element model
ω_n - Natural frequency measured in [rad/s]
FEA - Finite Element Analysis
μ - Mass ratio
a_g - Granular packing ratio
v_g - Volumetric filling ratio
CoF - Coefficient of Friction
CoR - Coefficient of Restitution
TMPD - Tuned mass particle damper

Chapter 3

HCP - Hexagonal close packing
DAQ - Data acquisition hardware
VI - Virtual instruments (name of LabView® codes)
VPF - Volumetric packing fraction
f - Excitation frequency measured in [Hz]

CONTENTS

1 INTRODUCTION

1.1 Overview

The field of noise and vibration (N&V) control is probably an endless field of study. Engineers and researchers around the world are constantly dealing with N&V issues, which are inherent to any flexible system. From rotating machines experiencing unbalancing forces to steel buildings subjected to wind load and earthquakes, from passenger vehicles to domestic appliances, any structure or machine is potentially susceptible to these issues and it is highly recommended them to be addressed as quickly and efficiently as possible due to safety, economic, environmental or even consumer complaints.

Some solutions employed to reduce or even mitigate these N&V issues can be grouped into two distinct concepts: the *active* and *passive* control approaches.

Generally speaking, in the former approach, a set of sensors and actuators are spatially allocated and arranged in a way to cancel out the structural response to external disturbances. Depending on the application and which phenomenon one wants to control the sensors can be accelerometers or microphones and the actuators can be loudspeakers or built-in force actuators. Introductory material on this subject can be found in Fuller and von Flotow (1995). On the other hand, passive control involves changes in the physical parameters – mass, stiffness, and damping – which will in turn alter the modal parameters – natural frequency, damping factor and modal shape. Several are the techniques employed to reach such objective and they go from changing the mass of the structure (Wong, 2002; Li and Li, 2008) to the use of subsystems like *tuned mass dampers* (TMDs, also called *dynamic vibration absorber*, or DVAs) and *resonant circuit shunted* (RCS) (Steffen Jr *et al.*, 2000).

When talking about altering the damping of the structure, the literature is full of resources that can guide engineers and technicians in such work. For example, a procedure that has become a commonplace is the use of viscoelastic patches adhered to large, lightweight sheet metals. Viscoelastic patches consist of a layer of viscoelastic polymeric material that dissipate the vibratory energy by cyclic deformation and restoration of their inner fibers (Kuram and Ozcelik, 2014, Chapter 5). Since the patches have to deform to-

gether with the structure, they are therefore placed in regions with large strain (da Rocha, 2014). The strain energy is consequently dissipated in the form of heat.

As an alternative for passively attenuate the structural vibration, particle damping has been explored for many years. Devices that use this principle are generally known as *Particle Impact Dampers* – hereafter called PIDs. Detailed information about them are found in Chapter 2.

Several papers have reported the efficiency of PIDs and their capability of dissipating the kinetic energy of the structure they are attached to. Due to the promising results found, the investigation of their dynamic behavior is still justified as there is a lack of a general theory for PIDs that would guide their design (Cempel and Natke, 1989). Note that this same statement is still repeated after twenty seven years by Zhang *et al.* (2016a,b).

Rongong and Tomlinson (2005) point out a very interesting reason for studying the dynamic behavior of particle impact dampers. According to the authors, the lack of knowledge about these passive control devices can lead to a *"suboptimal or ineffective"* design. The likelihood for this to happen is high enough to discourage designers to use particle impact dampers. Fowler *et al.* (2001) highlight that the process of trial and error may be very costly and then the development of a consolidated design methodology is of high appealing.

1.2 Motivation

Noise and vibration issues are not a concern just for the product development, but they are present in fabrication applications as well.

While from the consumers' point of view noise and vibration problems could change the way they recognize their desired product in terms of comfort and reliability, from the point of view of factory floor these problems could mean serious damage to the rest of workers' lives. In other words, noise and vibration can also play a significant role in occupational impairments and they have to be taken into consideration.

As it was already introduced in a previous work (de Melo *et al.*, 2015), numerous industries, such as aircraft manufacturing and aircraft maintenance, use sheet metal in various stages of their manufacturing processes. Because sheet metal components are in

general lightweight, stiff and can have a considerable surface area, the noise produced by them can reach levels that may potentially damage the workers' ears (Nelson *et al.*, 2005). Inside some facilities, considerable noise can be generated during stacking of sheet products, transportation among manufacturing shops (Eager and Williamson, 1996), and assembly or disassembly of components. Loud noise may be also radiated to the work place during other manufacturing operations like punching and power pressing (Eager and Williamson, 1996).

Lets take the example of workers that handle pneumatic tools like rivet and chiseling guns (Figure 1.1) during working hours. These type of tools are driven by compressed air, and due to a reciprocating mechanism, periodic impulses (*strokes*) are transmitted to the structure to be manufactured (Figure 1.2). It is known that this category of workers – the riveters – are potentially exposed to both *hand-arm vibration syndrome* (HAVS) and *noise-induced hearing loss* (NIHL). The former is characterized by a peripheral neuropathy where the vibration is responsible for injuring the peripheral nerves and cutaneous mechanosensory peripheral nerve populations, as well as vascular and musculoskeletal features (Raju *et al.*, 2011; Heaver *et al.*, 2011; Zimmerman *et al.*, 2015); the later is characterized by a hearing loss caused by high exposition to loud environments for an extended period of time (Lee *et al.*, 2007). According to Nelson *et al.* (2005), by the year of 2000, 16% average of adults worldwide with hearing loss were impaired due to occupational exposure to noise. By 2007, there were thirty million workers with NIHL in US and in Korea it represented over 50% of occupational disease (Lee *et al.*, 2007). In Brazil, there is no nationwide epidemiological data about NIHL (in Portuguese, PAIR - *perda auditiva induzida pelo ruído*), with studies being restricted to specific regions and labor activities (Brazil, 2006).

Figure 1.1: Picture of a Chicago Pneumatic 4X rivet gun (Adapted from de Melo *et al.* (2015))

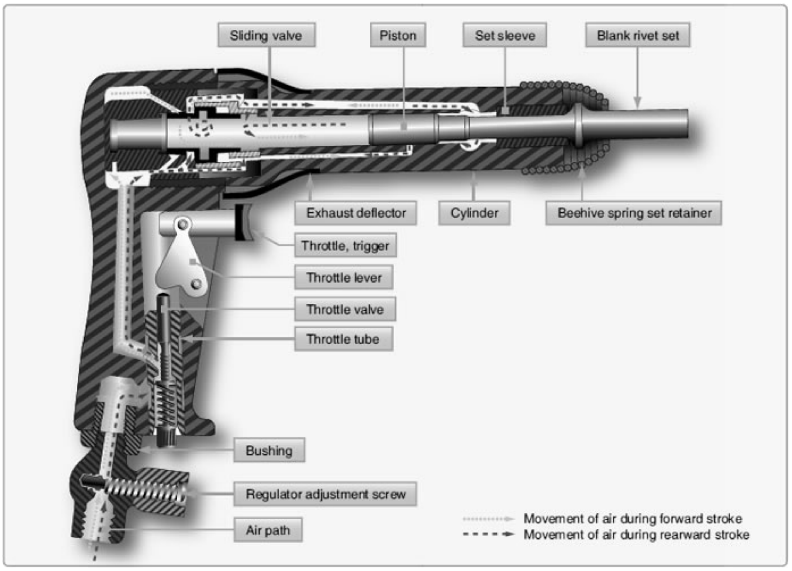

Figure 1.2: Diagram of the components generally found in a rivet gun. Adapted from *http://content.aviation-safety-bureau.com/allmembers/faa-h-8083-31-amt-airframe-vol-1/sections/chapter4.php*. Accessed in January 16th, 2017

Although currently wearable hearing protectors can be chosen to avoid hearing loss, complaints about comfort and voice intelligibility are reported by workers (Lee *et al.*, 2007). Misusing of hearing protections in real world conditions and the negligence of using it properly when and where it is mandatory also have to be considered when evaluating the effectiveness of such protectors (Arezes and Miguel, 2005).

1.3 Objectives

Considering the limitations of hearing protectors, a viable alternative to be considered to reduce the occupational hearing loss is the control of noise directly at its source: the vibrating component that is being manipulated by the workers. Some researches propose acoustical treatments in factory facilities (Lindqvist, 1983) and improvements in personal hearing protection. However, these practices may not lead to an acceptable level of protection (Eager and Williamson, 1996) and the use of hearing protection may impair communication between co-workers, as well as inducing fatigue and discomfort if worn continuously.

Therefore, bearing in mind the Motivation (Section 1.2), the present research intends to investigate experimentally the application of a particle impact damper to structures

subjected to impact-induced excitation, a test condition that simulates the situations aforementioned.

To accomplish such goal, the Thesis[1] is split into two parts: first, an investigation of the dynamic characterization of a PID under harmonic excitation is conducted and the results are compared with the literature. Later, it is carried out an evaluation of particle dampers subjected to impact-induced excitation. In this second part, an application of concept is presented along with a systematic investigation of a PID in a cantilever beam. Both vibratory and sound response are evaluated in this part. The scope of this Thesis is restricted to the PIDs in vertical direction (parallel to gravity).

By following the aforementioned path, this Thesis intends to shed some light upon the following questions:

1. *What are the trends and main findings found in the literature dedicated to the study of PIDs?* As it will be shown, the literature offers several information regarding the behavior of PIDs when subjected to harmonic, transient excitation and also when attached to a number of structures. In many of these studies, a parametric analysis is conducted and the trends observed are used as a reference to design guidelines. Therefore, it is worth compiling these informations as an effort to obtain a broader understanding on such dampers;

2. *What is the dynamic behavior of Particle Impact Dampers?* It is of particular interest investigating two different parameters proposed in the literature and used to quantify the dissipation, namely the *dissipated power efficiency* proposed by Yang *et al.* (2004) and the FRF analysis conducted by Zhang *et al.* (2016a,b). This comparative study is conducted as a way to assess the basic working principle of PIDs;

3. *What should be expected when exciting a PID with an impact-induced excitation?* This is investigated by attaching a single cavity PID to a cantilever beam.

4. *Is it possible to use an array of multiple PIDs for impact-induced excitations?* Impact-induced excitation leads to the excitation of several modes at the same time. Therefore, an array of PIDs placed on the structure is more likely to affect more than one mode (robust solution) and thus reduce the vibration amplitude.

[1] Although the English word *Thesis* may be more appropriate to Master's degree, this will be used as a literal translation of the Portuguese word *Tese* which is more suitable for PhD's final document in the Brazilian context.

1.4 Innovative aspects

This Thesis addresses the problematic of a particle impact damper subject to vertical, impact-induced excitation. As it is shown in the literature review found in Chapter 2, this problem seems not to be as treated as it does with PIDs under harmonic excitation.

In addition, this work proposes a design variation of conventional PIDs by gathering several cavities into an array of PIDs. The use of an array of PIDs is indicated as a robust solution with respect to dynamic variations of the structure to which it is settled. Moreover, an array of PIDs can spatially affect those several modes that are being excited at the same time due to the repetitive impacts. It is observed that using an array with multiple cavities of PIDs – or multi-particle damper (Saeki, 2005) – to suppress the vibration of a plate (and the consequent radiated noise) is an approach not deeply explored in the literature as far as I am aware.

1.5 Organization of the Thesis

This Thesis is divided into four chapters. **Chapter 2** comprehends the description of a particle impact damper, its advantages and drawbacks, and the physical mechanism behind its dynamic behavior along with the literature review. The research that has been conducted over time is presented along with the main findings and trends observed.

The experimental results and discussion are split into two chapters. **Chapter 3** presents the investigation on the dynamic behavior of PIDs under harmonic excitation. In **Chapter 4**, the experimental procedure and discussion on impact-induced PIDs is presented.

The last chapter (**Chapter 5**) is dedicated to the conclusions of this Thesis. Experimental enhancements and suggestions for continuity of this work are also enumerated.

2 Literature review

2.1 Overview

Granular physics are certainly another endless object of study, having several physicists devoted their career to it. The duty of an engineer studying particle impact dampers is gathering as much information as possible about the physics of granular matter and question him(her)self on how a PID can be optimally designed.

The literature review on particle impact dampers will be described next. It is intended to give an outline about the damper itself, how it is modeled and analyzed, what parameters researchers use to evaluate its performance and what are the verified trends when some design parameters are varied. Additionally, some works on structures experiencing impact-induced vibration will be presented.

2.2 Particle impact dampers

Particle impact dampers are devices used to passively control the vibration (and consequently the radiated noise) of vibrating structures – hereafter called *primary structures*. Such dampers absorb and dissipate the primary structure's kinetic energy by means of friction (conversion of energy into heat) and collisions between particles and walls, and also among particles themselves (dissipation by momentum transfer and acoustic radiation).

A PID usually consists of a hollow cavity fully or partially filled with granular materials, whose particles can be of different mechanical properties (density, elasticity, surface roughness) and shapes. It is a common practice to use metallic particles, frequently spheres – also known as *shots* (Figure 2.1). Sand[1], powders, other amorphous particles, and even polymer granules have also been studied focusing on their application (Lenzi, 1985; Friend and Kinra, 2000; Marhadi and Kinra, 2005).

[1]Sand has the advantage of being cheap and temperature resistant (Lenzi, 1985).

The literature proposes two main design concepts for PIDs: one consists of attaching an external cavity to the primary structure. This process can be temporary (de Melo *et al.*, 2015) or not. Another design concept of this category of dampers consists of drilling one or several holes in the structure to be treated and having them filled with the desired granular material (Panossian, 1992; Xu *et al.*, 2004b). The application of this second approach is conditioned to the possibility of drilling the holes onto the particular structure, and parameters like thickness and stiffness of the structure have to considered during the design process (Xu *et al.*, 2004a).

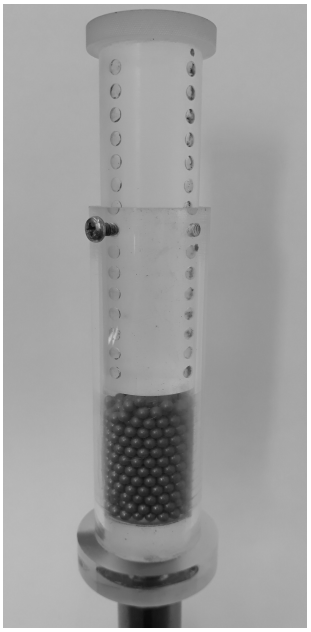

Figure 2.1: Particle impact damper cavity made of acrylic and filled with metallic spheres. The lid is adjustable and kept in position by two screws at the cavity's top edge.

The design concept of a PID is a consequent derivation of *impact dampers* (IDs), which consist of a single free moving mass inside the cavity. Unlike PIDs, the dissipation of energy provided by impact dampers is mostly due to the collision between the moving mass and the walls. Semercigil *et al.* (1992) proposed the use of an ID as the dissipation element in a singular DVA, which is formed by an inertia, a resilient element and a dissipative mechanism. It is known that the attachment of a DVA in a single degree of freedom (SDOF) system attenuates the amplitude at the resonance but creates two other resonant peaks in the vicinity of the original resonance – one in a lower frequency and other in a higher frequency than the original resonance. Hence, the objective of such study was to reduce the amplitude of the lower frequency resonant peak by using the damping capacity of the ID. This objective was satisfactorily achieved and the authors observed that the dissipation provided by the ID was directly related to the mass of the moving particle but it was not effective for systems with high inherent damping. Several other studies on IDs are vastly reported in the literature. Shaw and Holmes (1983); Bapat and Sankar

(1985b); Semercigil *et al.* (1988); Blazejczyk-Okolewska (2001); Li and Darby (2006) are examples of studies performed with dampers in horizontal vibration, while the studies conducted by Ema and Marui (1994); Duncan *et al.* (2005) are dedicated to dampers in vertical direction. One should not confuse the PID's concept with the concept of a multi-unit impact damper studied by Bapat and Sankar (1985a), whose model is reproduced in Figure 2.2. In this configuration, although more particles are employed, such particles are free to move inside independent cavities.

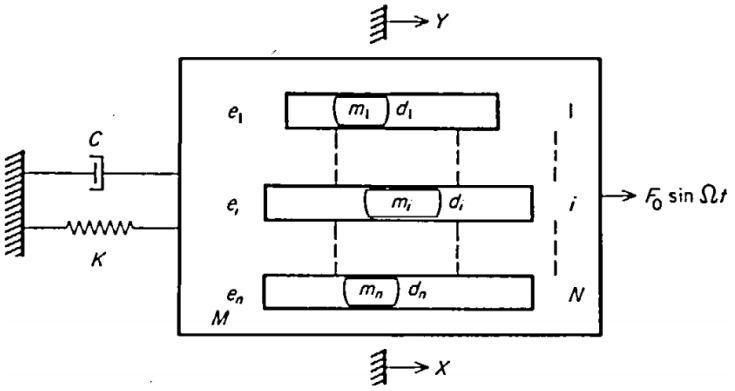

Figure 2.2: Model reproduced from Bapat and Sankar (1985a) used to simulate a multi-unit impact damper. Please refer to the original article for information about the parameters in this figure.

The term *particle impact damper* does not appear to be a consensual denomination in the research community as one can find some other variations related to them. Ramachandran and Lesieutre (2008) use the acronym *PID*, which is used throughout this text as well; Fowler *et al.* (2001) use the term Single-Particle Impact Damper (SPID) for those dampers with one single shot mass inside the cavity, and Multi-Particle Impact Damper (MPID) for dampers that work with several moving shot masses inside the same cavity. Other variations include particle dampers (PD) (Zhang *et al.*, 2016a), non-obstructive particle dampers (NOPD) (Panossian, 1992; Ben Romdhane *et al.*, 2013; Zhang *et al.*, 2016b), and shot impact dampers (SID) (Cempel and Natke, 1989). Du *et al.* (2008) call all of these types as conventional particle dampers (CID) in contrast with Fine Particle Impact Damper (FPID) which consists of a large mass sharing the same cavity with fine particles. Fine particles are used together with a larger particle so that when the small ones are compressed against the walls by the larger one, their plastic deformation contributes to the dissipation of energy.

2.2.1 Advantages and drawbacks

Some advantages of using PIDs as passive control devices were already extensively reported in the literature. A list containing some of them can be found in the following:

1. Conceptual simplicity (Zhang *et al.*, 2016b);
2. Little maintenance (Bannerman *et al.*, 2011);
3. Good stability as well as cost effectiveness (Fang and Tang, 2006);
4. No need to tune the particle impact damper to a particular frequency (Cempel and Lotz, 1993). In addition, it can work for stationary and transient vibration;
5. High damping with small weight penalty (Friend and Kinra, 2000);
6. Durability (Friend and Kinra, 2000);
7. Degradation insensitivity (Zhang *et al.*, 2016b) and no significant aging (Bannerman *et al.*, 2011);
8. May be considered as a good option for structures already constructed that are facing vibration problems (Booty *et al.*, 2014).

Several authors report the advantages of PIDs over IDs. In general, PIDs can dissipate more energy than IDs (Papalou and Masri, 1998; Olson, 2003). Additionally, PIDs seem to be a better choice compared to IDs because the later *"suffer from impact-induced high noise levels and surface degradations as well as high sensitivity to container size and input excitation"* (Friend and Kinra, 2000). Fowler *et al.* (2001) and Olson (2003) mention that as well. Although the noise generate by IDs is reportedly loud – Afsharfard and Farshidianfar (2012) model the acoustic response of a horizontal ID –, in the experiments conducted for this Thesis it was verified that PIDs are also very noisy, specially when subjected to high accelerations. This problematic is particularly addressed by Saeki *et al.* (2017).

The literature also highlights some advantages over other traditional passive damping techniques. PIDs do not require an anchor in order to restrict the motion of the structure, unlike other dampers (Bannerman *et al.*, 2011). Regarding the viscoelastic patches introduced in Section 1.1, PIDs have a potential effectiveness over a broad range of frequency and temperature (Olson, 2003; Zhang *et al.*, 2016b). Viscoelastic patches

have properties that are affected by temperature, frequency, strain and thus they are difficult to be used in environments with extreme temperatures or temperature gradients (Yang *et al.*, 2004). In addition, viscoelastic patches may degrade over time (Friend and Kinra, 2000). Comparing PIDs to friction dampers, although the latter is a robust solution specially for structural engineering (Pall and Pall, 1996; Hakimi *et al.*, 2004), they may degrade with wear (Olson, 2003) as damping is provided by friction at the interface of moving elements, a region of high contact stress. Thermal and other conditions affects its performance by degrading the contact interface (Fang and Tang, 2006). Shah *et al.* (2009) combine the friction damper with the particle damper concept by making a piston attached to the vibrating structure to move relative to a particle bed inside a cavity. Simulation of this concept is found in Bai *et al.* (2009).

Comparatively, particle impact dampers operating in optimal condition are able to reduce the vibration amplitude of the structure to which they are attached in the same order of magnitude as a DVA (Cempel and Lotz, 1993). Considering that DVA are applicable to structures with one distinguishable natural frequency or very close natural frequencies – which is not very common to find (Lenzi, 1985) and is not the only source of vibraton issue –, PIDs can actuate in a very broad range representing an advantage over the DVA usage.

Besides the advantages of using a PID, it is fair to mention, for the sake of good science, some drawbacks associated to this damper:

1. The determination of its dynamic behavior is not an easy task due to the response's dependency on many factors like cavity size and shape, particle size, material and others (Refer to Section 2.2.7);
2. Response is highly non-linear (Zhang *et al.*, 2016a,b; Fowler *et al.*, 2001). The response is amplitude dependent and may vary according to the acceleration of the attachment point.

Although these two aspects are listed as drawbacks, one could instead consider them as research challenges to be overcome.

2.2.2 Physical mechanisms of dissipation

The dynamic behavior of a PID under vertical excitation can be understood by two physical mechanisms – *transfer* and *dissipation* of energy (Bai *et al.*, 2009). According to Friend and Kinra (2000), *"The damping is achieved by absorbing the kinetic energy of the structure as opposed to the more traditional methods of damping where the elastic strain energy stored in the structure is converted to heat"*.

When PIDs are attached to the primary structure its motion is transfered to the cavity and consequently to particles. As pointed out by Bai *et al.* (2009), based in their simulations, the kinetic energy from the vibrating structure is transfered to the particles by means of momentum transfer between the particles and the cavity (collisions at the cavity's bottom and top). The particle bed can also be given some energy by static friction with the lateral walls, although this particular mechanism of energy transferring is particularly smaller than the transfer by collisions.

The kinetic energy is thus dissipated through friction and inelastic impacts, both among particles themselves and between the particles and the cavity walls. This mechanism of dissipation is mentioned by the majority of references found in this work.

Friend and Kinra (2000) observes that the dissipation on the kinetic energy—which corresponds to its transformation into heat—**is mainly attributed to the collisions between the particles and the cavity walls**. Controversially, Bai *et al.* (2009) observes that the main contribution factor of dissipation is the **friction** (in the interface particle-particle and particle-walls) rather than the collision. This behavior is material-dependent as the authors carefully state that collisions dissipating more energy than friction is generally true as long as the particles do not dissipate much energy when deforming after the impacts (inelastic collision) and do not have a very low coefficient of friction (CoF). This conclusion endorses the conclusion of Friend and Kinra (2000) although one has to be aware that these authors simulated a PID as an ID and have not considered the internal dissipation in their analysis. According to Fang and Tang (2006), friction is significant for very dense particle bed.

Sánchez *et al.* (2012) observe that at optimal dissipation, the interaction particle-particle is of irrelevant effect, being the collision the dominant effect in dissipation. This is achieved providing that a great number of particles is used and the particle bed moves as a single lumped mass.

Lu *et al.* (2017) conclude in their review that the mechanisms of dissipation and their individual contribution are still objects under discussion among researchers.

2.2.3 A note on the behavior of vertically shaken granular matter

When vertically shaken, a particle bed is known for exhibiting several motion regimes (or *motion modes*). Eshuis *et al.* (2007), in their experimental study with a quasi-2D cavity filled with glass beads, observed such regimes and established a phase diagram indicating each motion regime as a function of a shaking parameter and the number of particle layers F (Figure 2.3). Note that the term *phase* is related, in this case, to a distinguishable, separated spatial pattern described by the moving particles. Zhang *et al.* (2016a,b) also analyzed the motion mode of particles inside the cavity and described each of them.

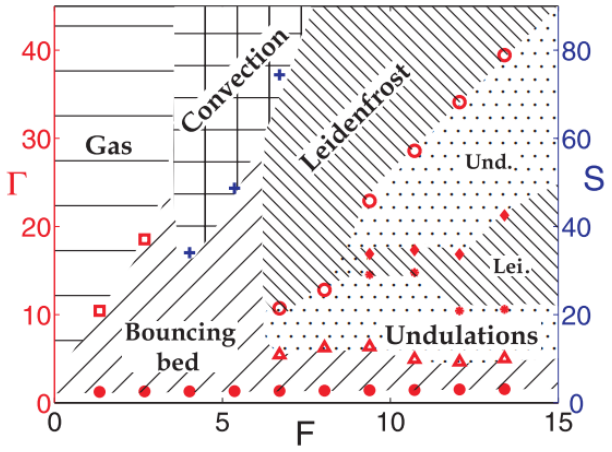

Figure 2.3: Example of a phase diagram reproduced from Eshuis *et al.* (2007) indicating the respective regime as a function of the shaking parameter and the number of layers.

The shaking parameters used by Eshuis *et al.* (2007) are the dimensionless acceleration Γ, in Equation (2.1), and the parameter S given by Equation (2.2).

$$\Gamma = \frac{a}{g} = \frac{A\omega^2}{g} \tag{2.1}$$

$$S = \frac{A\omega^2}{g d_p} \tag{2.2}$$

In Equation (2.1) the parameter a is the acceleration; A is the displacement; ω is

the excitation frequency and g is the gravitational acceleration given by $g = 9.81m/s^2$. In Equation (2.2), d_p is the particle diameter. Each of these equations is suitable for describing the particle motion depending on the excitation level to which the cavity is subjected.

Although the authors do not explicitly mention how to estimate the number of layers, at least two forms of determining F are found in the literature, as shown in Equations (2.3) and (2.4):

$$F = \frac{h}{d_p} \tag{2.3}$$

$$F = \frac{N_p}{N_{p1}} \tag{2.4}$$

In Equation (2.3), h is the height of the cylinder that circumscribes the particle bed. In Equation (2.4), N_p is the total number of particles and N_{p1} the number of particles in one layer, the very bottom for example.

Equations (2.3) and (2.4) are approximations and may underestimate the real number of layers by assuming that either no particle fills the voids formed by particles of the layer immediately below or by assuming that every layer has the same number of particles.

The motion regimes found in Eshuis *et al.* (2007) and Zhang *et al.* (2016a,b) are briefly described in the following:

1. Solid-like phase: in this phase there is perceivable relative motion among particles so the particle bed behaves like an added static mass, that is, the granular bed moves together with the cavity and never detaching from it. This regime appears for accelerations lesser than gravity;

2. Bouncing bed: for acceleration close to gravity and slightly above, the particles behaves like an inelastic bouncing ball. The transition from solid-like phase to bouncing varies linearly with the number of layers of particles;

3. Undulation regime: the granular bed appears to oscillate as a vibrating string revealing a standing wave pattern. This phase just appears if the number of layers is greater than 6. For number of layers smaller than 3, the bouncing bed regime is

followed by the granular gas regime. For number of layers between 3 and 6, there is the formation of convection rolls;

4. Local fluidization state: particles in the free layer start to fluidize, which means the particles in the upper layer have relative motion between each other. Lower layers remain in the solid-like phase;

5. Global fluidization: in this stage the particles are set in motion and there is relative motion between every particle;

6. Granular Leidenfrost effect: The *Granular Leidenfrost effect* was first experimentally observed by Eshuis *et al.* (2005) when a quasi-2D cavity filled with granular bed (glass beads) was vertically, vigorously excited. The terminology comes from the original *Leidenfrost effect* which is a phenomenon associated with a water droplet hovering over a very hot surface. The physical explanation for this is that when a droplet falls on a hot surface – at the Leidenfrost temperature –, part of the water on its bottom is turned into vapor which stays underneath the droplet avoiding it to evaporate quickly. Because of that, the droplet takes more time to evaporate than if it was on a surface with a temperature close to the ebullition point (Fig. 2.4).

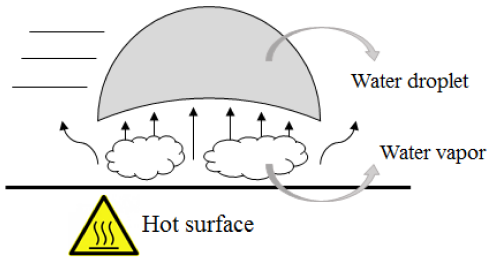

Figure 2.4: Schematic representation of Leidenfrost effect

The *Granular Leifenfrost effect* has a similar behavior but it is related with a particle bed vertically shaken in an especific amplitude (Fig. 2.5). Under this steady regime, part of the energy of the primary structure is converted into potential energy to sustain the bulk of particles, roughly at the solid state, above a gas-like phase.

Eshuis *et al.* (2005) observed that the granular Leidenfrost effect just happens when the number of layers F is greater than 10. For small values of F there is a transition from the solid phase of the granular matter to the gaseous-like phase without the Leidenfrost effect as a transition phase.

7. Buoyancy convection: convection that occurs inside the suspended layer in the granular Leidenfrost effect.

8. Convection rolls: in this stage the particles that are vibrating with high energy captured from the vibration tend to move upward and, in consequence, the surrounding

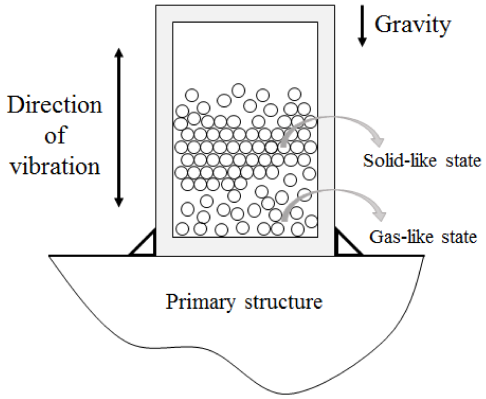

Figure 2.5: Schematic representation of Granular Leidenfrost effect. This illustration is based on the observation made by Eshuis *et al.* (2005)

particles tend to move downwards, thus changing their position among layers. This movement is related to the formation of rolls, very much like in an heat fluid;

9. Gas-like phase (Granular gas): *"a dilute cloud of particles moving randomly throughout the container"* (Eshuis *et al.*, 2007). This stage is only observed when the number of layers is smaller than 3, being the next phenomenon after bouncing bed in the case of less layers than 3.

2.2.4 Optimal dissipation

Fowler *et al.* (2001) mention that optimal dissipation is observed at an specific response level. This is in agreement with the remarks made by Friend and Kinra (2000); Olson (2003); Yang *et al.* (2004); Zhang *et al.* (2016a,b); Yin *et al.* (2017).

Zhang *et al.* (2016a,b) suggest, by analyzing their experimental results, that the optimal damping is achieved when the particles move in the Leidenfrost effect. On the other hand, Yin *et al.* (2017) affirm that the optimal dissipation occurs in the buoyancy convection motion mode. Procedures developed in both studies are not general and so the hypothesis of which state is the responsible for the optimal dissipation still deserves attention.

Yang (2003); Yang *et al.* (2004) found that the dissipation achieves an optimal value when analyzed along a dimensionless displacement, given by Equation (2.5).

$$\Delta = \frac{A}{L.F} \tag{2.5}$$

This dimensionless displacement takes into account the displacement of the base A, the gap clearance L and the number of layers F. The authors observed that the optimal peak is independent of frequency, number of particles, and particle mass. Results obtained for this Thesis, shown in Chapter 3, reveals that this behavior happens when analyzing the dissipation as a function of Γ (Equation 2.1) instead of dimensionless displacement.

2.2.5 Analysis approaches

Studies carried out up to the present moment focuses the analysis of PIDs on fundamentally two basic methods: the experimental and modeling approaches.

The main propose of carrying out an experimental study is to obtain the behavior of PID when varying some design parameters. This is achieved by either systematic experiments or analysis of application cases. Experimental investigations deliver valuable information about the real dynamics of a PID and are used to validate the models proposed by the researchers.

Although the present Thesis is mainly focused on experimental investigation, it is worth highlighting the modeling techniques employed in several papers. Some of them are briefly related in Section 2.2.5.1.

2.2.5.1 Modeling techniques

Some strategies can be found in the literature regarding PID modeling. One of the advantages of simulating a PID is the easiness to evaluate each parameter independently (Fowler *et al.*, 2001). This might not be possible in a testing procedure where some of the design parameters – mass and volume of a particle, for example – are dependent on each other by virtue of Nature.

One can consider a PID as an ID (Ramachandran and Lesieutre, 2008), which focus the simulations on the external loss mechanism – the dissipation provided by the colli-

sions between the particle bed and the inner cavity walls (Olson, 2003). Although the assumption that a PID behaves like an ID is computationally friendly, it will be shown later that the dynamics of each particle in the particle bed is important and should be considered as much as possible. When approximating a PID as a single mass, the impacts with the walls can also be modeled by either considering the impact an instantaneous event (Ramachandran and Lesieutre, 2008; Bannerman *et al.*, 2011) or by considering the impact as a finite event in time.

Another technique employed to simulate a particle damper is the Discrete Element Method (DEM), first proposed by Cundall and Strack (1979). In general terms, this method considers each particle inside the cavity as a rigid body prone to translational forces and torques. Each particle is assigned with six degrees of freedom and their equations of motion are integrated by using an explicit integrator. At the interface particle-particle or particle-wall, discrete stiffnesses and dampers are placed to simulate the contact. This approach allows the simulation of external and internal loss mechanisms. Discrete element method also has been widely used in geomechanics. More information can be found in O'Sullivan (2011) and Gomes (2014) (in Portuguese). Some open source softwares available include Yade [2], and LIGGGHTS [3]. Commercial softwares, like EDEM and Itasca, can also be employed. Studies using this approach comprehends Wong *et al.* (2007), where a methodology for determining the mechanical properties to be used as inputs of a DEM simulation are reported.

Wu *et al.* (2004) proposed a novel model based on multiphase flow theory. In their paper, the theoretical model is compared with the transient response of a cantilever beam's free end by means of the dissipative parameter proposed by Friend and Kinra (2000). Particles undergoing vertical vibration can be considered a multiphase gas-solid flow and thus are subjected to a drag force responsible for the external dissipation. Good correlation is observed between the simulation and experimental results. Wu *et al.* (2014) used an improved analytical model also based on multiphase flow theory to estimate the acoustic response of a box-type structure treated with PIDs. In this case, the viscous damping coefficient obtained from the modeling was inserted into a commercial finite element software. By inspecting the directivity pattern around the box, their simulation shows that particle impact dampers are able to reduce the far-field sound pressure level. The comparison between numerical and experimental validation also reveals a good agreement thus showing the feasibility of adopting the multiphase flow theory for modeling a PID.

It is worth noting that, from the point of view of modeling damper-structure inter-

[2]https://yade-dem.org/wiki/Yade

[3]http://www.cfdem.com/liggghts-open-source-discrete-element-method-particle-simulation-code

actions, some authors focus their study on particle impact dampers attached to SDOF systems while others analyze the PID behavior on MDOF systems (Du *et al.*, 2008).

It is important to observe that modeling is intrinsically related to the evaluation of PID's effectiveness, which is basically employed by analyzing how much dissipation a PID can provide. The next section assesses this topic.

2.2.6 Effectiveness and Design methodology

The literature offers several strategies to assess the effectiveness of PIDs. It also presents some guidelines and design methodologies in order to efficiently use this passive method. The need for a design methodology of PIDs arises from some factors, such as the complex interaction of the loss mechanisms and the large number of parameters affecting the damper performance, which makes the application of a particle damper very specific depending on the structure to which it is attached (Fowler *et al.*, 2001).

By using the modeling techniques in Section 2.2.5.1 or experimental results, some authors determine equivalent viscous damping coefficient for different levels of excitation (Liu *et al.*, 2005; Ben Romdhane *et al.*, 2013). These coefficients are obtained by fitting experimental or numerical results with a predetermined viscous model. This can be useful and a fast approach, specially when simulating complex structures using finite element method, where such coefficients are easily introduced in the nodes of the model. An evaluation of the viscous damping coefficient can thus assess the effectiveness of the given PID under analysis.

Fowler *et al.* (2001) suggest that the effectiveness of the particle damping can be assessed by comparing the time displacement of the primary system when untreated (without PID) and treated with the damper. In addition, to compare the relative effectiveness of two PID designs, the predicted displacement can be used. They also evaluate the effectiveness by comparing the damping capability with respect to the acceleration level. A maximum damping (peak) is found in a particular excitation amplitude.

Friend and Kinra (2000) analyzed the free response of a cantilever beam when treated with a PID. The cavity was placed at the beam's free end. The granular material adopted in their study is granular powder and the system is set into motion by different initial conditions (transient excitation). Although the authors recognize that the impact of particles with the cavity lid or bottom is finite in time, this time is unknown so they assume

that the particles behave as a single unit mass meaning that all the layers of particles impact the cavity instantaneously. This lead to the proposition of an *effective coefficient of restitution* which takes into account all the mechanisms involved in the dissipation of energy. So the authors assess their PID's effectiveness by means of a dissipation quantifier that is the ratio between the dissipated energy (variation of kinetic energy) and the maximum kinetic energy in a cycle, as shown in Equation (2.6).

$$\Psi = \frac{\Delta E_k}{E_k} \tag{2.6}$$

This parameter is used for transient excitation but Yang *et al.* (2004) develops this concept to harmonic excitation as well. In this study, an extensive analytical and experimental work shows the influence of the gap clearance on particle dampers vertically excited.

Marhadi and Kinra (2005) carried out a study in continuation to the one performed by Friend and Kinra (2000). The authors investigated experimentally the behavior of PID when attached to a SDOF (an equivalent model for the fundamental mode of a continuous beam) and subject to transient (free-decay) response. In this more comprehensive study, dissipation was analyzed when the following parameters were varied:

- Mass ratio;
- Number of particles;
- Particle material: lead spheres, steel spheres, glass spheres, sand, lead dust, steel dust, tungsten carbide pellets;
- Particle size;
- Gap clearance.

Zhang *et al.* (2016a,b) study the relationship between the particle motion modes and the damping performance of a PID. The authors evaluate the performance of a PID when attached to a cantilever beam and also when attached to a electrodynamic shaker head. After acquiring several frequency response functions (FRFs) related to different amplitude excitations, they made use of a phase diagram previously proposed in the literature (Eshuis *et al.*, 2007) to analyze the different particle motions found. The authors also conducted simulations using the discrete element method to understand a PID operating in optimal

conditions. One of the main conclusions is that for accelerations below $1g$ the particles behave like a static mass detuning the natural frequency due to mass loading effect.

One interesting observation reported by Zhang *et al.* (2016a,b) is the behavior of the system resonance for different accelerations. This behavior was already highlighted by (Liu *et al.*, 2005) but in a horizontal condition. According to them, the resonance peak tend to diminish in amplitude and frequency as the excitation amplitude increases; in the optimal condition, the amplitude is the lowest. As the acceleration continues increasing, the natural frequency tends to move towards the resonance observed when the primary system is added with the cavity without particles inside. The curve formed by the position of the resonances resembles a sigma-shape curve (Fig. 2.6).

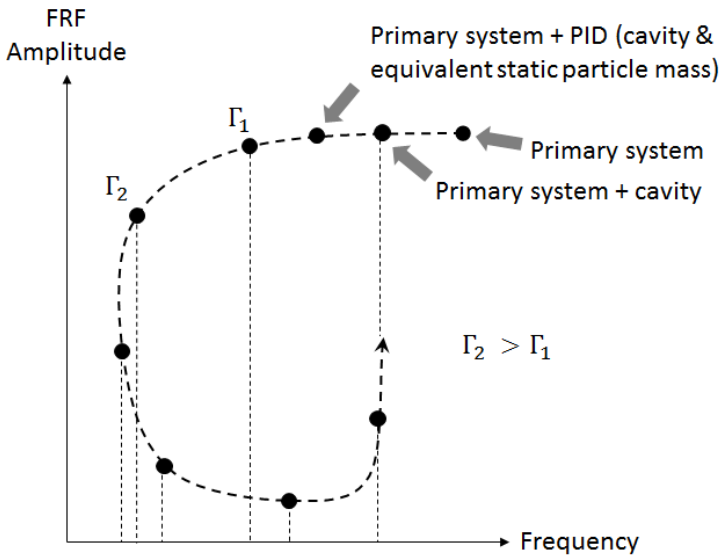

Figure 2.6: *Locus* of the system resonance

By placing a PID directly on a shaker, Zhang *et al.* (2016a,b) reproduced the same procedure reported by Yang (2003); Yang *et al.* (2004).

Yang (2003); Yang *et al.* (2004), using the experimental technique known as steady-state power measurement, proposed the use of master design curves as a tool for the fabrication of PIDs. Their master curves estimate dissipation by means of a dimensionless parameter called *dissipated power efficiency* (DPE), which is given by Equation (2.7). The DPE is a parameter similar to the one proposed by Friend and Kinra (2000), shown in Equation (2.6). The numerator is the averaged dissipated power per cycle and the denominator represents the maximum kinetic energy to be introduced into the system. As the DPE is dimensionless, the denominator has to have the unit of power and thus it is the first time derivative of the kinetic energy.

$$DPE = \Pi = \frac{P_{diss}}{P_{total}} = \frac{P_{diss}}{\dot{E}_k} = \frac{\frac{1}{nT}\int_0^{nT} F(t)v(t)dt}{m_{bed}|v||\dot{v}|} = \frac{\frac{1}{nT}\int_0^{nT} F(t)v(t)dt}{\omega m_{bed}|v|^2} \tag{2.7}$$

The dissipated power efficiency is evaluated along the dimensionless displacement, as shown in Figure 2.7. After obtaining the master curves, they were compared with the well known loss factor and a scale factor was determined so that the master curves could be applied in real structures.

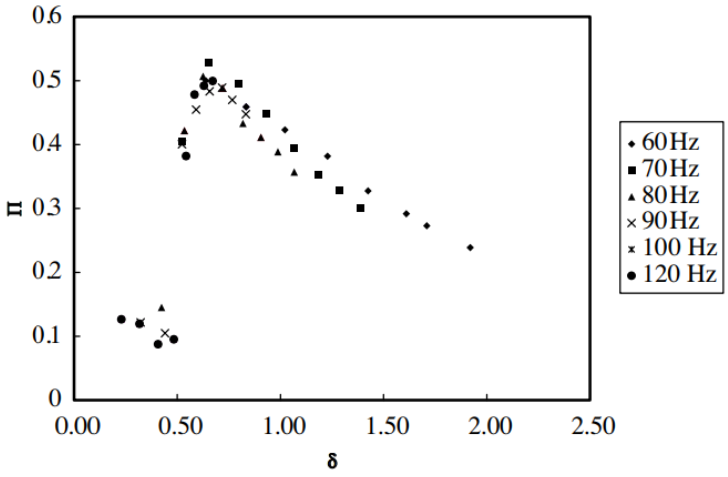

Figure 2.7: Example of master curves reproduced from Yang *et al.* (2004) and obtained for six frequencies, as detailed in the graph legend. One can note a peak dissipation in the DPE (vertical axis). One can also note the curves collapsing when analyzed as a function of δ ($\delta = \Delta.F$).

Fowler *et al.* (2001) proposed an analytical method focused on the development of a design methodology for PID. The analytical modeling is based on the assumption that the primary structure – a multi-degree of freedom system – can be approximated as a single-degree equivalent system at an specific mode of interest. The generalized mass m_α and stiffness k_α are the physical parameters of the equivalent system for an specific mode α. They are obtained by Equation (2.8) and Equation (2.9):

$$m_\alpha = \phi_\alpha^i M^{ij} \phi_\alpha^j \tag{2.8}$$

$$k_\alpha = m_\alpha \omega_{n,\alpha}^2 \tag{2.9}$$

Regarding damping, it can be estimated by either modal analysis algorithms or by

the *"expected intrinsic damping"* (Fowler *et al.*, 2001) of the material. After analyzing some parameters like excitation amplitude and particles size the following guidelines were proposed:

1. Determine the dynamic characteristics of the system without any treatments;
2. Determine whether particle dampers are suitable for the specific application or not;
3. Select a preliminary particle damper configuration;
4. Determine characteristics of the untreated system with additional mass;
5. Evaluate damper effectiveness using the particle damper simulation technique;
6. If necessary, modify damper configuration from Step 3 and repeat Step 4 and 5;
7. Verify chosen design experimentally.

Specifically for Step 3, the authors conduct a numerical study to assess the trends on some design parameters like total particle mass, particle size, and coefficient of friction.

Xu *et al.* (2004a) propose an empirical methodology for designing a PID based on its application to real structures. In their study, the PID was drilled on the structures. Their methodology has the steps listed in the following. Although the guidelines may not yield an optimal performance, the authors claim this can be a reasonable approach to suppress vibration.

1. Conduct a experimental or numerical (FEA) modal analysis of the structure;
2. Determine the feasibility of treating the structure with a PID by measuring the acceleration at several points;
3. Confirm the PID location;
4. Determine PID's characteristics (from parametric analysis);
5. Perform a stress analysis of the drilled structure;
6. Decide the packing ratio of particles.

Although it is a study on IDs, the work of Duncan *et al.* (2005) is worth mentioning. The authors propose a dimensionless parameter to quantify effectiveness, which is the ratio between standard deviation of the structure's position *without* damper divided by standard deviation of the structure's position *with* damper. This is a particular proposition that can also be used for PIDs. As a matter of fact, it was already investigated by Kocak and Cunefare (2016).

2.2.7 Conclusions about design parameters

Probably the most difficult part of designing a particle impact damper is to understand how the design parameters influence its dynamic behavior. In the following, an attempt to outline the main conclusions about the parameters that guide the design of a PID is presented.

2.2.7.1 Total particle mass (or mass ratio)

The relation between the particle and dissipation is fairly direct. It is reported by Fowler *et al.* (2001) that increasing the total particle mass the dissipation also increases. The opposite is also true. Friend and Kinra (2000) determined a relationship between the dissipation and the particle mass (or mass ratio μ) given by Equation (2.10), which was later confirmed by Marhadi and Kinra (2005).

$$\Psi = \frac{\mu}{(1+\mu)^2} \tag{2.10}$$

2.2.7.2 Number of particles

Marhadi and Kinra (2005) concluded that the specific damping capacity proposed by Friend and Kinra (2000) is dependent of the number of particles up to a certain limit. Above this limit there is no longer any dependency. Yang *et al.* (2004) recommends that the number of particles should be enough to complete three or four layers.

2.2.7.3 Particle size

When comparing the damping capability of PID with the excitation amplitude, it is found that, larger but fewer particles inside the cavity *"tend to peak at lower amplitudes while the more numerous, smaller particles favor the higher amplitudes"* (Fowler *et al.*, 2001). Moreover, dissipation peaks of smaller particles are narrower than the peaks of larger particles.

Xu *et al.* (2004a) recommend the use of different particle sizes as a robust solution to control several resonance frequencies.

Booty *et al.* (2014) claims that smaller particles tend generally to damp more.

2.2.7.4 Particle material

According to Marhadi and Kinra (2005), particle material plays an important role when a PID has a small number of particles. The effect of material disappears as the number of particles increases. Xu *et al.* (2004a) suggests that the higher the material's density the best. In their paper, tungsten is the chosen material.

2.2.7.5 Particle shape

Considering a cylindrical cavity, Xu *et al.* (2004a) recommend that the ratio of particle diameter and hole diameter should be about 1/5 to 1/10.

Sanchez *et al.* (2013) studied the influence of fragmentation and fusion of particles. They found that geometry of particles has no effect on PID's effectiveness. Additionally, particle fragmentation may not be a problem but particle fusion can impair the damper's effectiveness.

Booty *et al.* (2014) conclude that large irregular particles appear to be the most suitable when compared with small machine swarf particles. As pointed out by the authors, irregular particles could represent an important cost saving measure.

2.2.7.6 Gap clearance

According to Zhang *et al.* (2016a,b), the larger is the gap clearance the higher is the position of the bulk particles in the Leidenfrost state. That is, the more energy is transferred the more energy available to be dissipated. The relationship between the optimal gap clearance and the Leidenfrost Effect is not deeply explored though.

Marhadi and Kinra (2005) states that apparently, as gap clearance increases so does the specific damping capacity. However, conclusive tendency could not be completely inferred.

Ramachandran and Lesieutre (2008) mentions that high loss factor is found when there is double impact condition, thus suggesting the possible existence of an optimal gap clearance. As their approach is based on the simplification of a PID into an ID, this conclusion may not be valid for several particles inside the same cavity. The authors recognize the limitation of such assumption at the end of their study. Yang (2003) presents some indications that an optimal gap clearance exists.

As matter of fact, in some papers, the characteristic measure to quantify how the particles fill the room inside the cavity is the volumetric packing ratio, instead of the gap clearance. Fang and Tang (2006) report two important definitions regarding the cavity filling:

- Granular packing ratio:

$$a_g = \frac{\text{total volume of granules}}{\text{volume of the enclosure}} \tag{2.11}$$

- Volumetric filling ratio:

$$v_g = \frac{\text{volume occupied by the granules}}{\text{volume of the enclosure}} \tag{2.12}$$

The value of v_g is generally larger than a_g since voids are easily found in granular materials. Literature reports that the relationship between a_g and v_g is given by Equation 2.13.

$$a_g = 0.63 v_g \tag{2.13}$$

2.2.7.7 Coefficient of friction (CoF)

The increasing in CoF has little (or even slightly adverse) effect on damping (Fowler *et al.*, 2001).

Fowler *et al.* (2001) states that the coefficient of friction has more influence on an ID than on a PID. Rongong and Tomlinson (2005) reports that pouring lubricant enough to coat the particles tend to reduce energy dissipated by the PID. According to them, the heavier the lubricant the more significant the reduction in the dissipated energy. This observation shows that the friction between particles is an important mechanism of dissipation in PIDs. Yang (2003) also reports that higher friction between particles and cavity walls decreases PID's effectiveness.

2.2.7.8 Coefficient of restitution (CoR)

Duan and Chen (2010) affirm in their study that a velocity-dependent CoR should be more suitable for DEM simulations of PIDs. This assumption let them conclude that DEM simulation can deliver not only qualitative but quantitative information.

2.2.7.9 Cavity geometry

Wong *et al.* (2009) states that cavity geometry / shape can play a significant role in PID's effectiveness. Previously, although in a study of horizontal PID, Rongong and Tomlinson (2005) had already suggested that the cavity can influence the granular motion, which could be translated into alterations in the dissipation. The cavity can alter what is known as the mechanical temperature [4]. In general lines, a low mechanical temperature means close packing and high pressure, which is found in cavities with high aspect ratio (length/radius). Dissipation in granular materials at low mechanical temperatures occurs at high accelerations and are very narrow peaks. The opposite is also true: high mechanical temperature means low pressure and loose packing, with broad dissipation peaks occurring at lower accelerations.

[4]Mechanical impedance is a concept created to understand the behavior of a granular material under a combination of pressure and packing.

In their work, Booty *et al.* (2014) compared the rigid cavity with the *bean bag* configuration. The latter did not represent an improvement in terms of dissipation, as it was initially expected by the authors.

2.2.7.10 Orientation relative to the gravity

The orientation of gravity is reported (Fowler *et al.*, 2001) as a minor influencer in the damping capacity than it is for IDs.

2.2.8 Other studies and applications

Lu (2012) study the influence of a buffered particle impact damper on a building subject to controlled and real (earthquakes) excitations. A buffered PID means that the inner walls are covered with a resilient material, which improves the contact time between the particles and walls (with the consequent improvement in momentum transfer) and also reducing the noise created by the impacts.

More recently, Xiao *et al.* (2016) applied the technology of PID in gear pairs as a passive method to reduce its torsional vibration. Papalou and Strepelias (2016) used PIDs to control vibration in columns of monuments. Koch *et al.* (2017); Ahmad *et al.* (2017) explored the application of PID in honeycomb structures. Li and Tang (2017) proposed a hybrid particle impact damper, called tuned mass particle damper (TMPD) that incorporates advantages of a PID with the benefit of a tuned mass damper (that can primarily overcome the lack of effectiveness of a PID for accelerations below $1g$).

Duvigneau *et al.* (2016) applied the concept of a granular-filled cavity to the oil pan of an engine. The broadband reduction on the vibratory response of this automotive component has proven the effectiveness of PIDs.

Regarding sound insulation, Kuhl and Kaiser (????) tested the influence of sand and other granular materials in the loss factor of walls made of bricks and reinforced concrete, focusing on the reduction of structure-borne sound.

2.2.8.1 PID under horizontal excitation

Although this Thesis is restricted to PIDs under vertical excitation, for papers containing research on PIDs in horizontal direction, please refer to Papalou and Masri (1996, 1998); Saeki (2002); Liu *et al.* (2005); Heckel *et al.* (2012).

Papalou and Masri (1996) studied the behavior of particle impact damper filled with tungsten powder and ball bearings, attached to a SDOF system and subjected to horizontal random vibrations. By means of an experimental procedure, they analyzed the mass ratio, cavity dimensions, and intensity of excitation. An approximate analytical solution was proposed based on the experimental results and on the assumption that the particle bed can be analyzed as an equivalent ID. This model was used to predict the response levels of the primary system around the optimum combination of system parameters. The conclusion of this work were:

- For small cavity sizes, a PID tends to be less effective with the increase of the mass ratio. For larger cavities, PIDs are more effective with the increase of the mass ratio;
- For larger mass ratio, a small cavity is less effective than a larger one. This is because for small cavities the main dissipation mechanism is friction between the particles. As the cavity size increase the particles have more space to move and so the momentum exchange plays a major role in dissipating energy;
- If the excitation level decreases, PID is less effective. On the other hand, increasing the excitation level, PID is more effective up to a limit where the response is independent of the excitation level.

A similar study conducted by Papalou and Masri (1998) was dedicated to harmonic excitation.

Saeki (2002) performed a steady-state experimental and analytical analysis of a PID in a SDOF system and subject to horizontal sinusoidal excitation. In his work, the following parameters were investigated:

- Particle material: lead, stainless steel, steel, acrylic resin;
- Box-like cavity dimensions;

- Mass ratio: ratio between the total mass of particle bed and the mass of the primary system;
- Particle size.

Using the discrete element method (Cundall and Strack, 1979), the following conclusions were reported:

- Particle material is a parameter to be considered when designing a MPID and does affect its behavior;
- Cavity height and width have little influence on the response of the primary system. The cavity length (dimension parallel to the particles movement) is the main dimension to be considered;
- The mass ratio is inversely proportional to the response of the primary system. In addition, higher values of mass ratio increase the optimum cavity length;
- Higher values of particle radius also increase the optimum cavity length.

The work carried out by Heckel *et al.* (2012), in particular, shows the application of a multi-unit PID in the vibration control of an oscillatory saw. They compare the response of the machine under the treatment of a PID with the response when a solid mass is added to the saw.

2.3 Impact-induced excitation

The work devoted to understand systems subjected to impact is vast and it is included in the broader field of Non-linear Dynamics. The references in the following are restricted to studies carried out to analyze the dynamics of repetitive impacts.

Park (1967) studied a SDOF system subjected to repetitive impacts of a mass-spring-damper. Their model is illustrated in Figure 2.8. By considering that the momentum is conserved and the dissipation is introduced in the model by the coefficient of restitution, the author explored the response of the systems in terms of the excitation frequency, damping ratio, coefficient of restitution, initial gaps between the masses, mass ratio, and stiffness ratio. Simulations were validated by comparing them with experiments.

The author demonstrates that the higher the inherent damping the more attenuated the response is. On the other hand, for maximum response to repetitive impact, the mass ratio ($= m_3/m_2$) should be equal to the stiffness ratio ($= k_3/k_2$) and they both should be kept small. Damping factor should be low and the coefficient of restitution should be close to 1 (almost elastic collision).

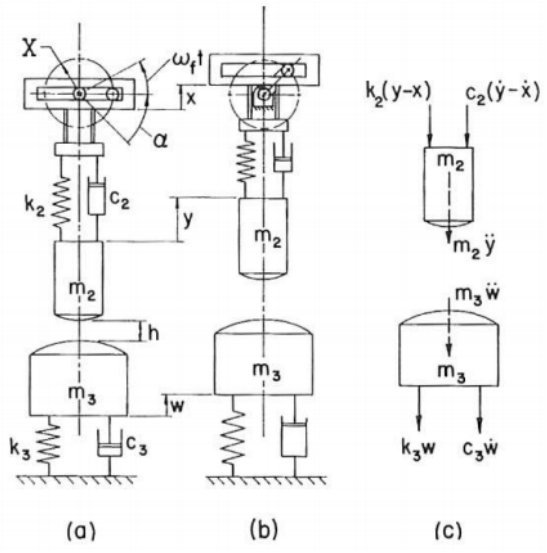

Figure 2.8: Model used by Park (1967). Please refer to the original article for information about the parameters on this figure.

Fang and Wickert (1994) studied the response of a single degree of freedom system periodically driven by an external impact-induced excitation. The authors experimentally analyzed the time response, spectra and state space trajectories of the main mass—also called *oscillator*. They also model the system using an implicit technique. Their model does not take into account the dynamic behavior of the mass that strikes the oscillator (Figure 2.9). The authors observed that the dynamic response of the cantilever beam followed a predictable pattern of resonance of a periodic solution, bifurcation and irregular (chaotic) vibration. Their model has qualitatively predicted this behavior.

Kember and Babitsky (1999) worked with a model where two grounded SDOF systems impact each other but, differently of Park (1967), the interface has a resilient element that exerts a contact force composed of an elastic and an dissipative element. Moreover, in this model the excitation is a force instead of a base excitation (Figure 2.10). The focus of this study was to propose a new tool to solve the equation of motion of the referred system. Observations of the system response show two types of resonances, namely *grazzing resonance* and *clapping resonance*. The former refer to a in-phase movement of the two masses (barely not contacting each other) while the latter refer to an out-of-phase movement with a single strong impact per cycle. The grazzing resonance is linear

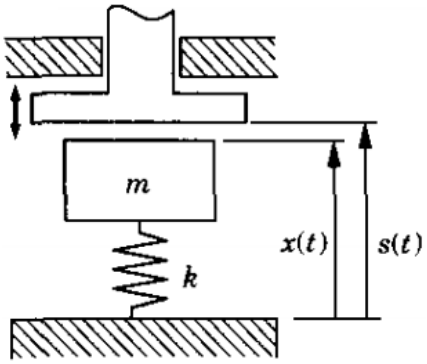

Figure 2.9: Model used by Fang and Wickert (1994). Please refer to the original article for information about the parameters on this figure.

(not dependent on the excitation amplitude) and dependent of the viscous damping; the clapping resonance refer to a non-linear behavior being dependent of the damping at the interface – the lower the dissipation at the interface the more prominent is the second resonance.

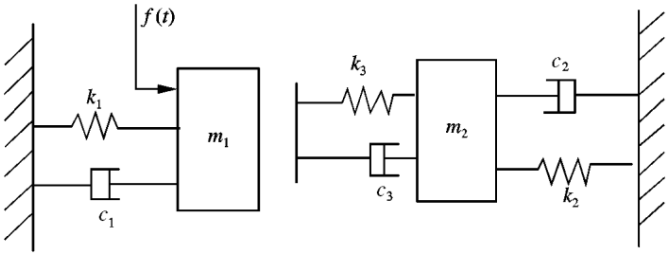

Figure 2.10: Model used by Kember and Babitsky (1999). Please refer to the original article for information about the parameters on this figure.

Kocak and Cunefare (2016) studied the influence of the excitation force and frequency in a particle impact damper subjected to repetitive impulses. Their model, depicted in Figure 2.11, takes into account the deformation of the PID's base as well as the physical limitation of its thickness (represented as a limit stop). The particles are lumped in a single mass. The authors concluded that, for the proposed model, for optimal performance the excitation frequency should be slightly larger than the natural frequency of the system. Moreover, the force amplitude should be numerically equal to the product between stiffness and gap clearance.

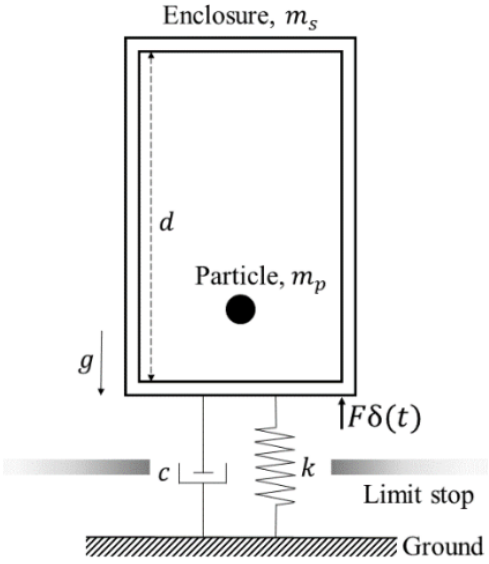

Figure 2.11: Model used by Kocak and Cunefare (2016). Please refer to the original article for information about the parameters on this figure.

2.4 Conclusions of the literature review

- Particle impact dampers are non-linear devices highly dependent of a myriad of parameters that still have to be deeply analyzed in order to achieve a one-size-fits-all general rule;
- The mechanisms of dissipation are: 1) inelastic impacts between the particle and the primary system; 2) Frictional losses due to slipping/rolling motion between the particles themselves and the particles with the primary structure (Ramachandran and Lesieutre, 2008);
- References on particle impact dampers are still incipient and thus this is a subject that worth it to be studied.

A very comprehensive review on particle impact dampers has been published recently (Lu *et al.*, 2017) and can be used as a first source of information by those who intend to start studying particle impact dampers.

3 Dynamic characterization of PIDs

3.1 Overview

This chapter aims to experimentally investigate the dissipation provided by a particle impact damper under harmonic excitation. The procedures proposed by Yang *et al.* (2004) and Zhang *et al.* (2016a,b), previously described in Chapter 2, are re-examined and compared with each other.

The dynamic characterization of PIDs under harmonic excitation is a well known procedure. What is not available, however, is a generalized methodology to design such dampers, as it was emphasized in Chapter 2.

But the question to be answered is: *Why should I compare two damping estimators?*

While exploring the behavior of particle dampers, I was intrigued by the number of ways one can determine the dissipation of such dampers and how they can lead to the conclusions about PID's design parameters. Zhang *et al.* (2016a,b) quantify dissipation through the analysis of linearized FRFs; Yang *et al.* (2004) conduct power measurements and claim the dissipation can be quantified without the need of the primary structure. It is of particular interest to investigate what information can be extract from these approaches when a parametric analysis is conducted. In other words, the main reason to conduct a comparison of dissipation indicators is to assess the possibility of two different parameters indicate different trends when performing a parametric analysis.

Carfagni *et al.* (1998) mention the difficulties of predicting damping in a structure. According to the authors, care should be taken when analyzing damping estimators obtained by different methods. They list three possibilities to evaluate damping in a structure:

- Reduction of the amplitude at resonances;
- Temporal decay of free vibrations;
- Spatial attenuation of forced vibrations.

Another estimation method that has been accepted as the most suitable damping estimator is the loss factor. Carfagni *et al.* (1998), therefore, devote some effort to analyze different definitions of loss factors found in the literature.

In another study, Ben Romdhane *et al.* (2013) perform an experimental characterization of a PID under harmonic excitation and perpendicular to the gravity by analyzing the loss factor provided by these dampers.

3.2 Re-examining the work of Yang *et al.* (2004): PID directly attached to a shaker

In this section, the dissipated power efficiency proposed by Yang *et al.* (2004) (Equation 2.7) is evaluated. To do so, the characterization of the particle impact dampers was carried out in two design generations which are detailed next.

3.2.1 Preliminary tests: First generation of PIDs

The first generation of PIDs (Figure 3.1) was designed and manufactured by the research group of Dr. Kenneth Cunefare from *Georgia Institute of Technology* (Atlanta, GA, USA) where I accomplished my PhD Internship. Initially, the intention of this preliminary test was to reproduce what it has been found in the literature and assess some basic understanding on how such dampers work. Replicating some of the results of Yang *et al.* (2004) appeared to be a reasonable starting point.

The cavities developed for this preliminary test have a hexagonal internal shape in order to accommodate the spheres according to the hexagonal close packing (HCP) configuration [1]. These first generation dampers were fabricated using a 3D printer. As they were designed to have a fixed height, three samples of different heights – $0.6in$ ($0.015m$), $0.8in$ ($0.020m$), $1in$ ($0.025m$) – were fabricated. PIDs with two different inner dimensions were also designed.

The cavity was fixed on the electrodynamic shaker (Figure 3.2). An impedance head measured the force and acceleration at its base. A four channel DAQ was used to

[1] It is worth noting that this assumption depends directly on the radius of the spheres and then it is not a general assumption for every particle size.

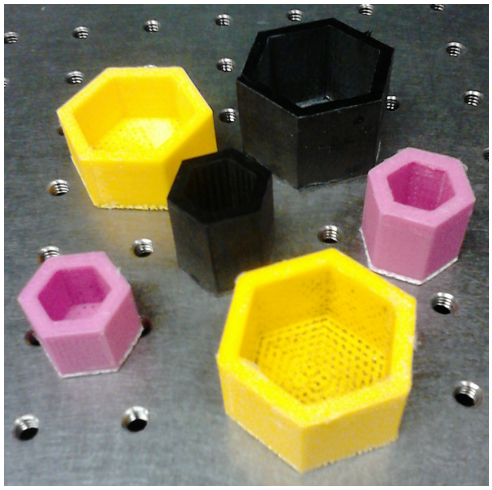

Figure 3.1: Ilustrative picture of first generation of PIDs with different heights and inner dimensions.

measure and generate signals to the power amplifier and then to the shaker. A LabVIEW VI was created, in association with Dr. Cunefare' students, to control the experimental procedure. The user interface allows the user to set several frequencies, and acceleration range, as it is desired. The acceleration is varied by changing the input voltage in the shaker, according to the voltage step also set initially. The user is allowed to choose the block time and the number of replicates for each acceleration as well. The setup is illustrated in Figure 3.3.

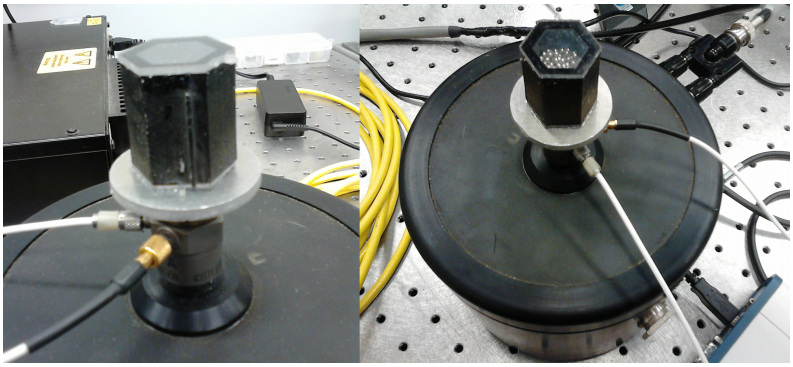

Figure 3.2: The cavity was attached to an impedance head which was then fixed on the shaker.

The equipment list used for the tests of the present Section are in Table 3.1.

Some results obtained are shown next (Figures 3.4 to 3.11). For the sake of brevity, only the results for two different cavity heights (same particle mass of $50g$ but different gap clearances) are displayed. They correspond to the yellow samples in Figure 3.1. Figures 3.4 to 3.11 depict the dissipated power efficiency as well as the dissipated power normalized

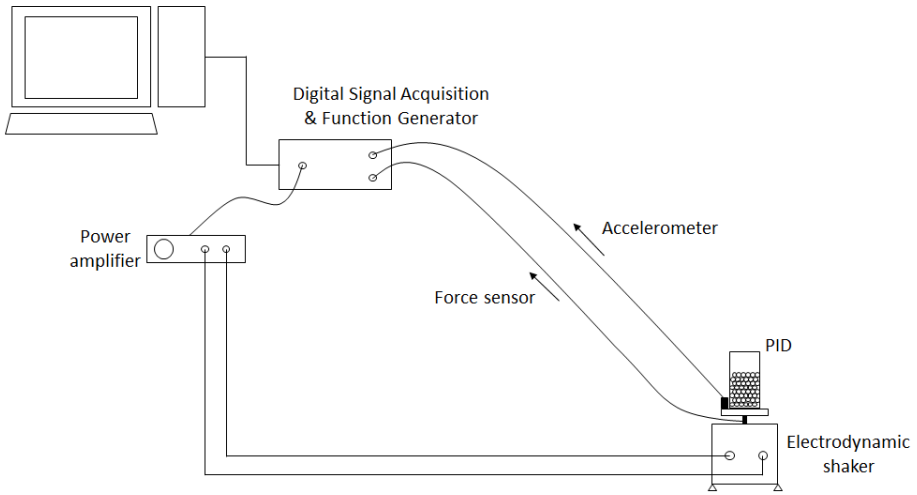

Figure 3.3: Experimental setup for the dynamic characterization of PIDs under harmonic excitation.

Table 3.1: Equipment list for tests with the second generation of PIDs.

Equipment	Manufacturer/Type	General information
DAQ	NI USB-4431	-
Electrodynamic shaker	B&K 4809	-
Power amplifier	B&K	-
Impedance head	Kistler 8770A50	$m_{force} = 34g$; $S_{acc} = 100mV/g$ $S_{force} = 22.6mV/N$

by the particle mass and the total mass (particles + cavity), velocity, and velocity squared. These quantities are used to compute DPE. Note that the slope of the velocity as a function of acceleration is the inverse of frequency. The dimensionless acceleration Γ was calculated by filtering the acceleration signal and extracting the amplitude of the response at the excitation frequency. One can compare these curves with those obtained by Yang *et al.* (2004) and reproduced in Figure 2.7. A compilation of curves shown in Figures 3.4 to 3.11 is found in Figures 3.12 and 3.13. More frequencies are added to verify the trends.

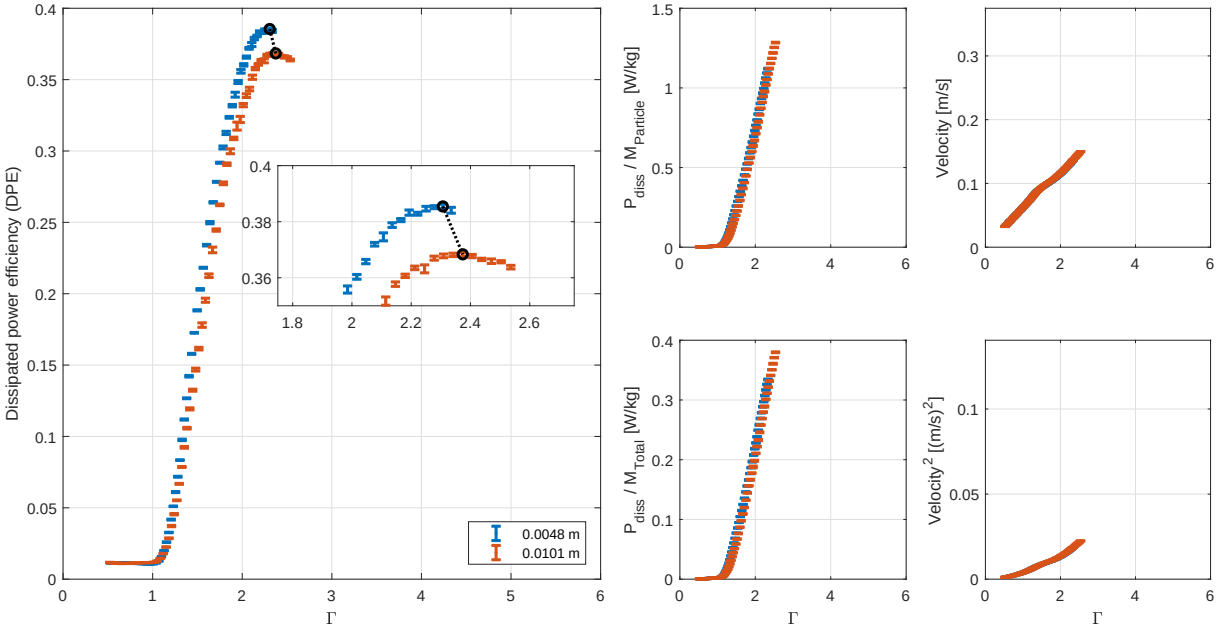

Figure 3.4: Gap clearance analysis. Curves represent two gap clearances – $0.0048m$ and $0.0101m$ – at 25Hz. Inset plot highlights the averaged peak value and the error bar of ten replicates at each acceleration. Other plots include DEP normalized by particle mass, DPE normalized by total mass, velocity and velocity squared.

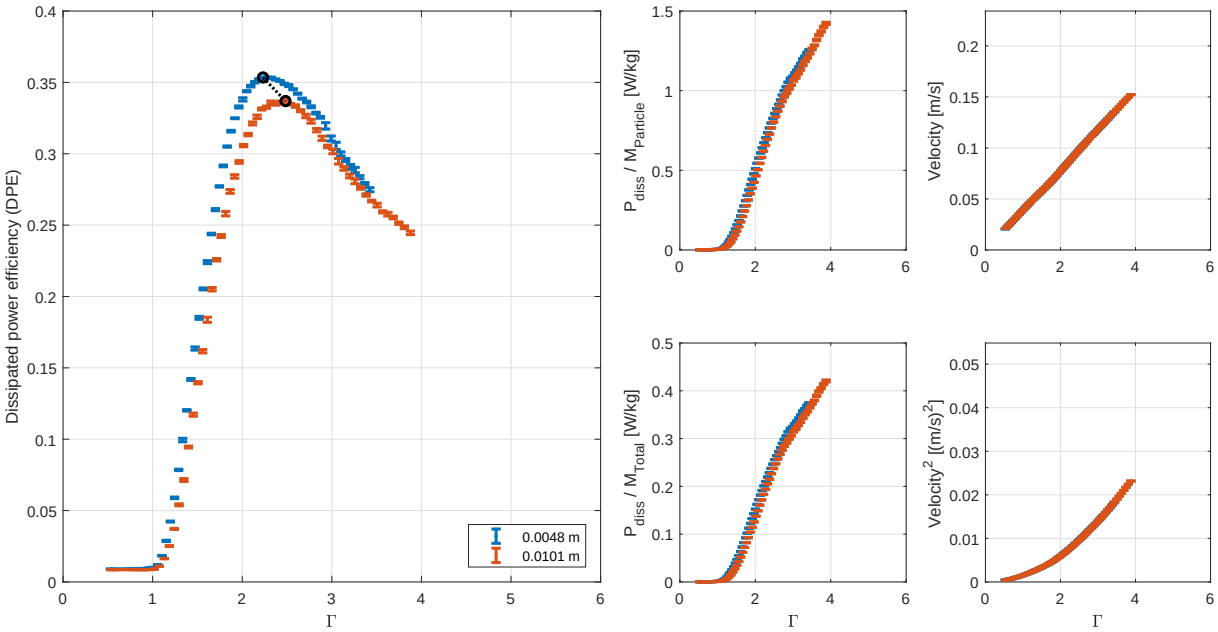

Figure 3.5: Gap clearance analysis. Curves represent two gap clearances – $0.0048m$ and $0.0101m$ – at 40Hz

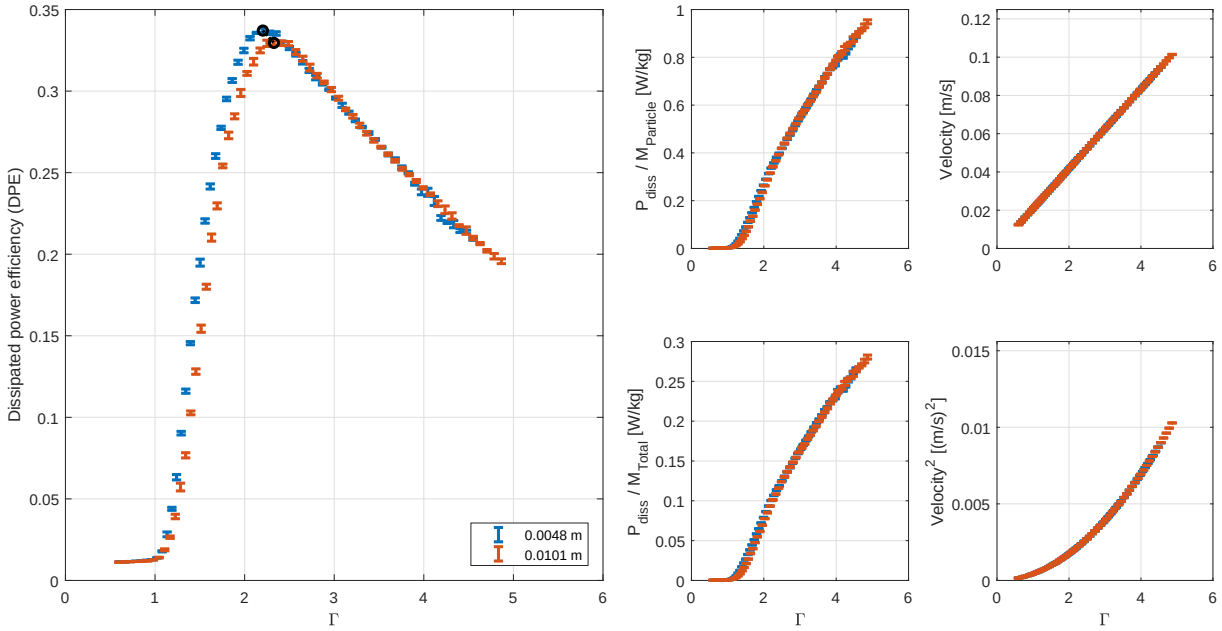

Figure 3.6: Gap clearance analysis. Curves represent two gap clearances – $0.0048m$ and $0.0101m$ – at 75Hz

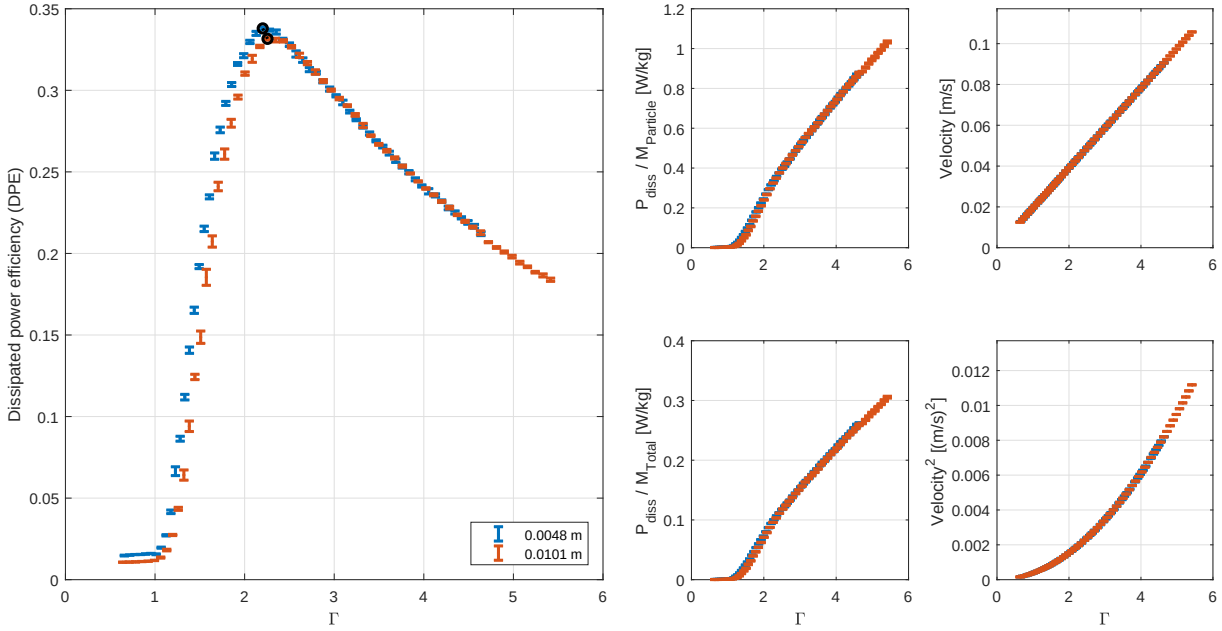

Figure 3.7: Gap clearance analysis. Curves represent two gap clearances – $0.0048m$ and $0.0101m$ – at 80Hz

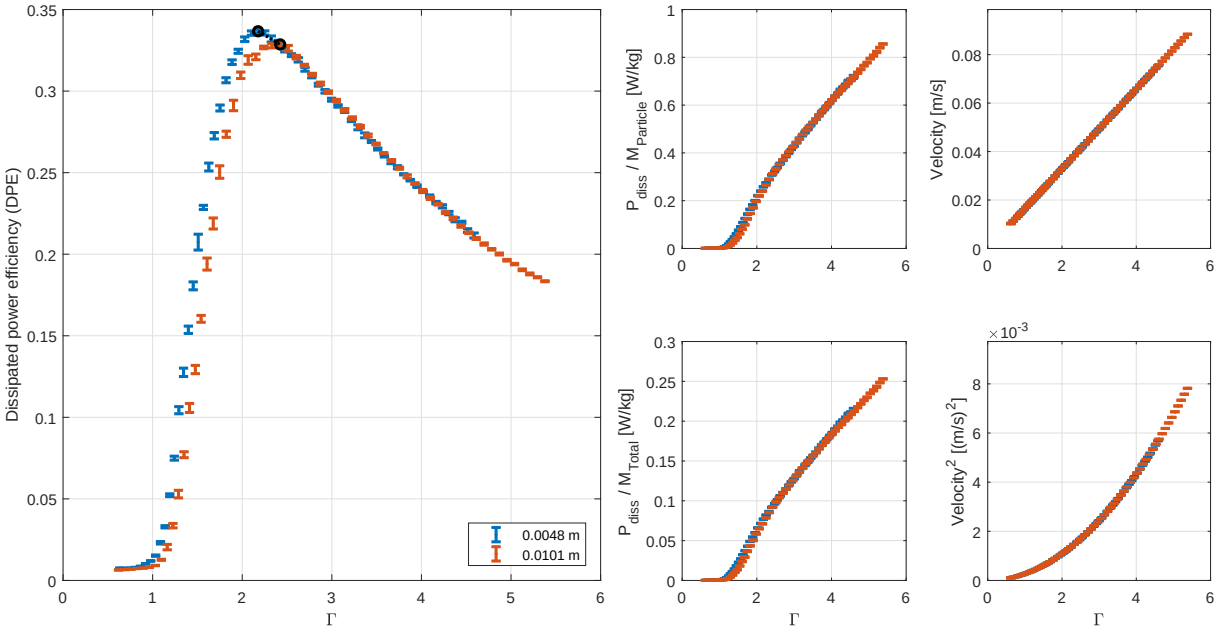

Figure 3.8: Gap clearance analysis. Curves represent two gap clearances – $0.0048m$ and $0.0101m$ – at 95Hz

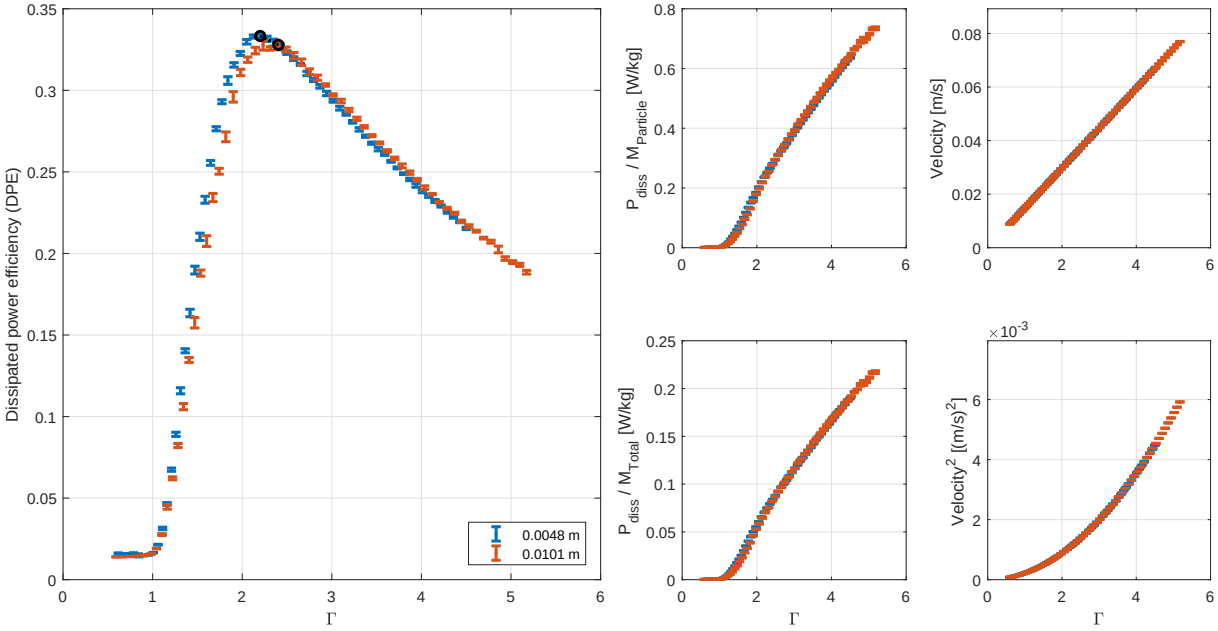

Figure 3.9: Gap clearance analysis. Curves represent two gap clearances – $0.0048m$ and $0.0101m$ – at 105Hz

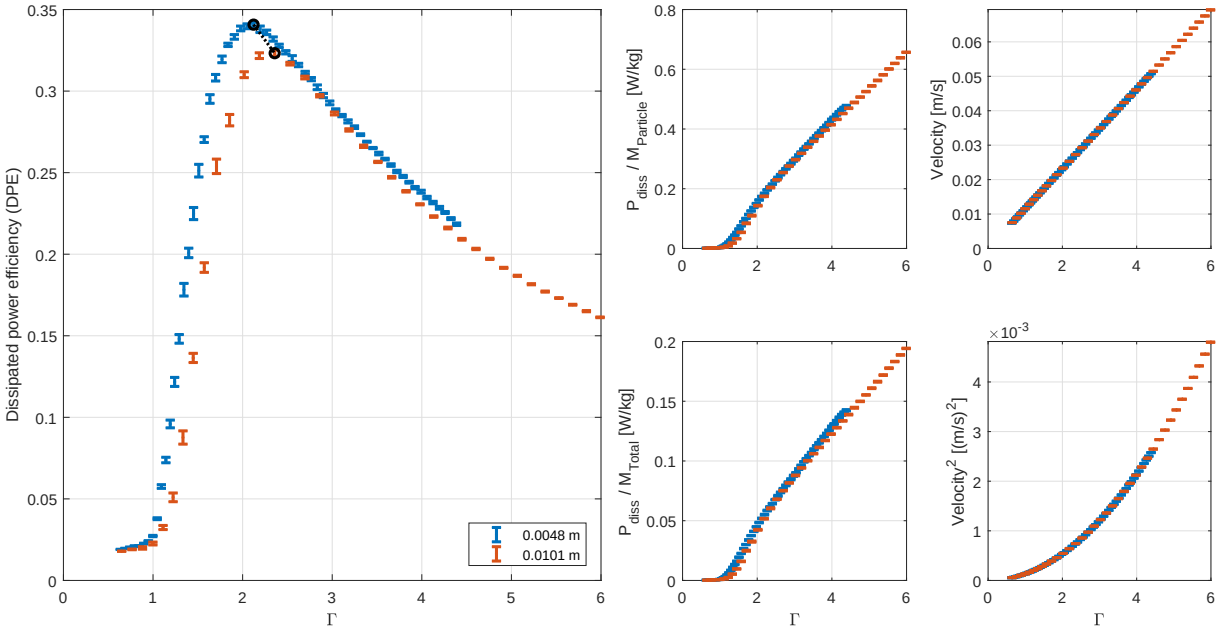

Figure 3.10: Gap clearance analysis. Curves represent two gap clearances – $0.0048m$ and $0.0101m$ – at 135Hz

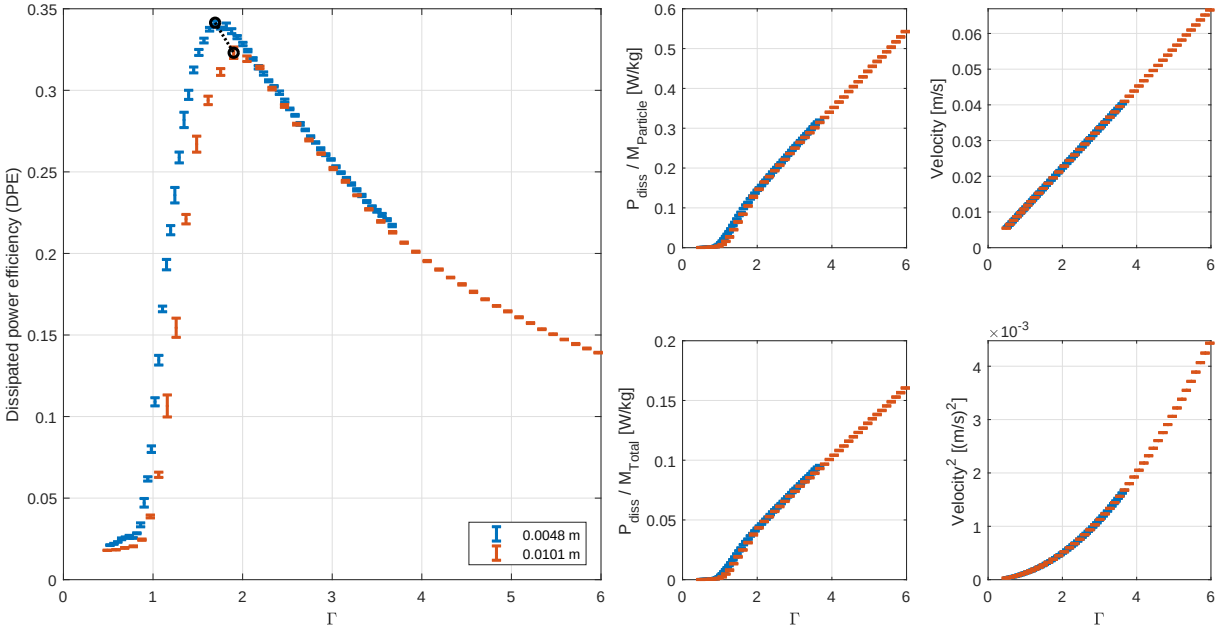

Figure 3.11: Gap clearance analysis. Curves represent two gap clearances – $0.0048m$ and $0.0101m$ – at 140Hz

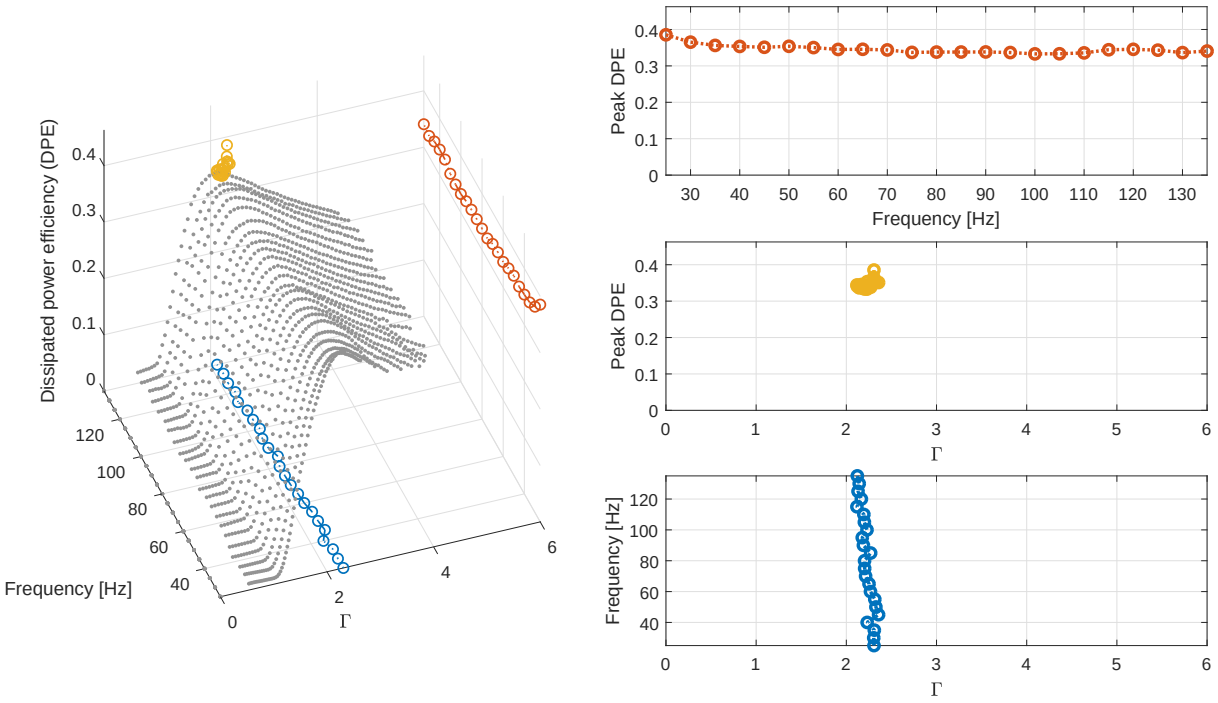

Figure 3.12: Curves related to the sample with gap clearance of $0.0048m$.

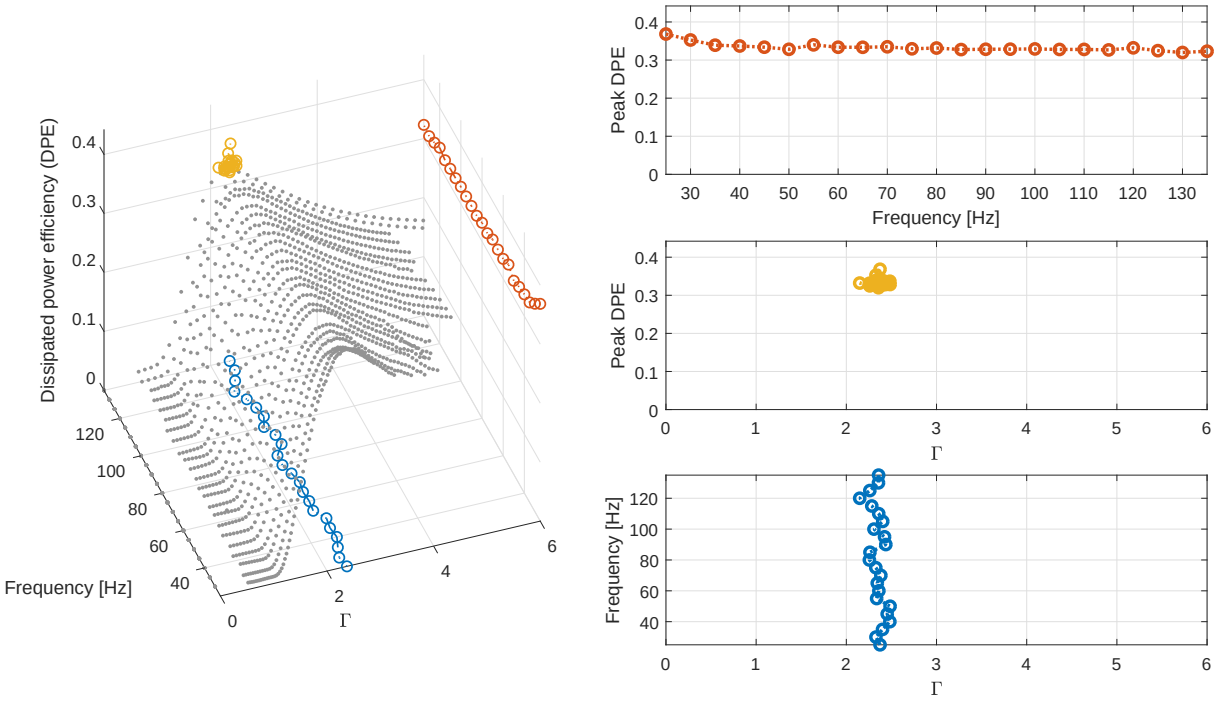

Figure 3.13: Curves related to the sample with gap clearance of $0.0101m$.

One can clearly observe from Figures 3.12 and 3.13 that DPE curves collapse with respect to the acceleration the damper is subjected, which means that the optimal peak is located roughly at the same acceleration for every frequency. This conclusion differs from what was exposed by Yang *et al.* (2004) in their study. If data provided by Figures 3.4 to 3.11 were plotted as a function of displacement, as proposed by Yang *et al.* (2004), curves would display as they are in Figures 3.14 and 3.15.

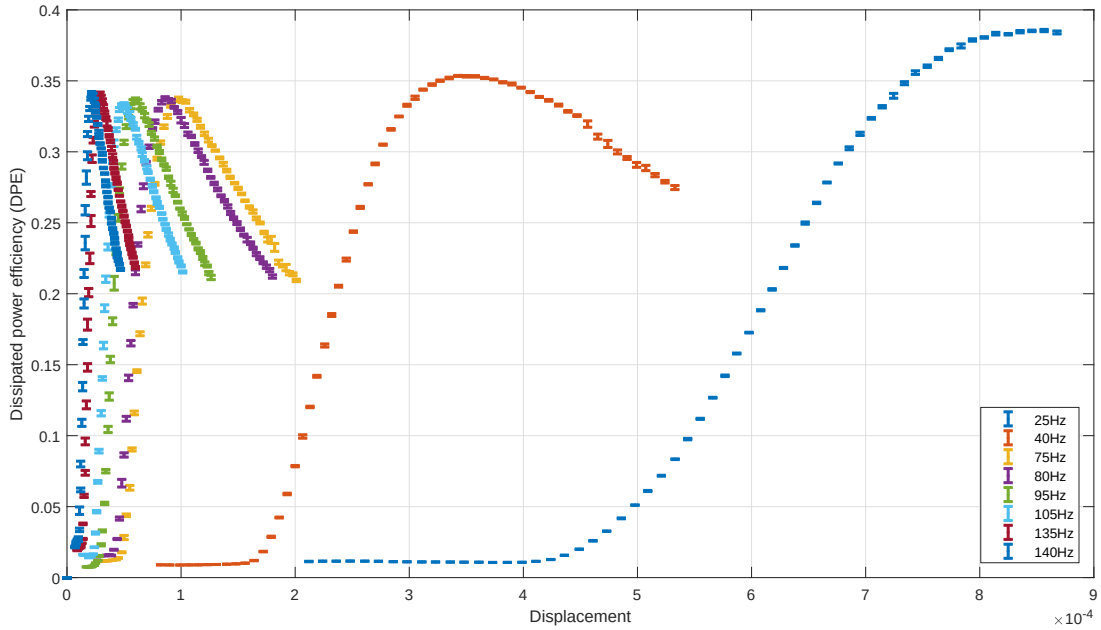

Figure 3.14: Curves related to the sample with gap clearance of $0.0048m$. Dissipation as a function of displacement.

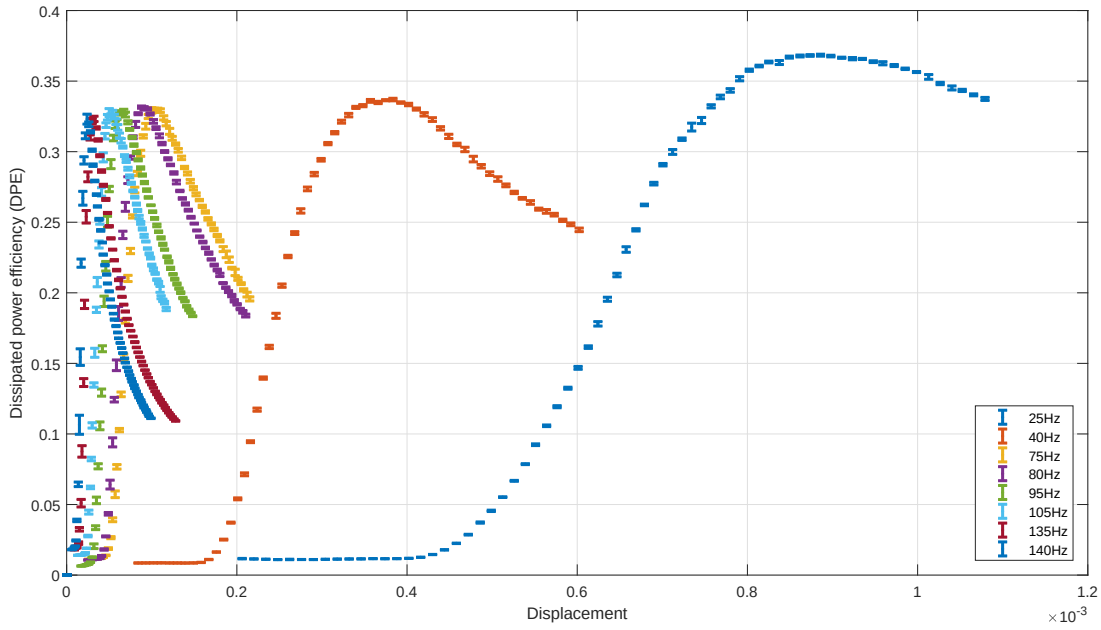

Figure 3.15: Curves related to the sample with gap clearance of $0.0101m$. Dissipation as a function of displacement.

The dissipation provided by the damper is also constant along the frequency. As the curves for the two gap sizes provide the same dissipation, one can also conclude that the damper behaves similarly, providing that the particle mass is the same and the particles do not hit the ceiling – which is the case here.

In order to go deeper in the experimental analysis, a second generation of PIDs were implemented. Note that, in the first generation, it was difficult to observe what was happening with the particle bed while vibrating. Thus, a transparent cavity was required for such task. The need for a simpler geometry – one without corners – also motivated the design and fabrication of the second generation. By designing and manufacturing a different cavity with different features, the effects related to the cavity itself could be analyzed and its influence could be assessed.

3.2.2 Second generation of PIDs

Particle impact damper of the second generation was fabricated using an acrylic tube with inner diameter of $24mm$ and wall thickness of $3mm$. The PID has an adjustable lid, also made of acrylic, which can be locked by screws at predetermined positions $5mm$ away from each other (Figure 2.1).

Again, the cavity was attached to the shaker (Figure 3.16). In the tests of the present Section, the impedance head was replaced by a force sensor and an accelerometer, both attached to the PID's base. The equipment list is in Table 3.2.

Table 3.2: Equipment list for tests with the second generation of PIDs.

Equipment	Manufacturer/Type	General information
DAQ	NI USB-6251	-
Electrodynamic shaker	B&K 4808	-
Power amplifier	B&K 2712	-
Signal conditioner	PCB 482A16	-
Force sensor	PCB 208C03	$m_{force} = 22.48g$; $S = 2.27mV/N$
Accelerometers	PCB 356A11	$m_{acc1} = 4.00g$; $S = 10.27mV/g$
	PCB 353B68	$m_{acc2} = 4.55g$; $S = 108.60mV/g$

The tests with this PID were conducted in order to evaluate the following parameters: gap clearance L, particle size and particle mass. For each parameter, the dissipation at each acceleration in a desired range was also tested.

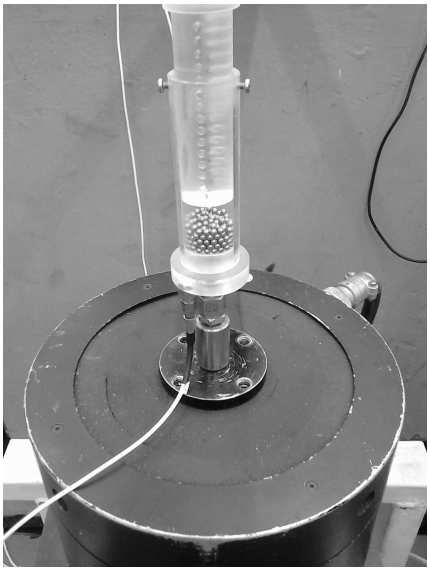

Figure 3.16: PID directly attached to a shaker. The accelerometer and the force sensor are attached to the PID's base.

3.2.2.1 Varying the normalized acceleration

Figure 3.17 shows the DPE for $26.31g$ (approximate 233 particles) of $3mm$ steel particles at $f = 70Hz$, $L = 12mm$. One can observe that an optimal acceleration is also obtained. These results clearly corroborates with the previous results obtained with PIDs of first generation. This indicates that the behavior observed is independent of the sample and the presence of an optimum condition of dissipation is intrinsic to the damper. Curves for a set of frequencies are found in Figures 3.18 and 3.19.

3.2.2.2 Varying the gap clearance

From now on, the curves depicted in Figures 3.17 and 3.18 are represented by their peak location. Three gap clearances were selected, namely $0.002m$, $0.012m$, and $0.022m$. By analyzing the gap clearance, one can find the curves plotted in Figures 3.20, 3.21, and 3.22. Figure 3.20 shows the peak *locus* of the DPE curve as a function of the excitation frequency. Figure 3.21 depicts the peak *locus* as a function of the normalized acceleration. Finally, Figure 3.22 shows the location of the peak acceleration in terms of the tested frequencies.

Consider Figure 3.20. For the three gap clearances analyzed, they have barely the

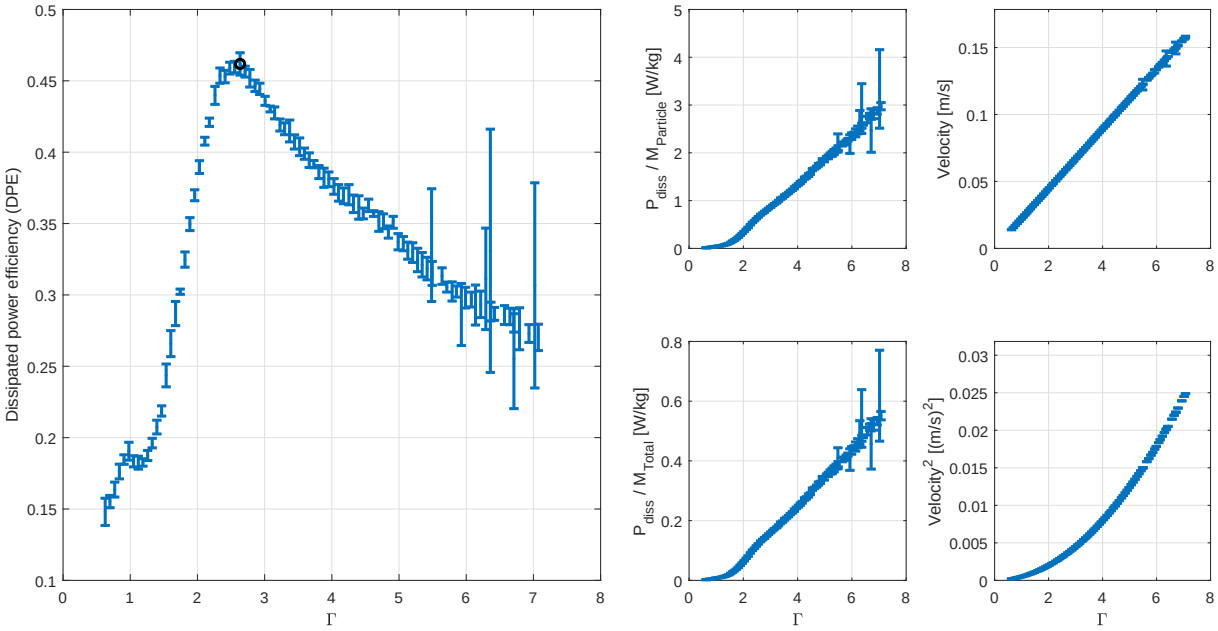

Figure 3.17: Dissipated power efficiency curve at $70Hz$.

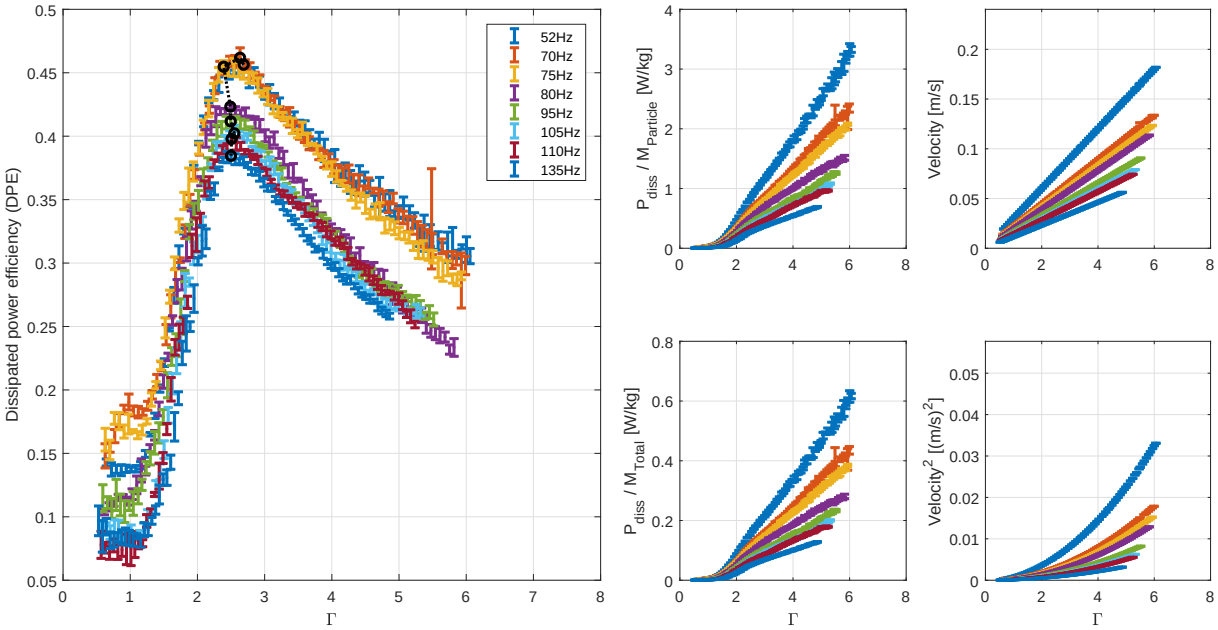

Figure 3.18: Dissipated power efficiency for $52Hz$, $70Hz$, $75Hz$, $80Hz$, $95Hz$, $105Hz$, $110Hz$, $135Hz$.

same level of dissipation. It was verified that, for gap clearance of $L = 2mm$, a double impact condition is achieved for $f = 52Hz$, which implies that the dissipation level at this specific frequency is higher than at the others. Moreover, when the particle hit the ceiling of the cavity, another peak is formed at a higher acceleration. This is clearly show in Figures 3.21 to 3.23. As the particles do not hit the ceiling for other frequencies, the dissipation and peak location are almost the same for the whole range. The little changes

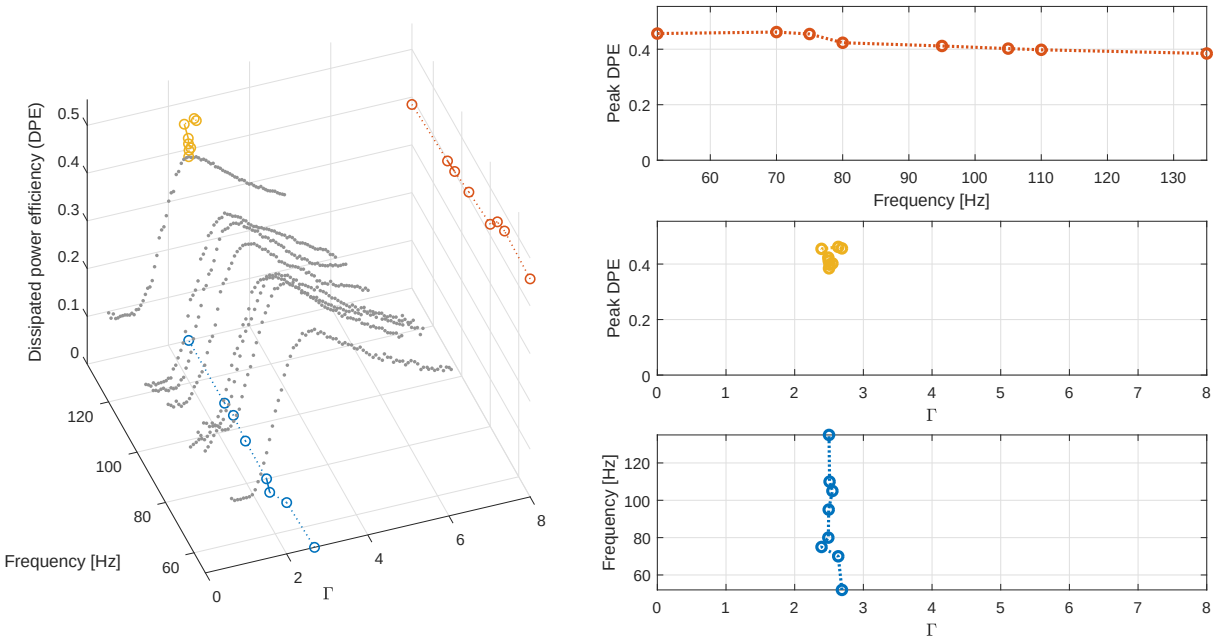

Figure 3.19: Dissipated power efficiency for $52Hz$, $70Hz$, $75Hz$, $80Hz$, $95Hz$, $105Hz$, $110Hz$, $135Hz$.

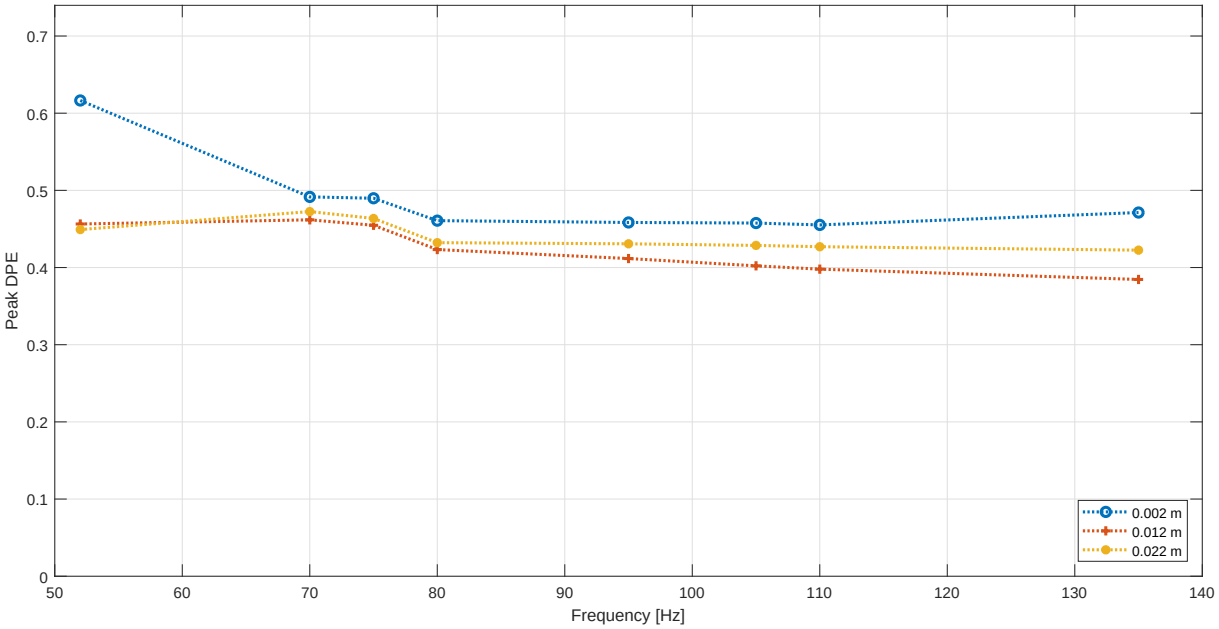

Figure 3.20: Gap clearance analysis: Peak DPE as a function of Frequency.

in the peak DPE, although very close in terms of amplitude, could be attributed to the cushioning effect of the air film above the particle bed trapped inside the cavity. A deeper investigation has to be conducted to validate this hypothesis (by allowing the pressure inside the cavity to equal the external pressure).

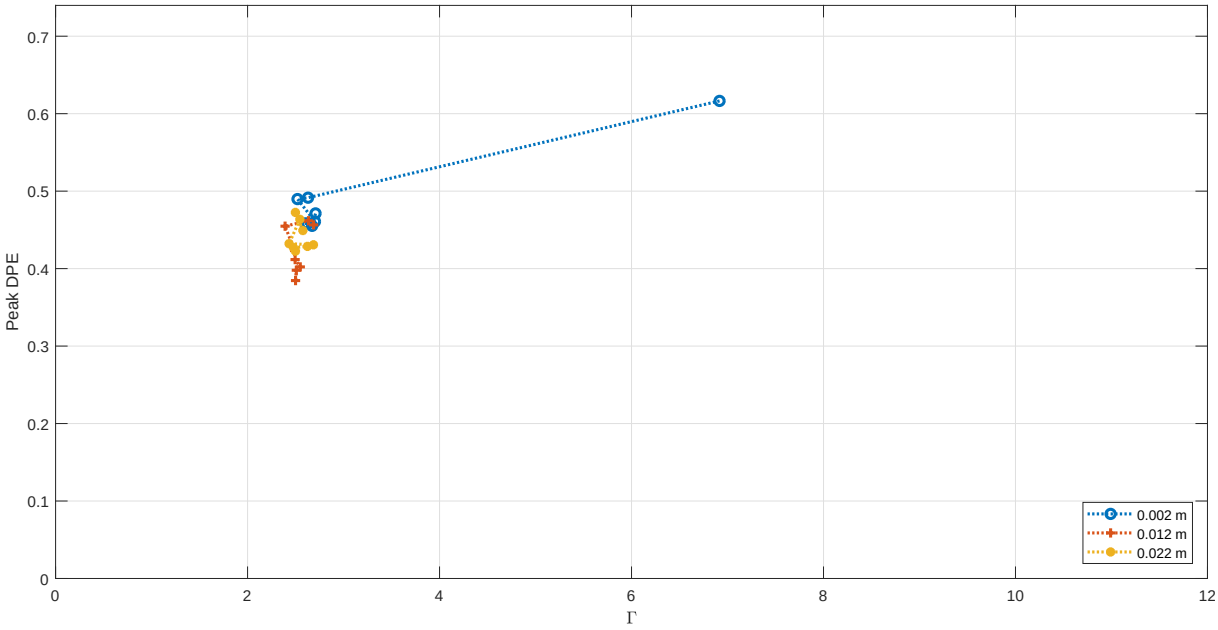

Figure 3.21: Gap clearance analysis: Peak DPE as a function of Γ.

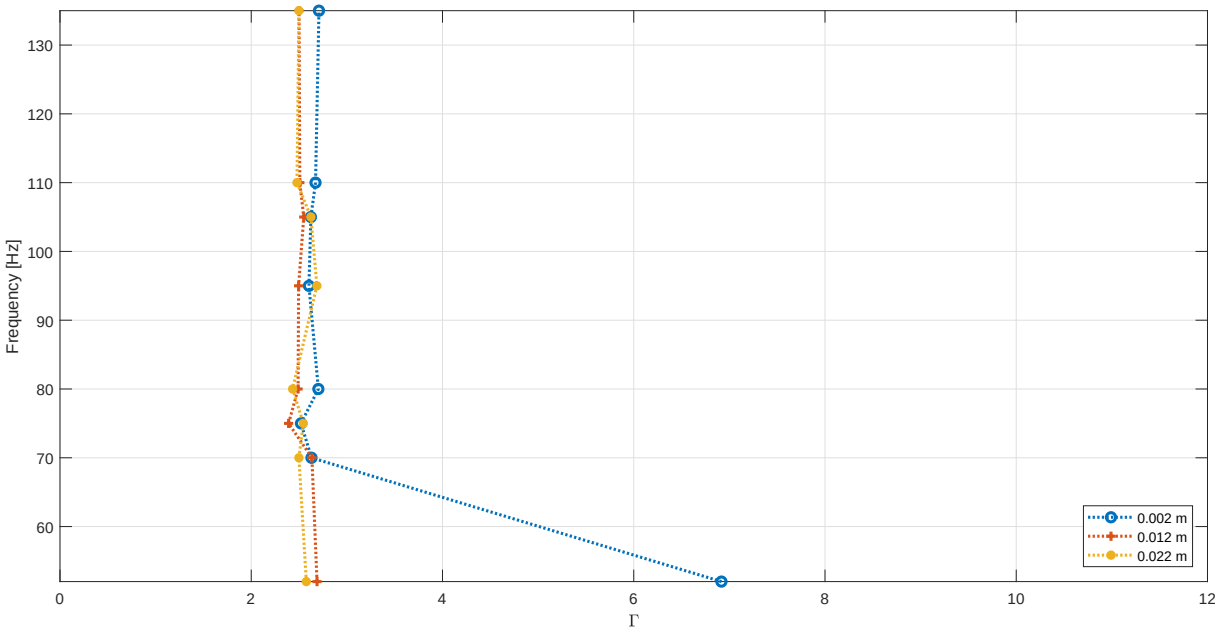

Figure 3.22: Gap clearance analysis: Peak DPE location plotted as a function of excitation frequency and Γ.

3.2.2.3 Varying the particle size

The influence of particle size in PID's behavior was tested in this Section. Three different diameters were chosen: $3mm$, $4mm$, and $5mm$.

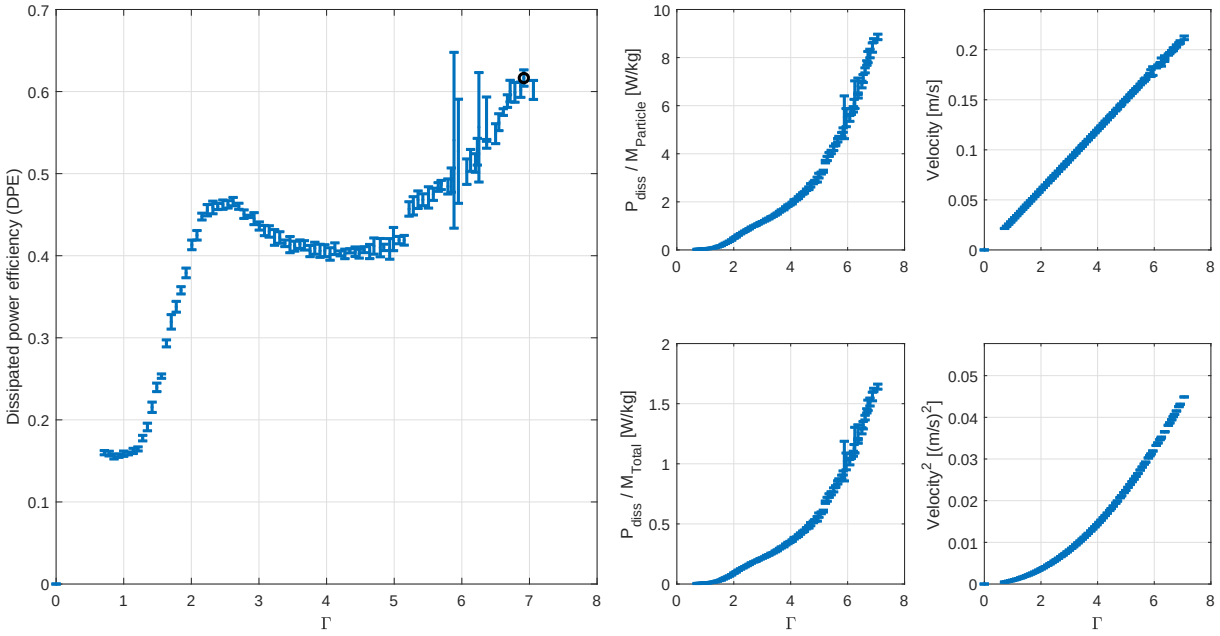

Figure 3.23: Dissipated power efficiency curve at $52Hz$. Higher accelerations were not tested so the right location of this second peak is inconclusive for this sample

For particles of different sizes, Figures 3.24, 3.25, and 3.26 show that smaller particles dissipate slightly more energy than bigger particles. Again, the particles with diameter of $4mm$ (100 particles) and $5mm$ (52 particles) have their optimal dissipation at lower accelerations. The jump observed $110Hz$ for $4mm$ particles could be attributed to variations inherent to the behavior of granular material, specially when the number of particles is reduced.

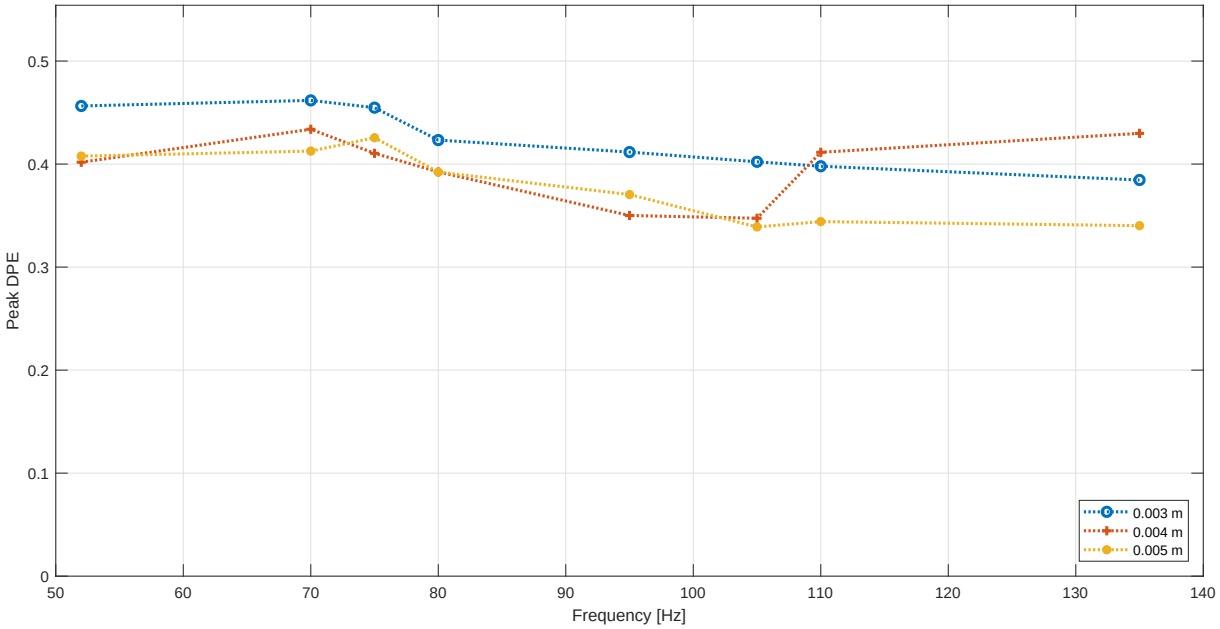

Figure 3.24: Particle size analysis: Peak DPE as a function of Frequency.

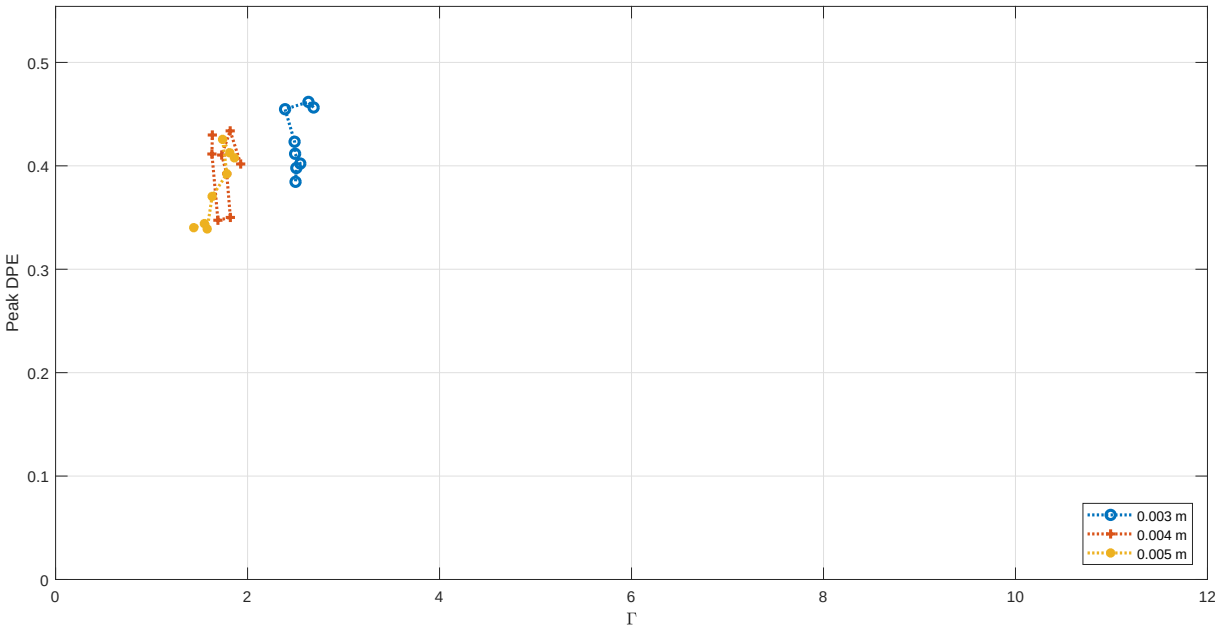

Figure 3.25: Particle size analysis: Peak DPE as a function of Γ.

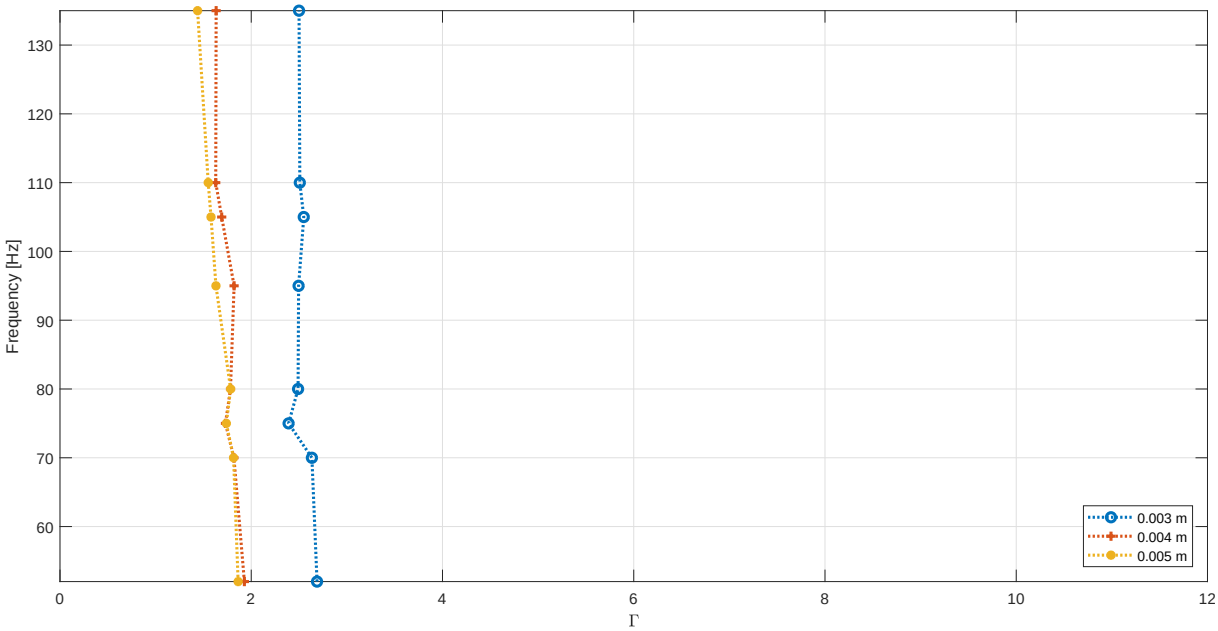

Figure 3.26: Particle size analysis: Peak DPE location plotted as a function of excitation frequency and Γ.

3.2.2.4 Varying the particle mass

By characterizing the PID dissipation through the dissipated power efficiency and analyzing the system when the particle mass is changed, one can observe an odd phenomenon. The DPE for a heavier particle bed is lower than the DPE for the lighter ones

(Figure 3.27). Yang *et al.* (2004) showed that the DPE is not sensitive to mass variation, with different masses appearing to have the same dissipation. That is not expected as the particle mass is reported to be directly proportional to the dissipation (Fowler *et al.*, 2001). By inspecting the DPE formula (Equation 2.7), if the particle mass is increased, the denominator is consequently increased and the DPE tends to reduce. Moreover, although more particles would result in more dissipation, due to the difficulties faced by particles to move in a more dense particle bed, the numerator is not increased proportionally. That would justify why, in the present tests, such behavior was demonstrated.

That observation about particle mass is intriguing and, although more masses were not tested, it endorses the need to proceed with caution concerning the dissipation estimator when performing a parametric analysis of a PID.

Particle bed with different mass may have their peak location precisely at the same acceleration, as shown in Figures 3.28 and 3.29.

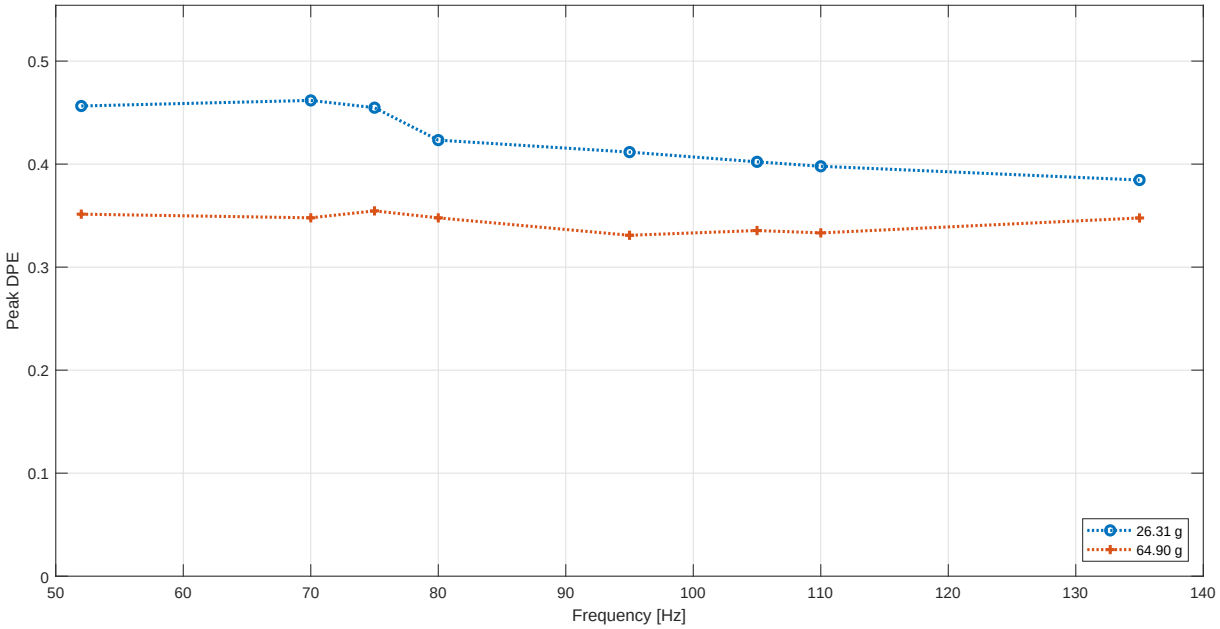

Figure 3.27: Particle mass analysis: Peak DPE as a function of Frequency.

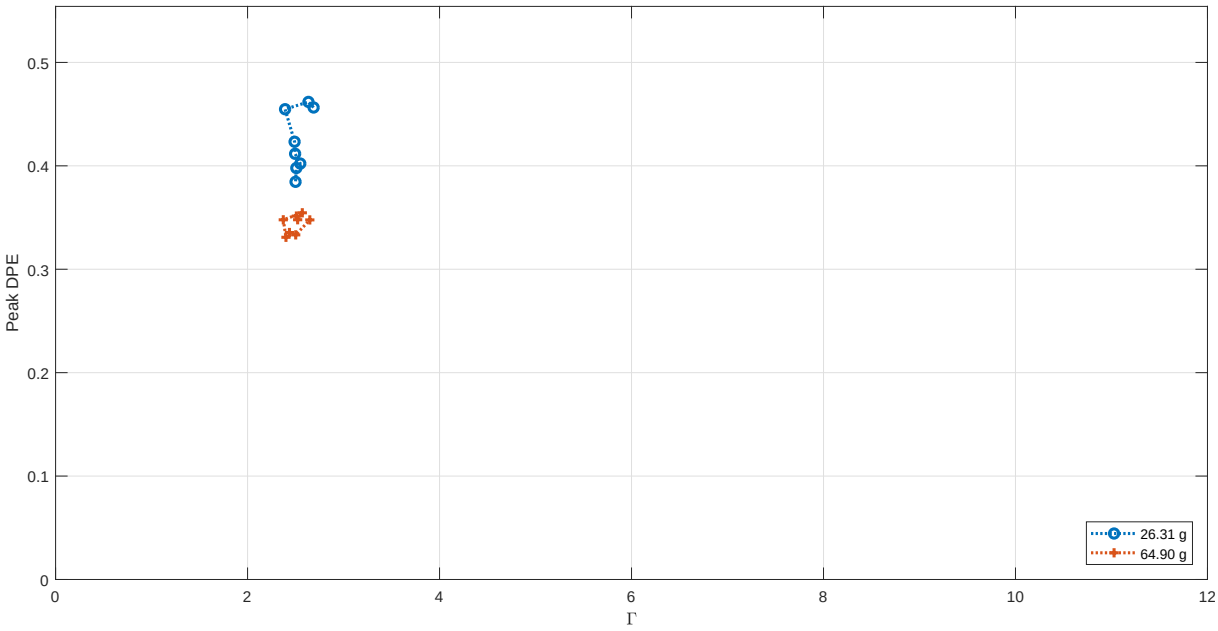

Figure 3.28: Particle mass analysis: Peak DPE as a function of Γ.

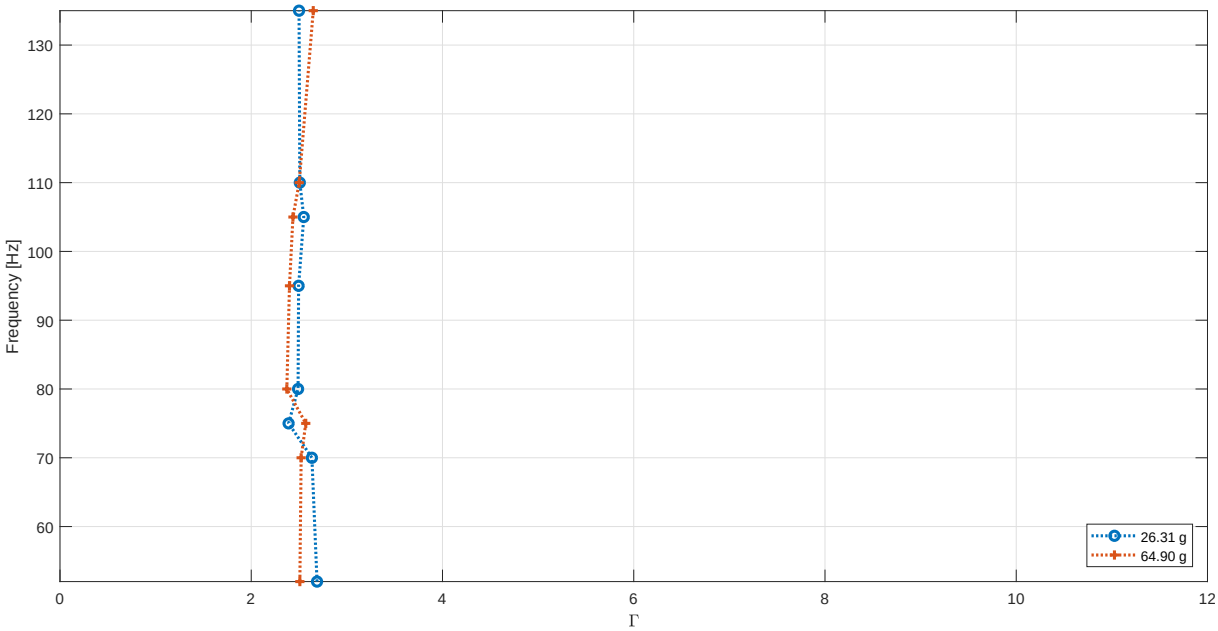

Figure 3.29: Particle size analysis: Peak DPE location plotted as a function of excitation frequency and Γ.

3.3 Re-examining the work of Zhang *et al.* (2016a,b): PID on a cantilever beam

The studies conducted by Zhang *et al.* (2016a,b) are another example on how the researchers are devoting so much efforts to understand a PID behavior. In Zhang *et al.*

(2016b), the authors established a comparison with two different estimators of PID's dissipation but did not explored their trends when varying the design parameters. Moreover, they established a correlation with tests conducted in two different setups but their results and conclusions seemed to be not extrapolated to structures other than the cantilever beam they used. Their work is re-examined in the following sections.

3.3.1 Varying the normalized acceleration

The same PID used in Section 3.2 was placed at the cantilever beam's free end. This beam is identified as Beam #1 (please refer to Table 3.3 for beams' dimensions). An electrodynamic shaker excited the structure also at the free end so that the drive point accelerances (FRF) could be estimated. The experimental setup is illustrated in Figures 3.30 to 3.32.

Table 3.3: Dimensions of the beams used in the present Section.

Beam	Length [mm]	Width [mm]	Thickness [mm]
Beam #1	220.0	31.90	6.450
Beam #2	273.5	38.30	6.600

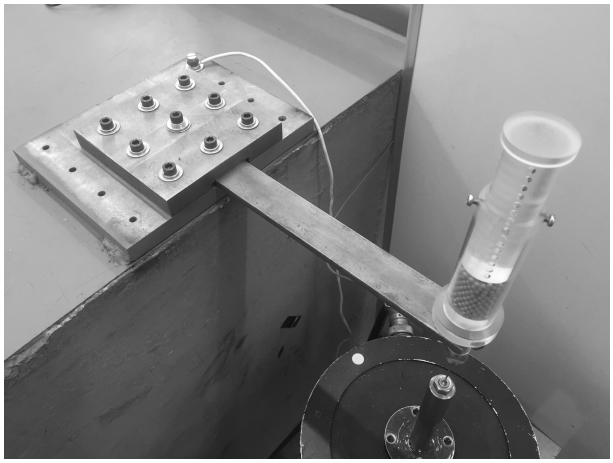

Figure 3.30: PID attached to the cantilever beam.

Each FRF was obtained using a closed-loop stepped sine routine implemented in LabVIEW to ensure the same acceleration response at each frequency. These frequency response functions were reconstructed using a modal identification method called rational fraction polynomial method (RFP) (Maia, 1997) and assuming the system is SDOF. The LabVIEW program searches for the desired acceleration, inputted by the user, by

Figure 3.31: Detailed image of force sensor and the accelerometer used in the test with the PID on a cantilever beam.

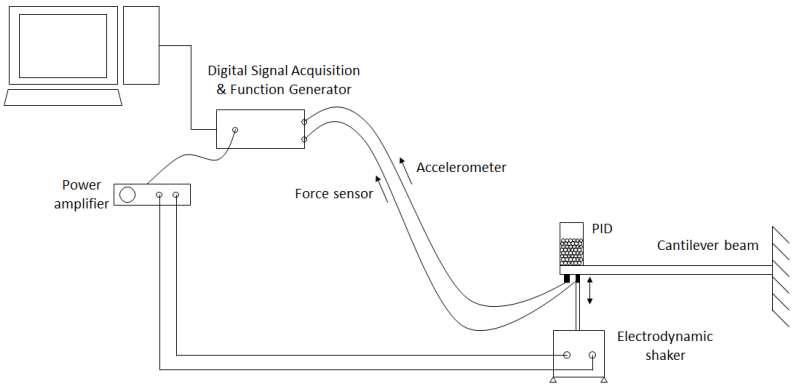

Figure 3.32: Sketch of the experimental setup for the comparison of dissipation indicators.

changing the shaker voltage. The desired acceleration is extracted from the signal by filtering the fundamental component and obtaining its amplitude. Once the acceleration is found, amplitudes and phases of both acceleration and force signals are saved, FRF is calculated, and the excitation frequency is updated. The flowchart of the routine is in Figure 3.33. The frequency step used was $0.1Hz$.

Using $64.90g$ of $3mm$ diameter steel particles, gap clearance $L = 28.5mm$, cavity height $H = 60mm$, we obtained the FRFs. Reconstructed FRFs are depicted in Figure 3.34. The curve named *No Sample* is the FRF of the cantilever beam itself and the curve *Empty Sample* is related to the system *beam + empty PID*. Each curve corresponds to a constant normalized acceleration Γ, given by Equation 2.1.

For the sake of clarity, the resonant peak *locus* of each FRF in Figure 3.34 is shown in Figure 3.35. This representation is used in subsequent figures throughout this section,

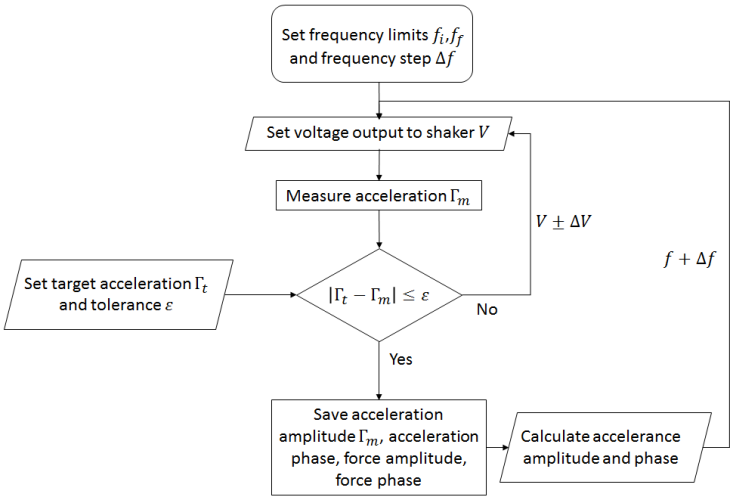

Figure 3.33: Flowchart of LabVIEW routine.

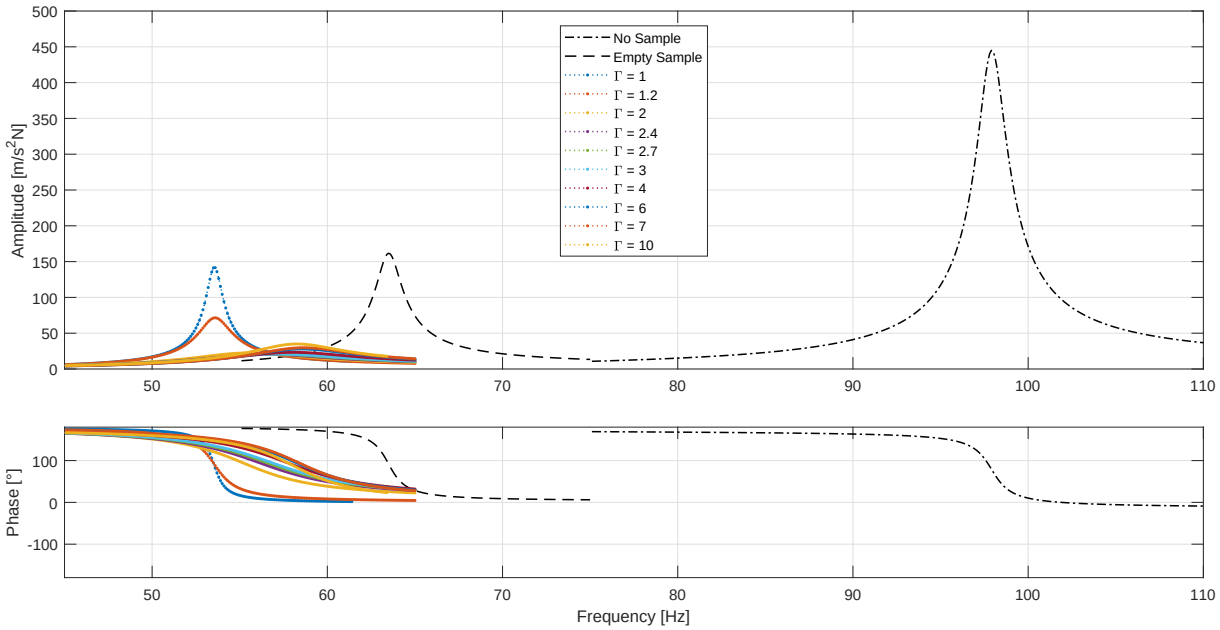

Figure 3.34: Beam #1 first-order drive point accelerances obtained for different normalized response accelerations.

with phase information being omitted. It is important to note that the lines connecting each resonant peak do not represent dependency, being used just to illustrate the order in which each peak occurs.

In Figure 3.35, one observes that, as the acceleration increases, a minimum amplitude condition is achieved. According to Zhang *et al.* (2016b), for accelerations higher than the optimal, the peak should tend to the condition of empty sample (Figure 2.6). We observed in our case that the resonant peak tend to a frequency that is 90% of the natural frequency for empty condition. This can be attributed to the number of particles

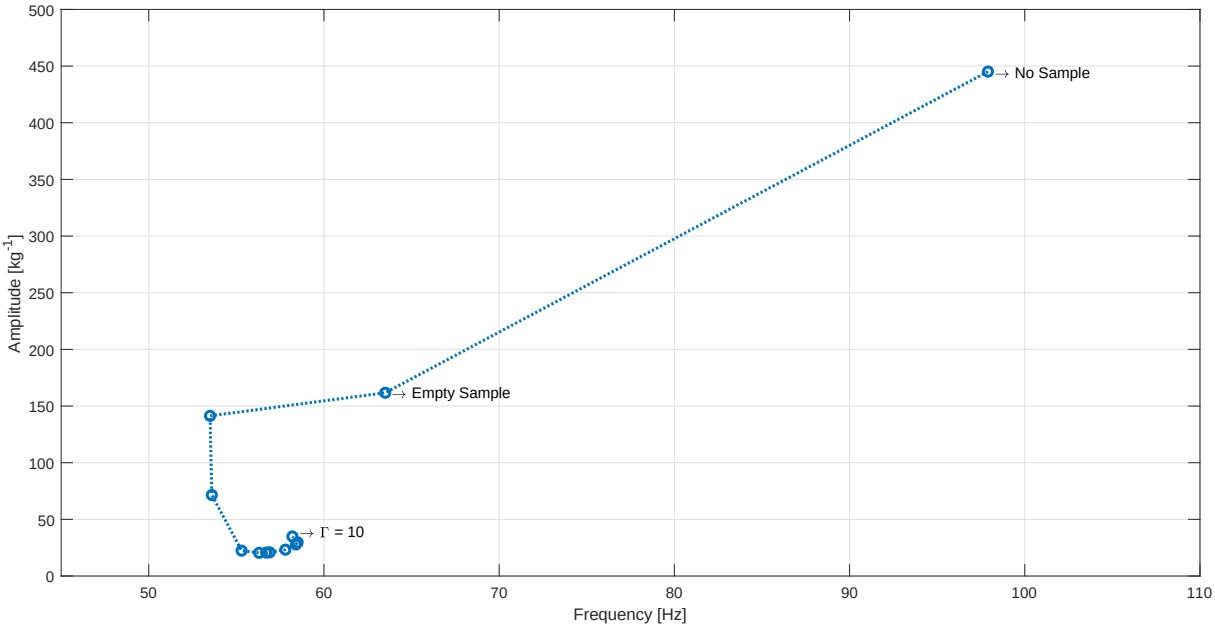

Figure 3.35: Resonant peak *locus* of the FRFs shown in Figure 3.34.

inside the cavity and the difficulty for particles to overcome the load of the upper layers, which impair their motion. This directly impacts the effective mass of the system which cannot reach the empty sample condition. This effect is more evident in Figure 3.36, left, where the natural frequency tends to stabilize at a value other than the natural frequency of the empty sample system. In Figure 3.36, right, one observes that, for this specific case, the higher modal damping ratio occurs at $\Gamma = 2.7$.

It is worth noting the similarity of Figure 3.36, right, with the curves obtained for DPE (Section 3.2), with the peak dissipation happening at the same acceleration (Please refer to Figures 3.28 and 3.29 for comparison).

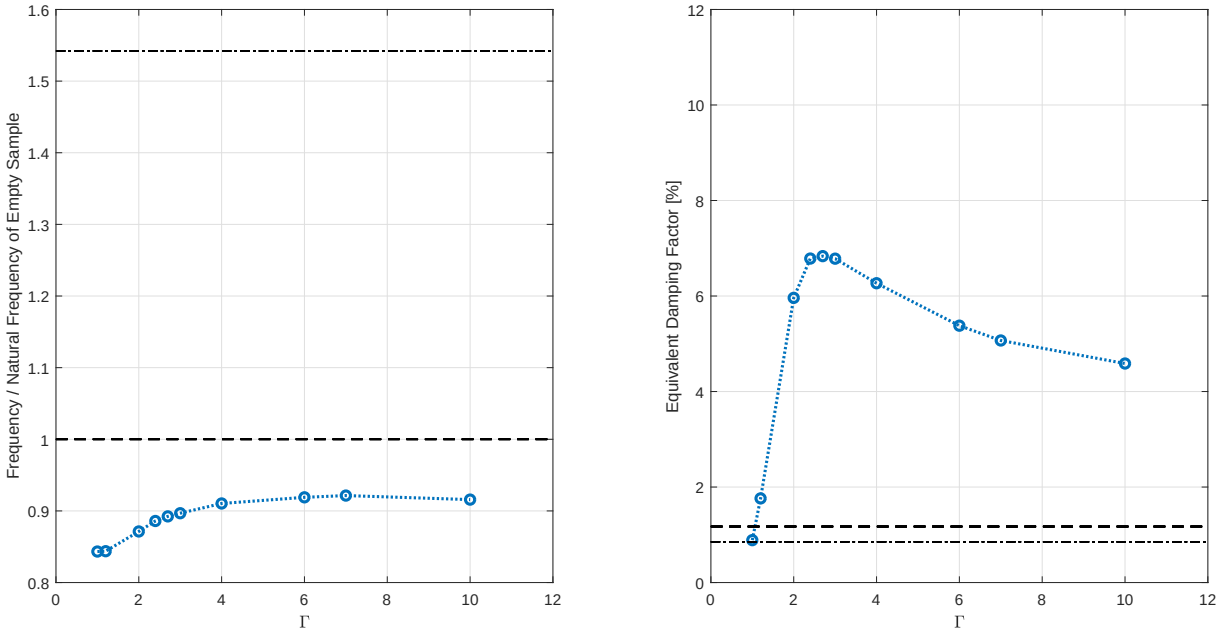

Figure 3.36: Ratio between natural frequency of the system and natural frequency of empty sample as a function of normalized acceleration Γ (*left*); Equivalent viscous modal damping ratio as a function of normalized acceleration Γ (*right*). Dash-dot line corresponds to the *No Sample* condition; dashed line is related to *Empty Sample*.

3.3.2 Varying the beam

The same PID was then attached to a less stiff beam, here named Beam #2. One can observe in Figure 3.37 that an optimal acceleration is also obtained and the natural frequency at this optimal condition is lower than the one obtained with the first beam. This phenomenon should be somehow expected. We can infer, therefore, that the natural frequency at the optimal condition is not a characteristic of the PID itself. Rather, it is a property of the system "beam + PID". As the acceleration is kept constant throughout the analysis, the velocity in which particles are set into motion is higher for Beam #2 due to low frequency range. This implies that particles are in the air for a longer period than when in Beam #1. That would explain why the peak tends to be closer to empty condition in Beam #2 than in Beam #1 (Figure 3.38).

As pointed out in Chapter 2, Zhang *et al.* (2016b) claim that the natural frequency at the optimal condition is linked to a phase diagram of particle motion. In such diagram, several particle motion modes are identified by varying the normalized acceleration and the excitation frequency. The relationship between natural frequency and motion mode lead the authors in Zhang *et al.* (2016b) to conclude that the *granular Leidenfrost effect* (Eshuis *et al.*, 2005, 2007) is occurring at the optimal condition. Although the phase diagram does

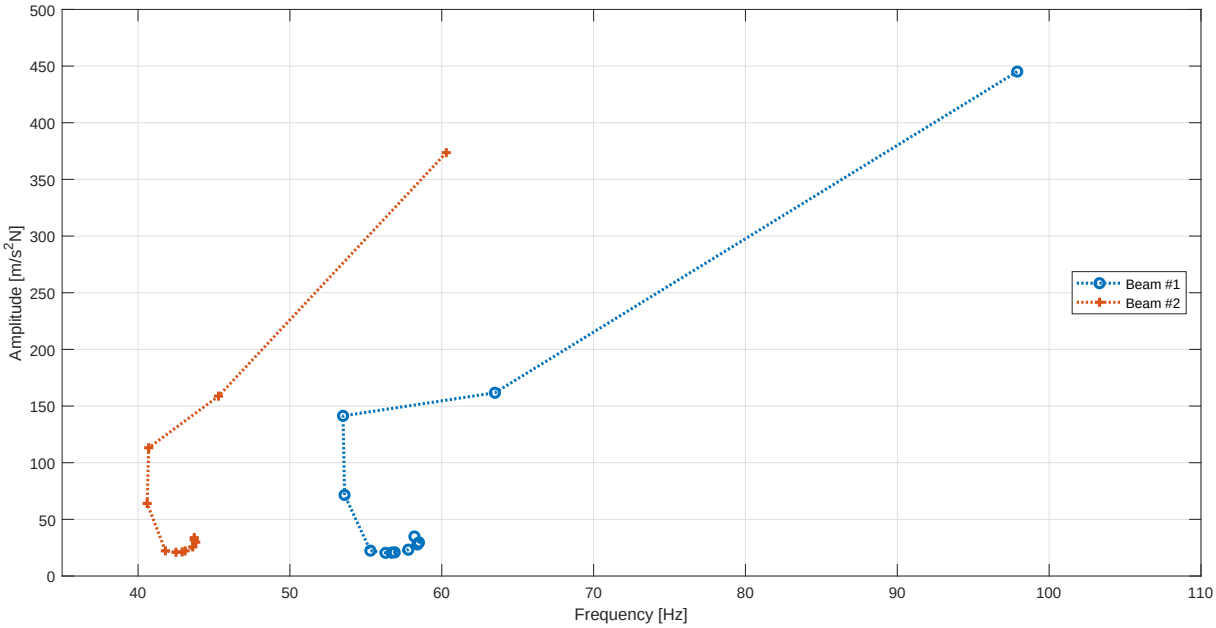

Figure 3.37: Resonant peak *locus* of the FRFs for two different cantilever beams.

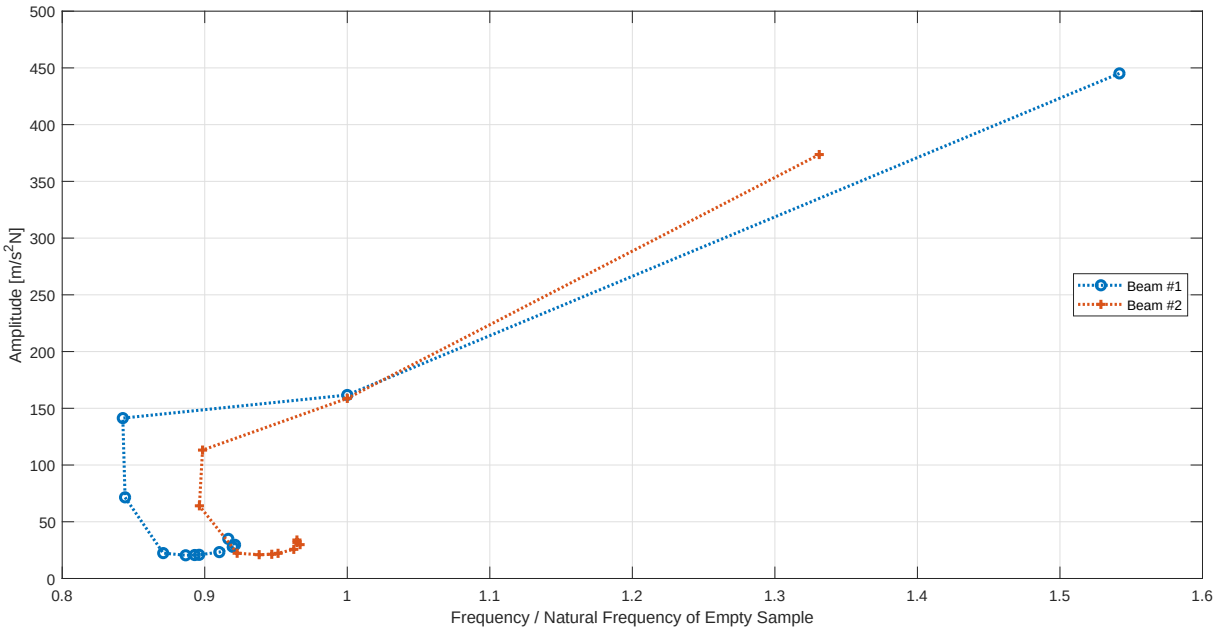

Figure 3.38: Resonant peak *locus* of the FRFs as a function of normalized frequency.

show the Leidenfrost effect at the specific pair of acceleration and frequency, the fact that the same PID behaves differently depending on the beam to which it is attached shows that natural frequency should not be used to infer about the optimal motion mode. In addition, as the curves depicted in Figure 3.38 behaves somehow equivalently (with a difference for every acceleration of approximately 5%), it suggests that the phase diagram should also be normalized.

3.3.3 Varying the gap clearance

Continuing the analysis, five gap clearances were tested using Beam #2. Due to height limitations of our PID, it was used $26.31g$ of the same previous particles. Lets look at the equivalent modal damping ratio obtained for the gap clearances in Figure 3.39. When the gap clearance is wide enough so that no particle hits the ceiling for any tested frequency (double impact), the modal damping ratio behaves as it was presented in Figure 3.36 for the Beam #1 (the dissipation is also lower due to less mass). However, for a narrower gap clearance, if the acceleration is high enough so that the particles do hit the ceiling, then another peak is formed, as it is observed for $L = 2mm$ in Figure 3.39. In addition, the natural frequency tends to move away from the natural frequency of the system with the empty cavity. This characteristic is particularly evident when turning the attention to the resonant peak *locus* inset plot in Figure 3.40. This diverse behavior was also presented for DPE when in double impact condition (Figure 3.23).

The presence of a new peak in the modal damping ratio, higher than the first one, opens a new possibility where a particle impact damper can be *tuned* in the sense of the acceleration levels.

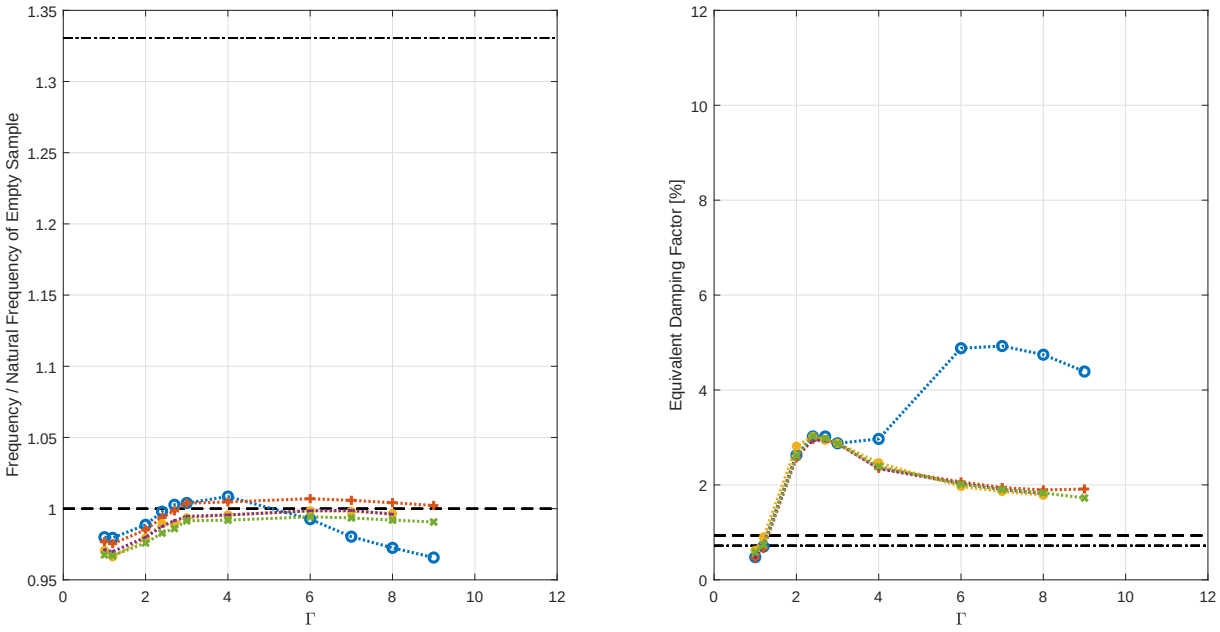

Figure 3.39: Natural frequencies *(left)* and equivalent viscous modal damping ratio for five gap clearances *(right)*. $-$o$-$ $L = 2mm$, $-+-$ $L = 7mm$, $-*-$ $L = 12mm$, $-.-$ $L = 17mm$, $-$x$-$ $L = 22mm$

By drawing two imaginary vertical lines parallel to the y-axis of Figure 3.39, right, at $\Gamma = 2$ and $\Gamma = 7$, one can verify that the FRFs peaks do not follow the same trend

as that observed in Zhang *et al.* (2016b). Figures 3.41 and 3.42 depicts the resonant peak *locus* of the FRFs at these two accelerations. At $\Gamma = 2$ the peaks are roughly the same in terms of frequency and amplitude, a behavior that diverge from the observations made by Zhang *et al.* (2016b) when the acceleration is varied at a constant gap clearance. On the other hand, at $\Gamma = 7$, the peak relative to gap clearance $L = 2mm$ is located far from the cluster of peaks relative to other gap clearances. It is worth noting that in Zhang *et al.* (2016b) nothing is mentioned whether the particles hit the ceiling or not. Our results show that this is an important information to be reported. With the results presented here, it was not possible to assess whether an optimal gap clearance occurs in a vibrated vertical PID because of the constructive aspect of the PID. However, there is an indication that, if it does occur, so it happens in a very narrow range of gap clearances. This again is not in consonance with that reported by Zhang *et al.* (2016b).

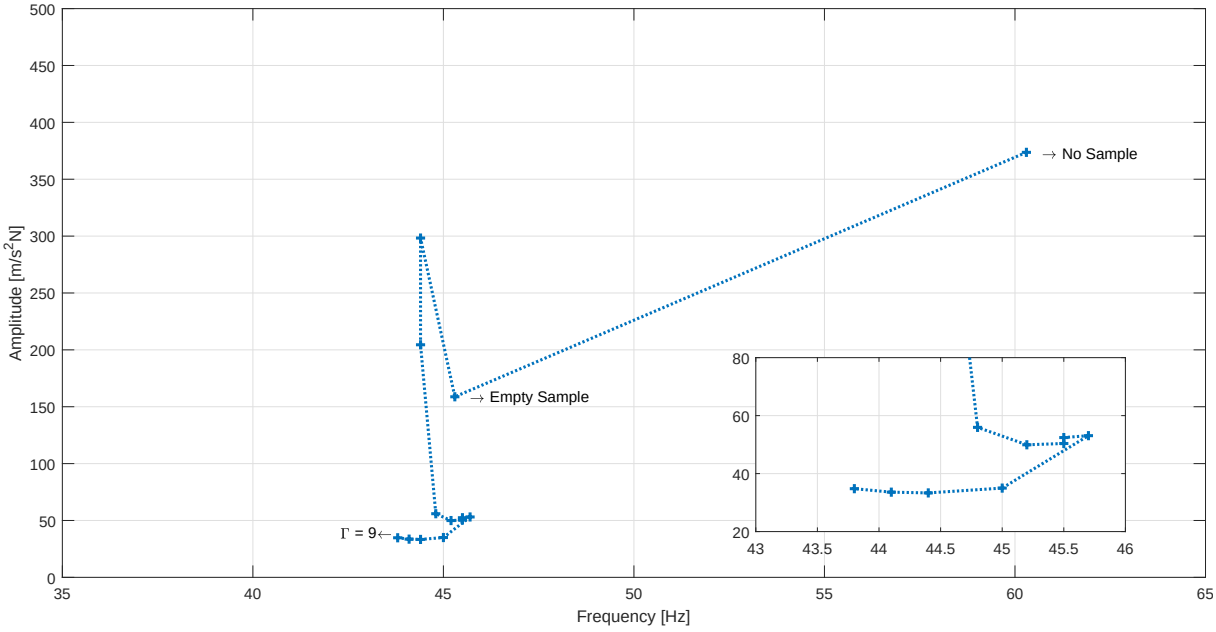

Figure 3.40: Resonant peak *locus* for $L = 2mm$.

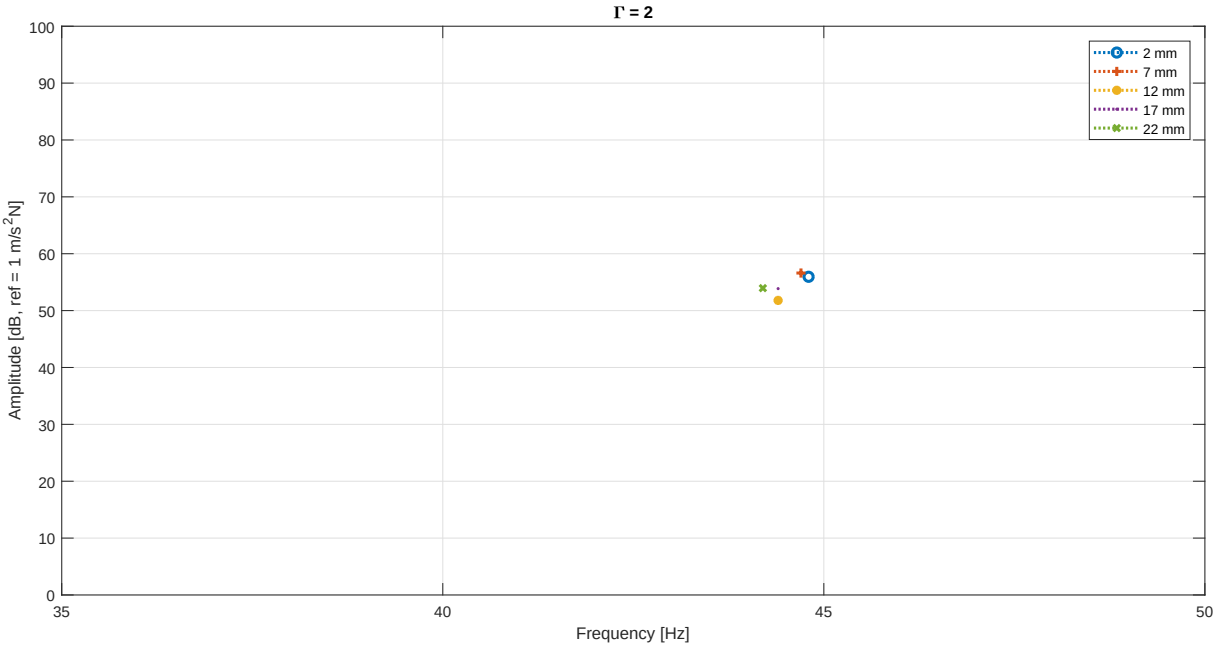

Figure 3.41: Resonant peak *locus* for $\Gamma = 2$ (please refer to Figure 3.39, left). The peaks are roughly at the same location indicating the PID behaves the same way when the particle do not touch the ceiling.

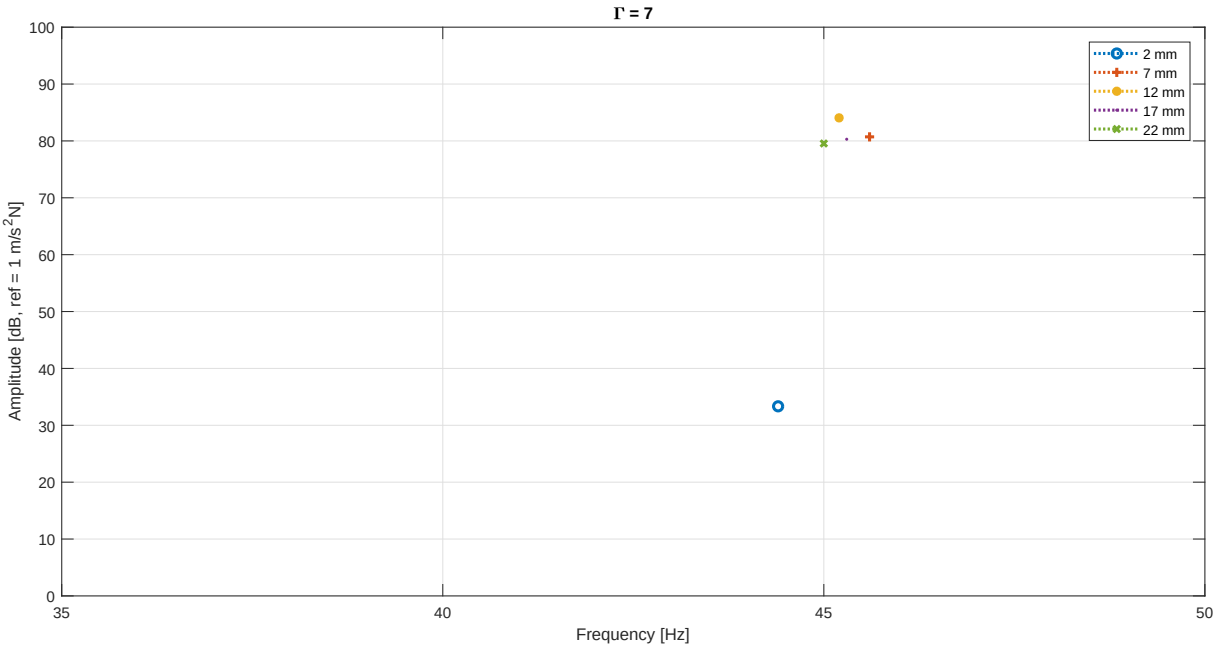

Figure 3.42: Resonant peak *locus* for $\Gamma = 7$ (please refer to Figure 3.39, left). In this case, all the peaks are again roughly except the one corresponding the gap clearance $L = 2mm$ which has a fairly lower amplitude than the others.

3.3.4 Varying the particle size

To verify whether the behavior presented up to this moment is valid, a PID with three different particle sizes was tested. For this condition the particle mass was kept constant (having the number of particles necessarily changed). Figure 3.43 shows how they behave. It is interesting to note that for particle diameters $4mm$ and $5mm$ the first peak occurs at an acceleration slightly lower than the optimal acceleration for $3mm$ particles. For $5mm$ particles, the second peak tend to occur before that for other sizes. Again, this is attributed to the number of particles inside the cavity—for the same mass, less particles of bigger size are required, which in turn means that particles inside the cavity are more prone to be set into motion at low accelerations than for smaller particles.

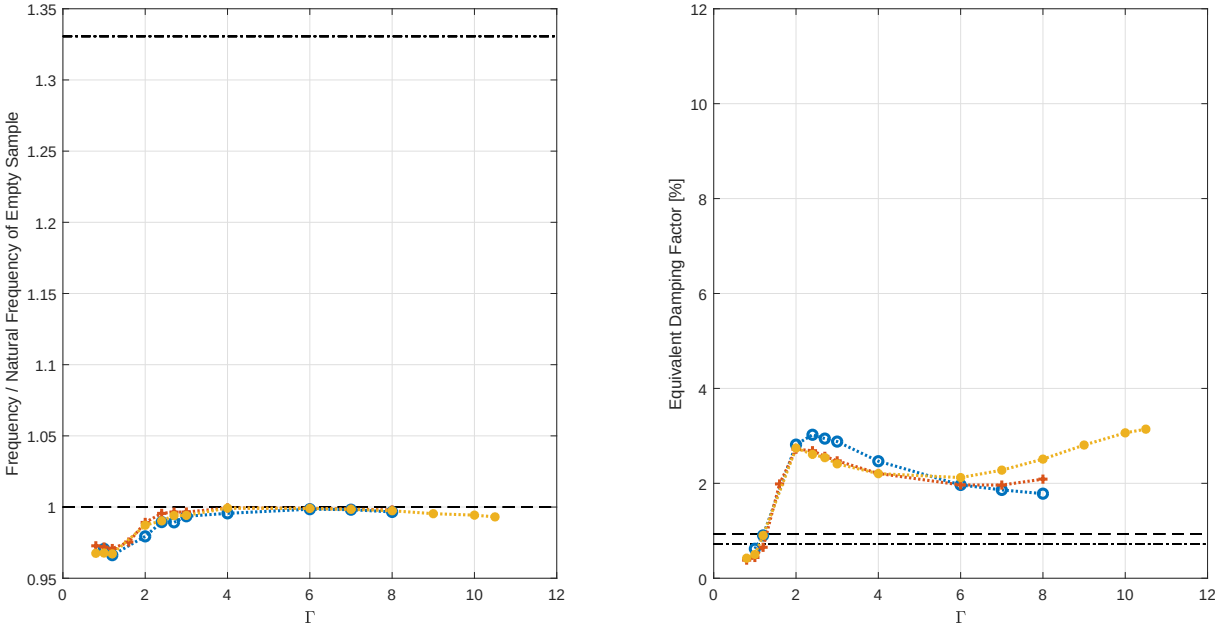

Figure 3.43: Natural frequencies *(left)* and equivalent viscous modal damping ratio for three particle sizes. $-$o$-$ $3mm$, $-+-$ $4mm$, $-*-$ $5mm$

Figure 3.44 depicts how the $5mm$ particles behave in terms of the resonant peak *locus*. Again, as the double impact condition is achieved, the resonant peak tend to diverge from the peak of empty sample condition.

One can note that, for $5mm$ particles, the second peak was not clear in the DPE analysis.

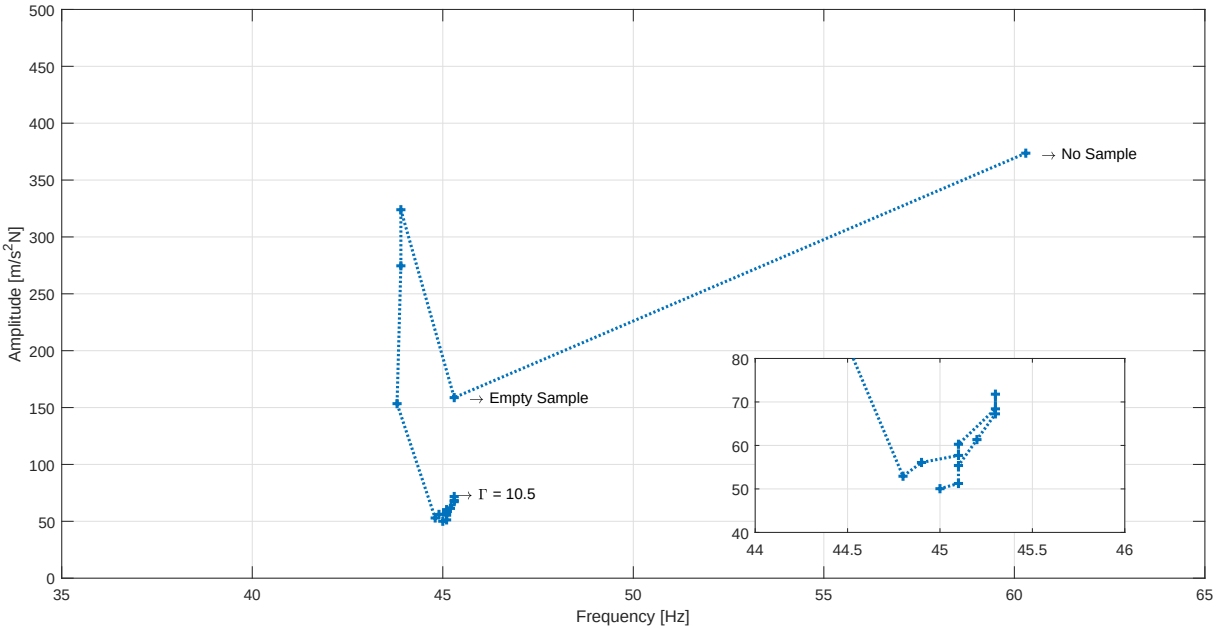

Figure 3.44: Resonant peak *locus* for particle size $d = 5mm$.

3.3.5 Varying the particle mass

As analyzed in Section 3.2, the particle bed mass were also investigated by Zhang *et al.* (2016b). Figure 3.45 depicts how the system behaved when particle mass was changed.

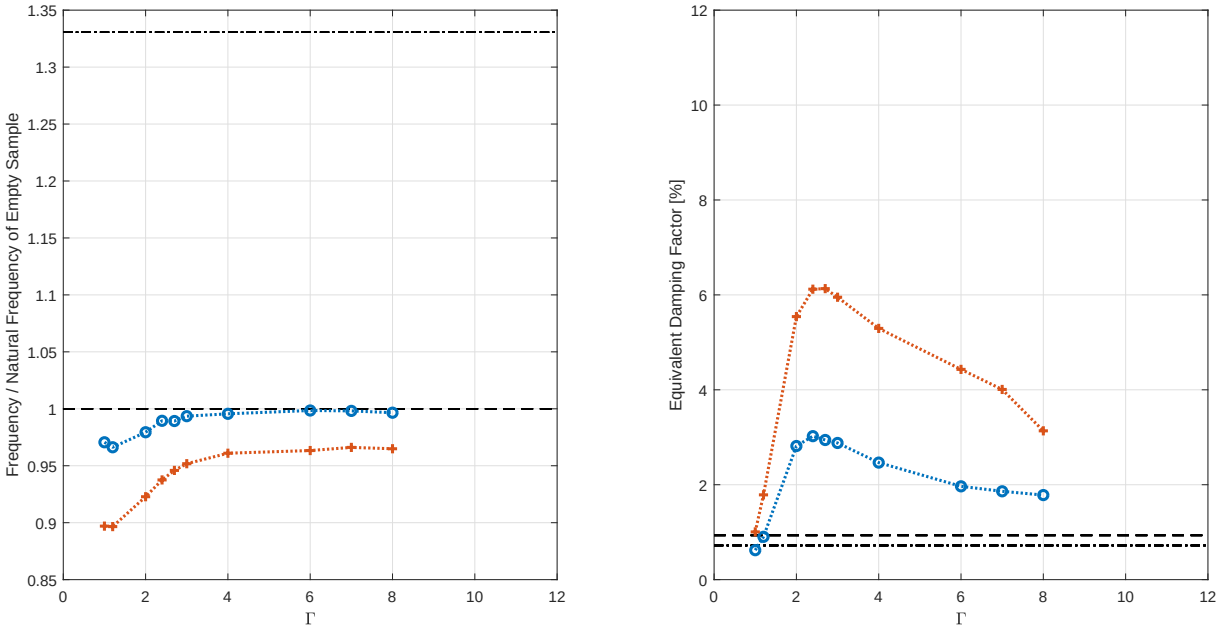

Figure 3.45: Natural frequencies *(left)* and equivalent viscous modal damping ratio for two particle masses.

One observes that, for higher mass, again the natural frequency was not precisely the same of the empty cavity due to the reason aforementioned. Interestingly, the damping provided by higher mass is also higher, which endorses what the literature has already reported. In this case, an increase of 2.46 times in mass has doubled the damping factor.

3.3.6 Conclusions of the comparative analysis

One can conclude from the comparative analysis that the two chosen approaches to estimate the damping provided by a particle impact damper have some similitudes but may also diverge, as in the case of particle mass. Experimental observations, although still limited, suggests that both approaches could be used as complementary information when choosing the right PID for an specific application.

Based on what was reported in this chapter, a guideline to the design of a single PID can be outlined:

1. The appropriate cavity should be selected so that the particles are able to hit the ceiling in most of the operation conditions. That would require an evaluation of the acceleration levels at the PID's attachment point;
2. It appears to be appropriate also to design a PID that accommodates more than one cavity so that more than one particle size can be chosen. Consequently, this will make a PID to work optimally in a broader range of accelerations (robust solution);
3. As more mass appear to dissipate more, one should adopt the approaches analyzed in this Chapter in conjunction with other criteria (mass target, availability, etc.) to obtain the desired dissipation.

In the next chapter (Chapter 4) is reported a first attempt to use an array of PID to control the vibration of an extended structure.

4 PID under impact-induced excitation

4.1 Overview

In this chapter, the experimental evaluation of PIDs under impact-induced excitation will be presented. The proposal of the experiments described in the following is to analyze the dissipation provided by PIDs in two cases: one refers to an application of concept – a motivational study conducted to assess the PID's effectiveness –; later in this Chapter, an investigation is conducted to understand the dynamic behavior of a cantilever beam subjected to repetitive impulses and treated with a particle impact damper.

4.2 Application of concept

Recalling the Motivation (Section 1.2) of this work, it is proposed in this section the use of particle impact dampers for noise control on extended sheet metal structures subject to metal-working – impact-induced – operations. The concept is the use of extended, cellular arrays of PIDs, configured to be readily attached and removed from a workpiece. The results presented in this section were reported in de Melo *et al.* (2015).

One or more arrays of PIDs, each comprising 48 cells of PIDs (measuring $0.25m$ x $0.24m$), were attached to a representative aircraft panel in order to reduce its vibratory response when subjected to the successive impacts of a riveting gun. The following design parameters were investigated in terms of their effects on noise reduction:

1. Volumetric packing fraction of shot within the PID cells;
2. Position of the array or arrays relative to the excitation point;
3. Number of arrays.

The motivation for using a distributed array is because impact excitation induces the transient response of the structure in a broadband frequency range, which means

that several natural modes are being simultaneously excited. A distributed array can, therefore, spatially affect several modes at the same time. As particle impact dampers are already known for being robust with respect to temperature (Li and Tang, 2017), the use of an array of particle impact dampers is intended to be also a robust solution with respect to variations in the dynamic characteristics of the work piece and to variations in the disturbance frequency around those encountered in real operational conditions.

4.2.1 Experimental apparatus

An aluminum panel – a representative fuselage panel – was placed and clamped horizontally in a frame constructed with slotted hole strut channels[1] as shown in Figure 4.1. The representative panel had reinforcements made of transversal and longitudinal ribs as shown in Figure 4.2. The dimensions of the panel are found in Figure 4.3.

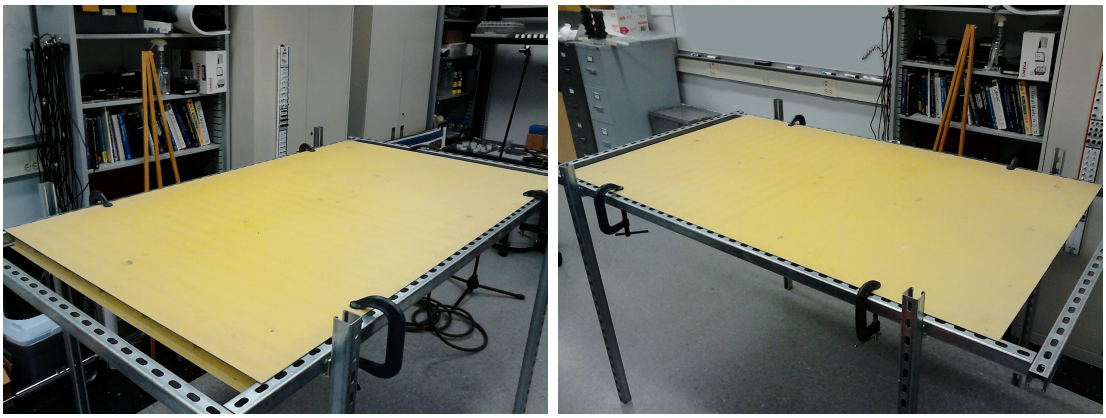

Figure 4.1: Representative fuselage panel placed and clamped horizontally in a frame constructed with slotted hole strut channels.

Using a PCB Accelerometer Y352C33, a PCB Impact hammer 086B01, and a NI USB-4431 Dynamic Signal Acquisition, the driving point accelerances of two points of interest were obtained. These points are also illustrated in Figure 4.3.

A Chicago Pneumatic 4X riveting gun (Figure 1.1) was used to excite the panel. The radiated noise was measured using a Larson-Davis model 824 Sound Lever Meter positioned at $1m$ above the plate. The complete experimental setup is illustrated in Figure 4.4.

The arrays of PIDs, shown in Figure 4.5, were fabricated with Ecoflex® Rubber

[1] in Portuguese, *perfilados perfurados de aço*

Figure 4.2: Detailed image of the reinforcements made of transversal and longitudinal ribs.

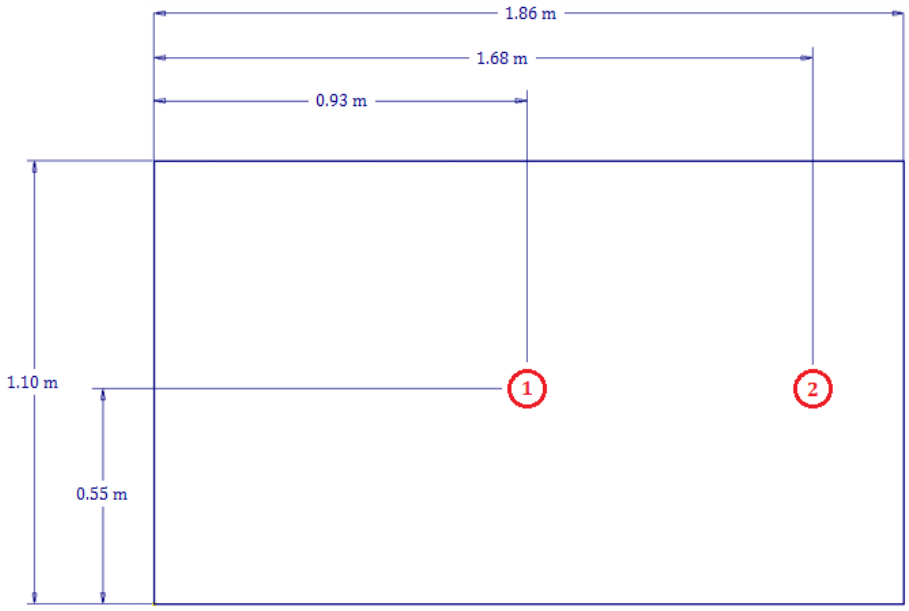

Figure 4.3: Dimensions of the panel and the points of interest.

poured into the steel mold depicted in Figure 4.6, left. After cured and removed from the mold (Figure 4.6, right), the rubber array was filled with Nickel-plated lead shots of 2.1mm nominal diameter, as exemplified in Figure 4.7. As the arrays must be easy-removable, it is proposed to place them over the fuselage in such a way that they held in position by either their own mass, and surface adhesion between the material and the skin.

For the FRF test, the accelerometer was placed on the underside of the test panel,

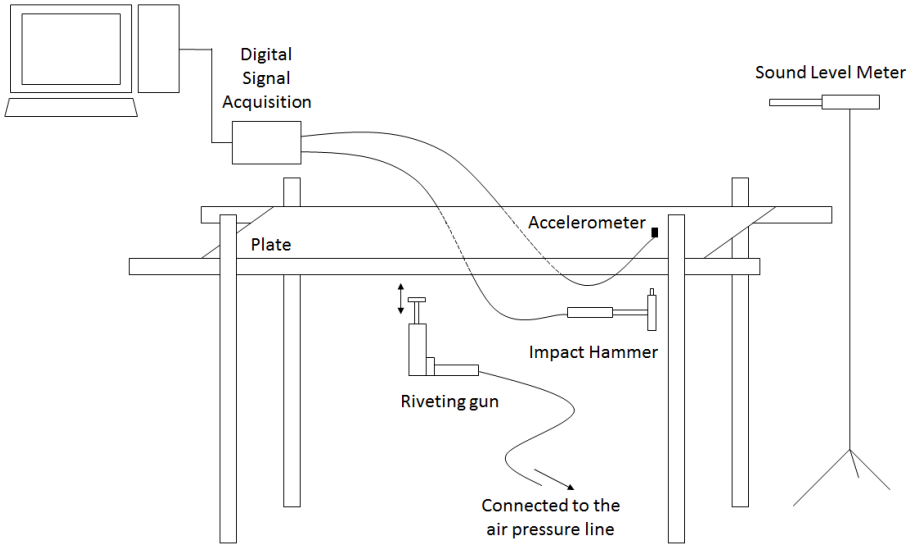

Figure 4.4: Schematic representation of the complete setup.

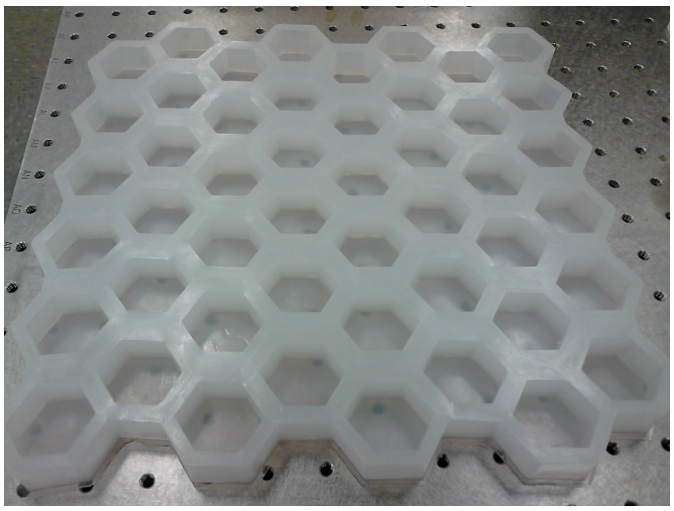

Figure 4.5: Array of cavities made of Ecoflex® Rubber.

which was impacted by the hammer from below. For the noise tests, the panel was struck with the riveting gun, which has a nominal impact frequency of $30Hz$. Ten trials were performed and the average value and standard deviations were obtained. The two categories of testing were carried out in both undamped and damped condition, with the PIDs rested atop the panel, as illustrated in Figure 4.8. The test parameters were varied according to Figures 4.9 to 4.12. Points in red represent where the test panel was struck.

There are three possibilities for volumetric packing fraction – empty array, uniformly-filled array, and randomly-filled array. The empty array case is intended to assess the impact of the added mass or just the array cell structure alone. The uniformly-filled case assess the impact of having all cells filled to the same volume fraction. The randomly-

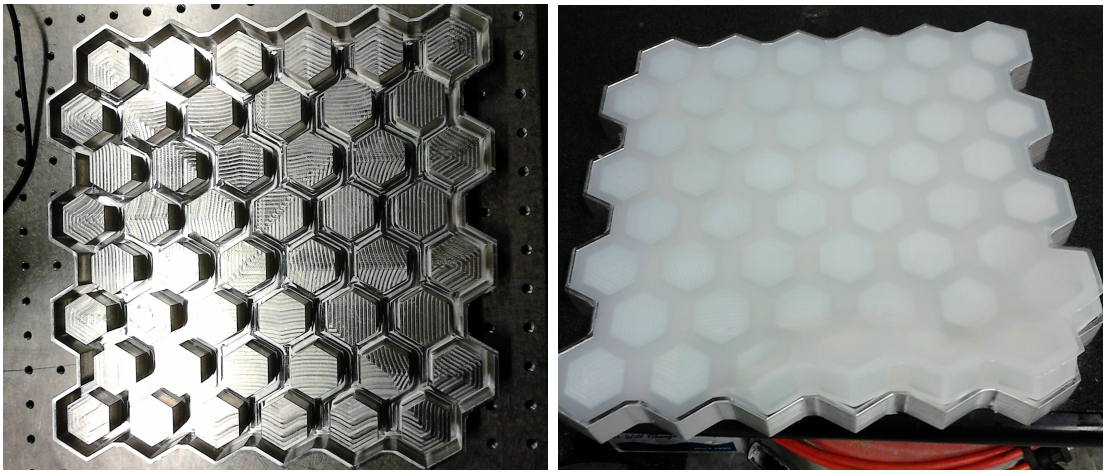

Figure 4.6: Steel mold (*left*). The rubber array after being cured (*right*).

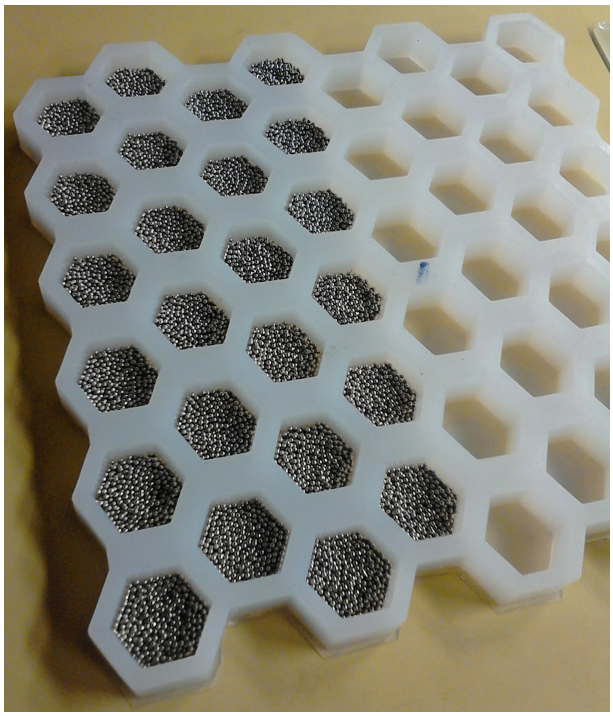

Figure 4.7: Array filled with Nickel-plated lead shots. Although in this figure there are some empty cavities, all cavities were filled in order to test the array.

filled array case is to assess the impact of having each cell filled to a different, randomly distributed, volume fraction. Regarding the position of the array relative to the excitation point, two configurations are considered – *on* the excitation point (Figure 4.9) and *far* from the excitation point (Figure 4.10). Tests were also carried out with two and three arrays over the surface, as can be seen in Figure 4.11 and Figure 4.12. It is important to note that for the FRF test, only one array was tested ON the excitation point. The procedure is based on that performed by Itankar and Sujatha (2013).

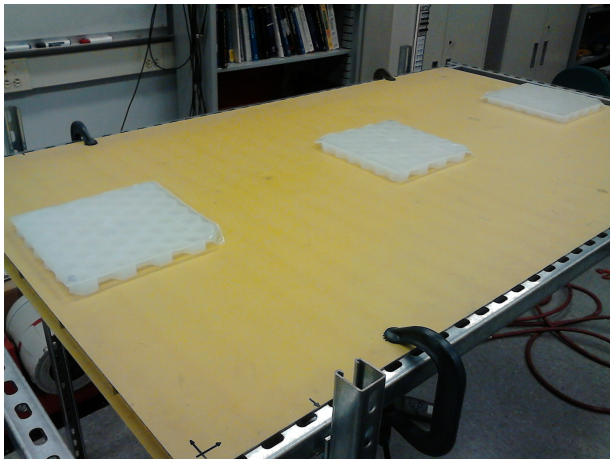

Figure 4.8: Three arrays placed atop the panel illustrating how the panel was treated with the damper.

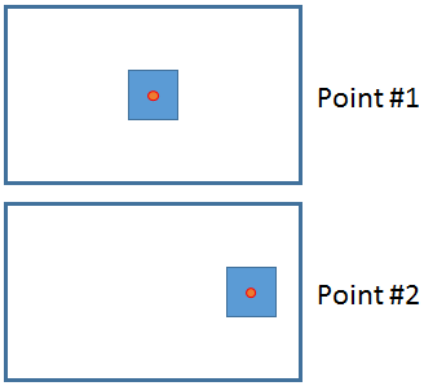

Figure 4.9: Relative position of the array to the excitation point (EP): *ON* the EP.

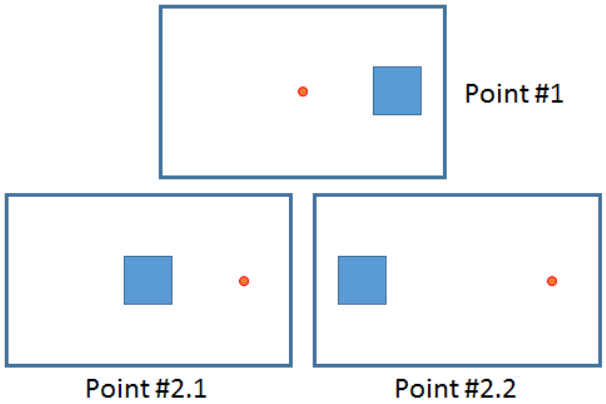

Figure 4.10: Relative position of the array to the excitation point (EP): *FAR* from the EP.

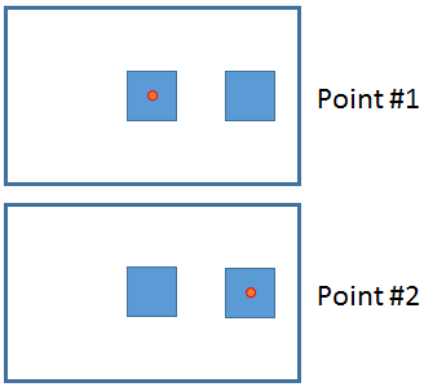

Figure 4.11: Test configuration for the analysis of the number of arrays: 2 arrays.

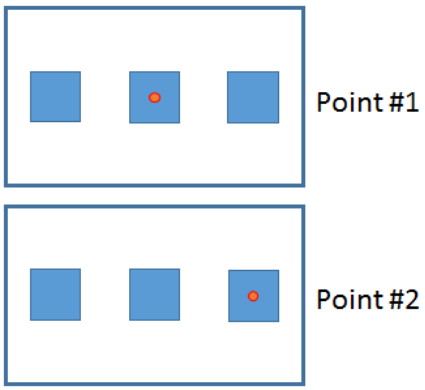

Figure 4.12: Test configuration for the analysis of the number of arrays: 3 arrays.

4.2.2 Discussion

Figures 4.13 and 4.14 show the FRFs for Point #1; curves in Figures 4.15 and 4.16 are the FRFs of Point #2. Figures 4.13 and 4.15 depict the accelerance curves from zero to $50Hz$ while Figs. 4.14 and 4.16 show the accelerance curves from zero to $300Hz$. Blue curve represents the undamped system; the orange curve is related to the empty array; the yellow one is related to the uniformly distributed array and purple curve represents the damped system with randomly distributed array.

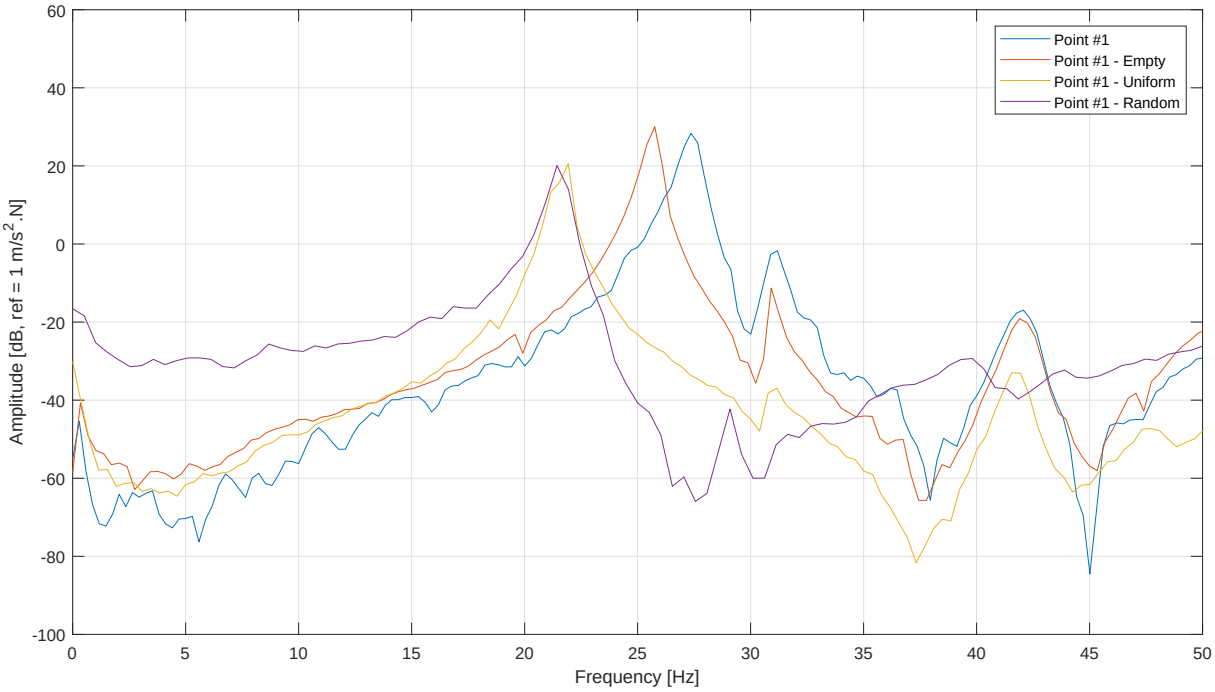

Figure 4.13: Driving point FRF of Point #1 (0 to $50Hz$)

One can note that, for lower modes, the mass loading effect of the dampers is more prominent while for higher modes a very heavy damping effect is observed. It is also noteworthy that the damping effect provided by both randomly and uniformly distributed arrays is similar. This behavior can be seen in the ranges from $130Hz$ to $210Hz$ and from $230Hz$ to $270Hz$ for Point #1. For Point #2, this is observed in the ranges from $70Hz$ to $150Hz$ and $170Hz$ to $210Hz$. Further studies will be conducted in order to understand the dynamic characteristics of the modes in these ranges.

For the noise test, the measured values of sound pressure level L_n are found from Tables 4.1 to 4.5. Table 4.1 presents the measured sound pressure level for the untreated system. Table 4.2 reports the measured values of sound pressure level when the panel is struck ON the excitation point. This table is split into three columns that represent the

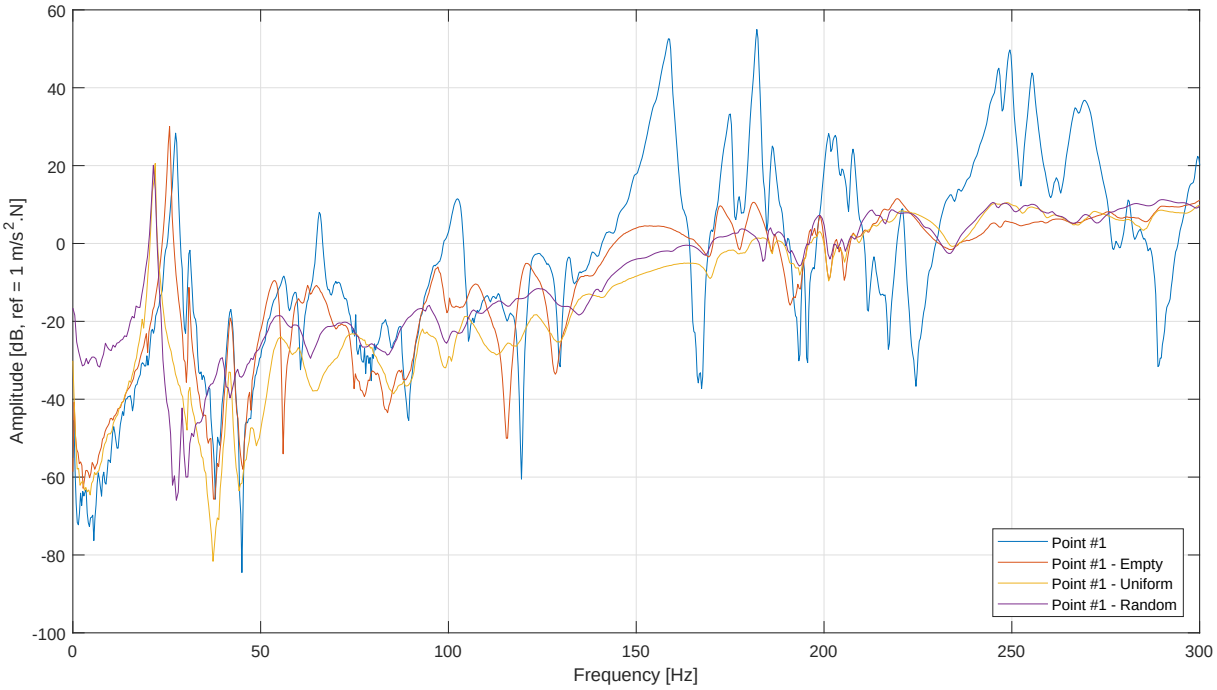

Figure 4.14: Driving point FRF of Point #1 (0 to 300Hz)

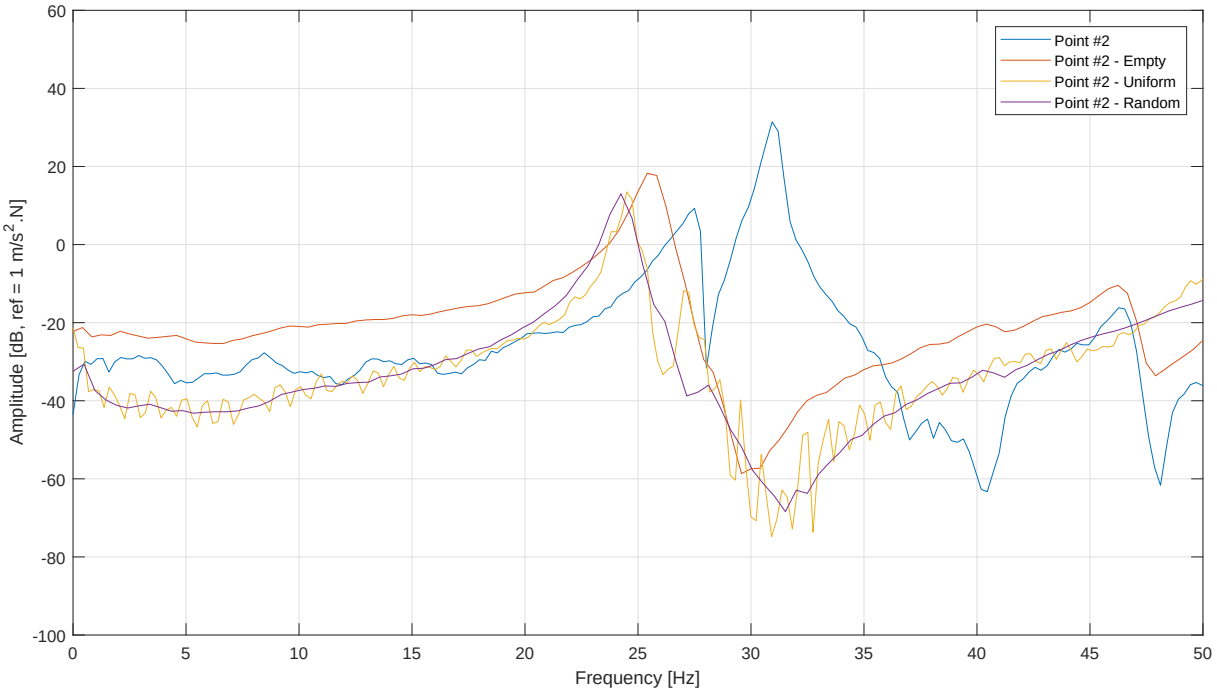

Figure 4.15: Driving point FRF of Point #2 (0 to 50Hz)

array completely empty; the array with cavities randomly filled; and the array with shots distributed uniformly for the two points. These columns are also found from Tables 4.3 to 4.5.

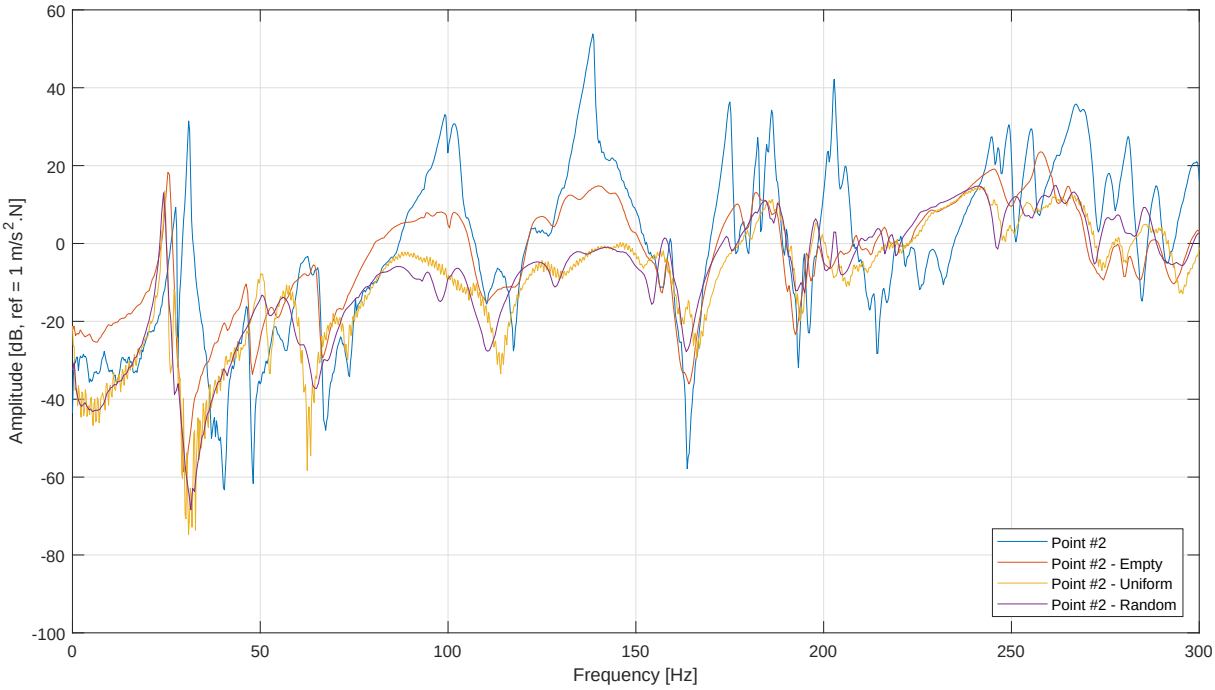

Figure 4.16: Driving point FRF of Point #2 (0 to 300Hz)

Table 4.3 shows the measured values of sound pressure level when the panel is struck FAR from the excitation point. In this case, attention must be paid to the two possibilities for Point #2: one is when the array is placed on Point #1 – called Point #2.1 or just *far* – and the other is when the array is far from the Point #1, in the opposite edge of the panel, called Point #2.2 or *very far*. Table 4.4 shows the measured values of sound pressure level for two arrays over the work piece and finally Table 4.5 reports the measured values of sound pressure level for three arrays placed over the work piece.

Table 4.1: Sound Pressure Level for the untreated system

	Untreated	
	Point #1	Point #2
Average (A)	110.7	110.7
Standard Deviation (B)	1.1	1.0

Table 4.2: Sound Pressure Level for the arrays *on* the excitation points

	On the excitation points (One array)					
	Empty		Random		Uniform	
	#1	#2	#1	#2	#1	#2
(A)	106.4	105.1	101.0	102.0	104.9	102.0
(B)	0.6	0.9	1.5	0.7	0.9	0.8

Based on the information presented on the tables, it is possible to note that when the array is on the excitation point, the larger noise reduction observed for Point #1 is 9.6dB, which corresponds to the randomly distributed array. Note that the empty array

Table 4.3: Sound Pressure Level for the arrays *far* from the excitation points

	Far from the excitation points (One array)								
	Empty			Random			Uniform		
	#1	#2.1	#2.2	#1	#2.1	#2.2	#1	#2.1	#2.2
(A)	107.6	108.7	106.9	102.7	107.6	107.7	103.7	108.0	107.6
(B)	0.8	0.8	1.0	1.2	0.5	0.8	1.2	0.9	0.8

Table 4.4: Sound Pressure Level for two arrays over the panel

	Two arrays					
	Empty		Random		Uniform	
	#1	#2	#1	#2	#1	#2
(A)	105.0	106.3	100.5	102.4	99.5	100.7
(B)	1.0	0.6	0.7	0.8	1.0	0.9

Table 4.5: Sound Pressure Level for three arrays over the panel

	Three arrays					
	Empty		Random		Uniform	
	#1	#2	#1	#2	#1	#2
(A)	105.5	106.1	99.6	100.8	99.4	100.5
(B)	0.6	0.9	1.0	1.1	1.4	0.9

also provides a reduction in the noise radiation. This is because the unfilled array adds both mass loading and some damping to the structure. When the excitation is on Point #2, both the randomly and uniformly distributed array contribute to the same larger reduction – $8.6dB$.

If the array is placed far from the excitation point, the random array is still the best one for Point #1. It provides a reduction of $8.0dB$. Although this value is lower than the one previously found, it is still a considerable reduction. For Point #2 (far), again both the random and uniform array provide nearly the same reduction (around $3dB$). This value corresponds to $5.6dB$ less than the value found when the array is on the Point #2. For Point #2 (very far), both random and uniform arrays provide the same noise reduction – $3dB$ – though this is not the largest noise reduction found in this configuration. In this case, the empty array is the one that provides the best noise reduction, $3.7dB$. One can note, however, that the standard deviation of this measurement is a little bigger than that found for the other two arrays. This can be an indication that the empty array might provide nearly the same noise reduction as the random and the uniform array.

Regarding the number of arrays over the structure, one can observe that, for Point #1, two and three arrays can damp the structure nearly in the same way. Reductions around 10 and $11dB$ were observed for the random and uniform arrays. Considering the

average value and the standard deviation of the trials, the two configurations can provide the same noise attenuation. For Point #2, again the layout with two and three arrays provide almost the same noise reduction, indicating that perhaps the limit of diminishing returns has been reached. However, for this point, the largest reduction is observed for the uniform array (around $10dB$). It is important to highlight that the reductions found with two or three arrays are not substantial compared to that found with just one array. Therefore, the choice for just one array may be suggested for real applications.

4.2.3 Conclusions of the application of concept

For two points of interest tested in this study, it was observed that the largest noise reductions, approximately around $10dB$, were obtained when the array was placed *on* the excitation point itself. In practical terms, the increase in the number of arrays did not yield significant benefit in terms of increased noise reduction, which indicates that the use of just one array should be considered.

Comparing the uniformly-filled and the randomly-filled arrays, one can see that both of them impacted the structure behavior similarly. This can be observed both in the FRF test and the noise test. Further investigations have to be conducted in order to optimize the arrays in terms of its size, material, volume packing fraction and concept design.

4.3 PID on a cantilever beam

It is clear from the application of concept that an array of PIDs can reduce the radiated noise of a structure struck by repetitive impulses.

The potential of such method to passively control vertical, impact-induced vibration verified in the last section (Section 4.2) lead to the proposition of a more systematic study. In the present section the particle impact damper was then investigated when applied to a cantilever beam.

The lack of an unified (and consensual) methodology to design a PID naturally drives a researcher to conduct experiments (or simulations) to understand how a set of design parameters contributes to the final system's response. That said, the following

design parameters were investigated in terms of how they change the dynamics of the beam:

1. Shaker displacement;
2. Particle size;
3. Particle mass;
4. Gap clearance.

4.3.1 Experimental apparatus

The acrylic cavity used in Chapter 3 was again placed at the free end of Beam #1. An electrodynamic shaker, equipped with a brass impact head, was employed to strike the beam also at the same location. A force sensor, attached to the impact head, measured the striking force while one accelerometer was placed underneath the PID, at the bottom face of the beam. Another accelerometer was employed to measure the shaker acceleration and estimate its displacement (Figure 4.17). Finally, a microphone – G.R.A.S – was positioned close to the PID to measure the noise radiated from the PID in motion (Figure 4.18). The complete experimental apparatus is depicted in Figures 4.19 and 4.20. Please refer to Table 3.2 for the equipment list.

As matter of fact, it is worth noting that, both in the application of concept and in the present Section, the noise measurements were conducted inside the laboratory without the employment of any acoustically treated chamber. As pointed out by Verma and Li (2003), noise measurements in a ordinary laboratory is similar to those noise measurements performed at a *"practical workplace, which is neither a free-field nor a reverberant-room"*. Thus, the results obtained in the present Chapter are of *"practical importance"* and are used to assess the differences in noise radiation caused by the dampers.

The signal acquisition was done using a LabVIEW VI. The procedure implemented into the software was quite similar to that employed in Section 3.3 but, in the present case, the variable to be controlled was the displacement of the shaker (and not the acceleration). The routine works in a loop where the input voltage is continuously changed in order to reach the target displacement. Once the measured displacement reaches the tolerance, the quantities are saved and the loop proceeds to the next frequency. With this procedure,

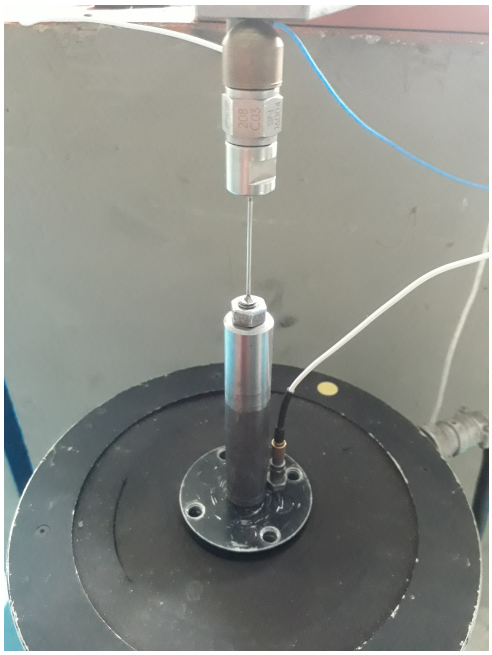

Figure 4.17: Shaker accelerometer.

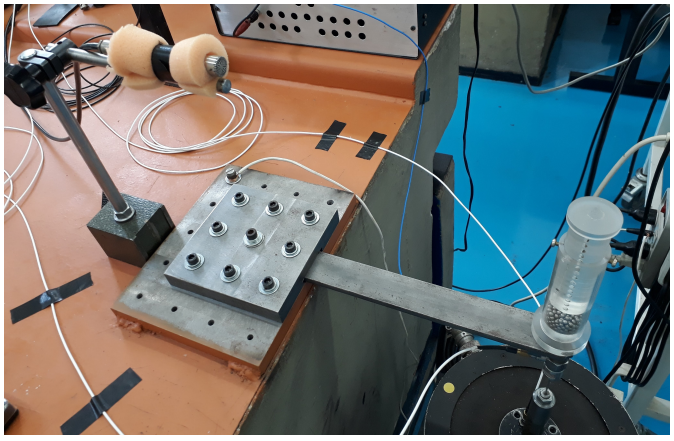

Figure 4.18: A microphone was used to measure the noise radiated from the PID.

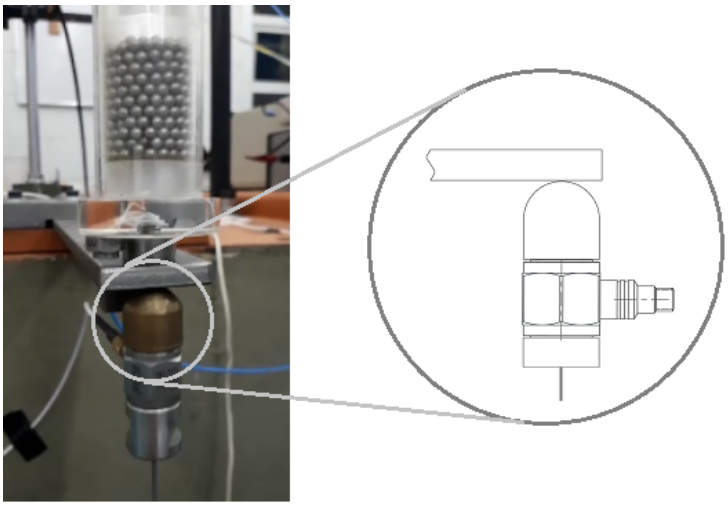

Figure 4.19: Detail of the brass impact head and the force sensor both coupled to the electrodynamic shaker. The impact head is initially set to be aligned with the bottom face of the beam. The accelerometer is right behind the impact head.

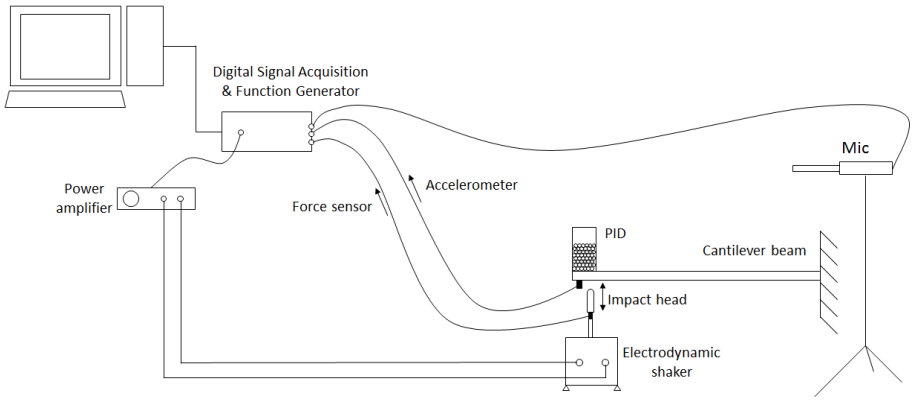

Figure 4.20: Experimental setup for the evaluation of a single PID in a cantilever beam under impact-induced excitation.

it is possible to obtain the spectra of the measured signals for a constant displacement condition.

Note that, due to the non-linear behavior of the system, the variable under control – shaker displacement – is determined by filtering the shaker's acceleration, extracting its first harmonic amplitude and dividing it by the frequency squared. This procedure neglects the energy of other harmonics than the fundamental and assumes that the motion of the shaker is not affected by the dynamics of the system under test. The difference between target and measured displacements determines whether the routine increase or decrease the input voltage.

4.3.2 Discussion

Initially, the behavior of the beam without treatment was tested. Figure 4.21 shows the spectra of acceleration and force for two shaker displacements, namely $0.4mm$ and $0.3mm$. Three replicates for each condition were tested. One can clearly observe that shaker displacement determines how intense is the structural response: as the shaker displacement is decreased, less force is exerted on the structure.

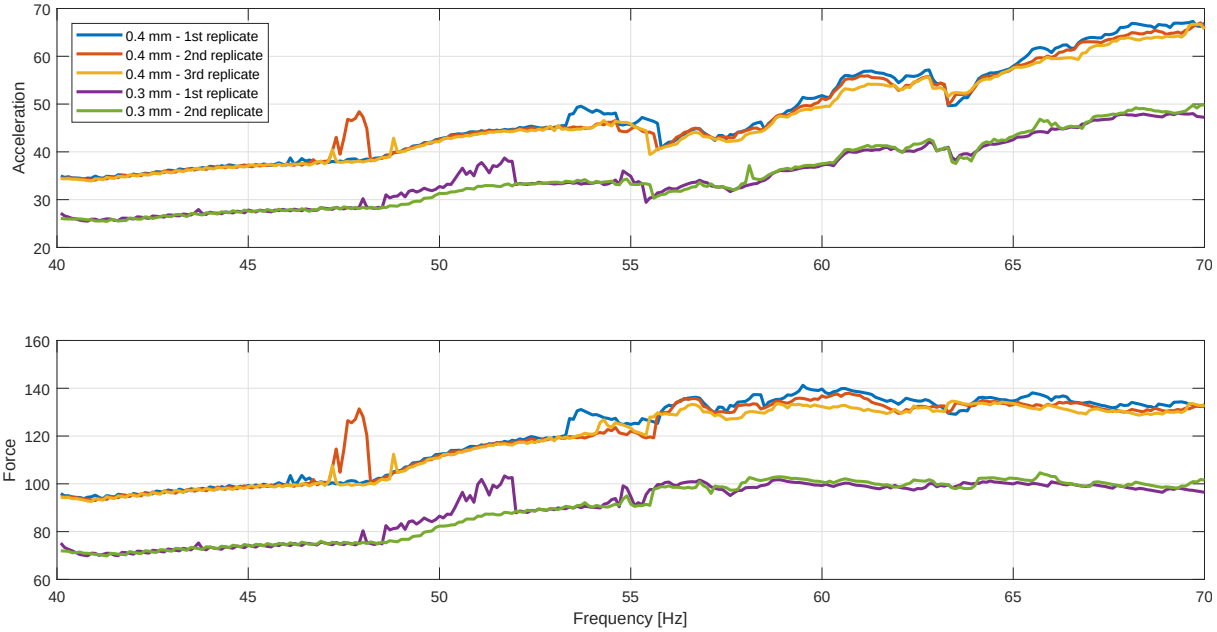

Figure 4.21: Spectra of acceleration and force of the untreated beam. Bear in mind that the amplitudes plotted here correspond to the signals' first harmonic. The third replicate of the $0.3mm$ test could not be plotted.

Figures 4.22 and 4.23 depicts the amplitude of five harmonics. One notes that, in the

range between $55Hz$ and $65Hz$, the response is dominated by the second harmonic. This is the range where the control routine had more difficulty to reach the target displacement, as it is shown in Figure 4.24. The upper plot of Figure 4.24 shows the shaker acceleration as a function of frequency. One could expect that, by controlling the displacement, the acceleration would be a square function of frequency. Indeed, data follows the theoretical square function (dashed curve). The bottom plot shows the shaker displacement, which is constant along the frequency. It is possible to observe that most of the points are close to the lower tolerance limit, which is $0.01mm$. Dashed line shows the target displacement.

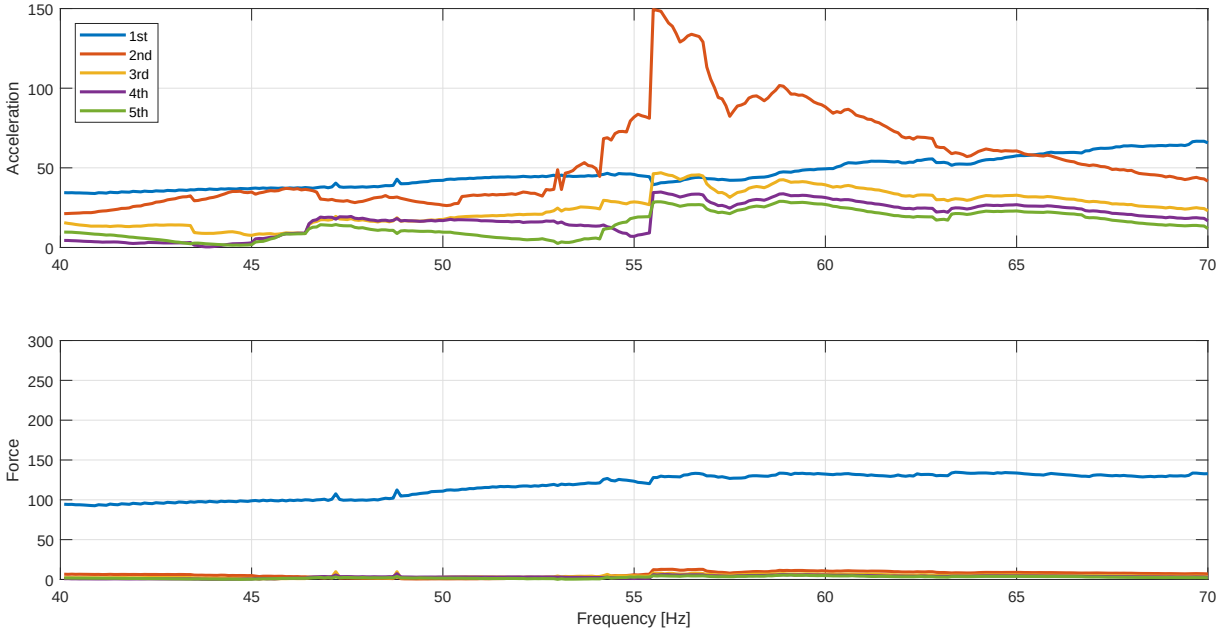

Figure 4.22: Amplitudes of five harmonics of acceleration and force (shaker displacement of $0.4mm$ / 3rd replicate).

Regarding radiated noise, the same trend observed for acceleration and force is verified when sound pressure level is plotted as a function of frequency (Figure 4.25). Sound pressure level is shifted downwards by $2.5dB$ along the whole range. It is interesting also analyze the third-octave band spectra of the radiated noise, depicted in Figures 4.26 and 4.27. One can observe that the noise is dominated by the excitation frequency of the shaker. In this particular case, there is no apparent evidence that the structure dynamics contributes to the noise though.

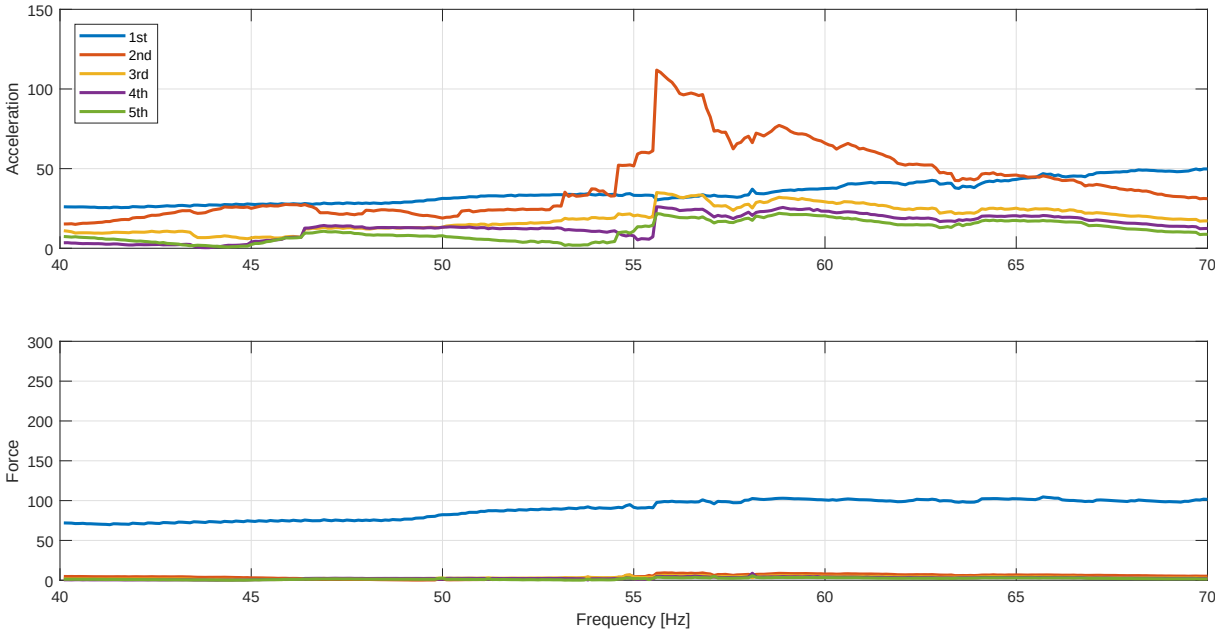

Figure 4.23: Amplitudes of five harmonics (shaker displacement of $0.3mm$ / 2nd replicate).

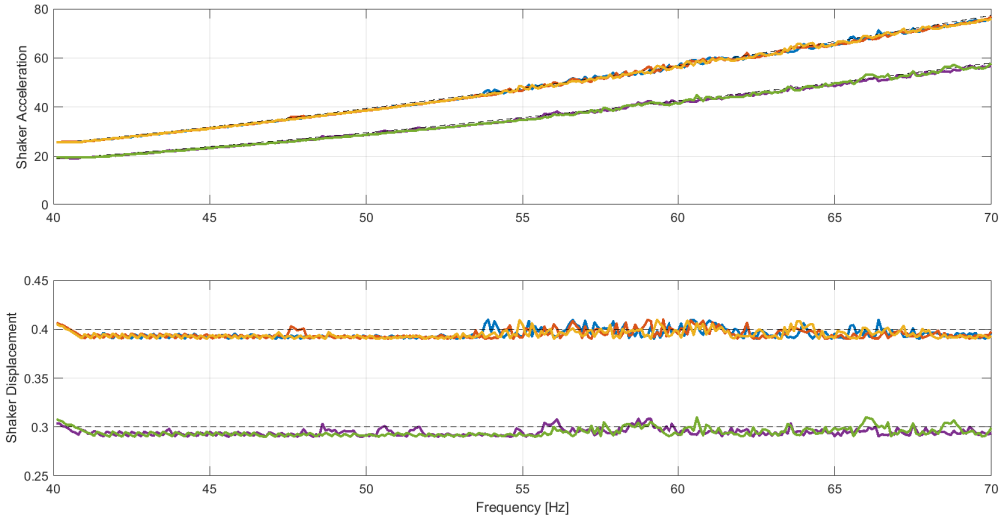

Figure 4.24: Shaker acceleration and displacement. Note that in the range of $55Hz$ and $65Hz$ had more dificulty to reach the target displacement (dashed line).

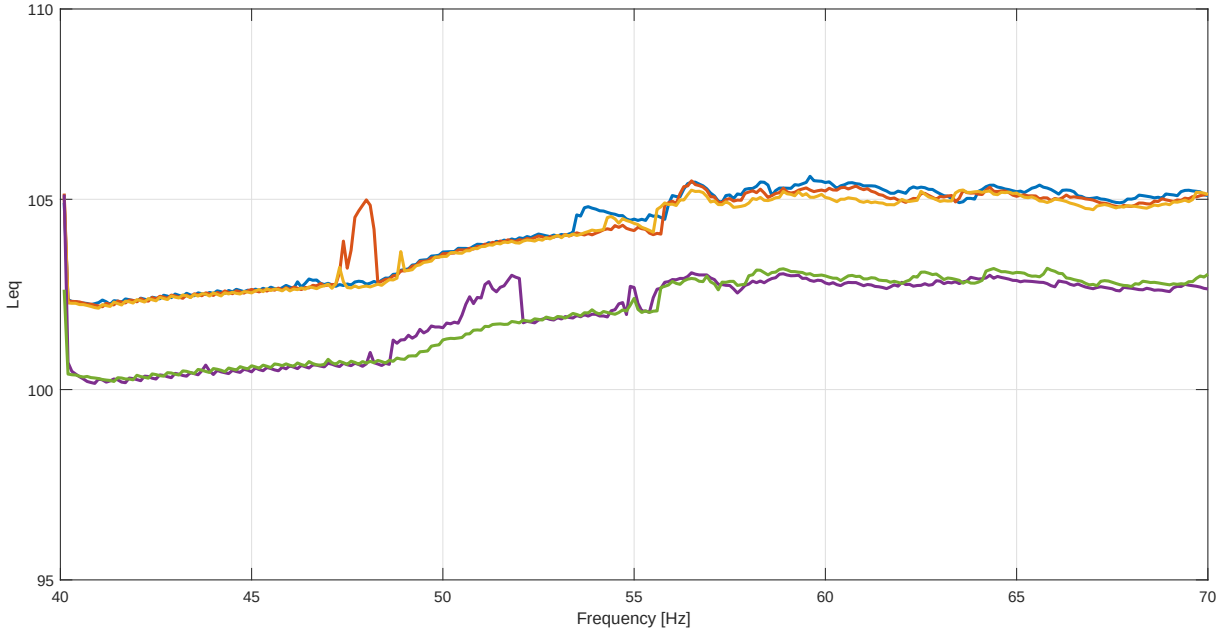

Figure 4.25: Sound pressure level as a function of frequency for the untreated beam.

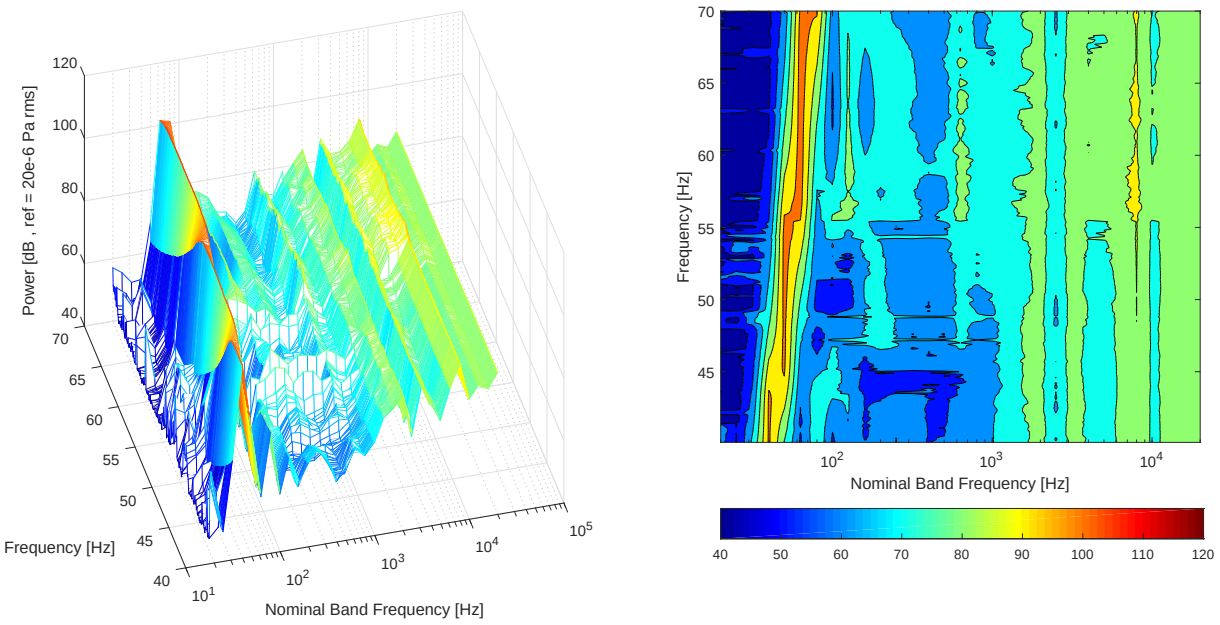

Figure 4.26: Third-octave spectrum of noise (shaker displacement of $0.4mm$ / 3rd replicate).

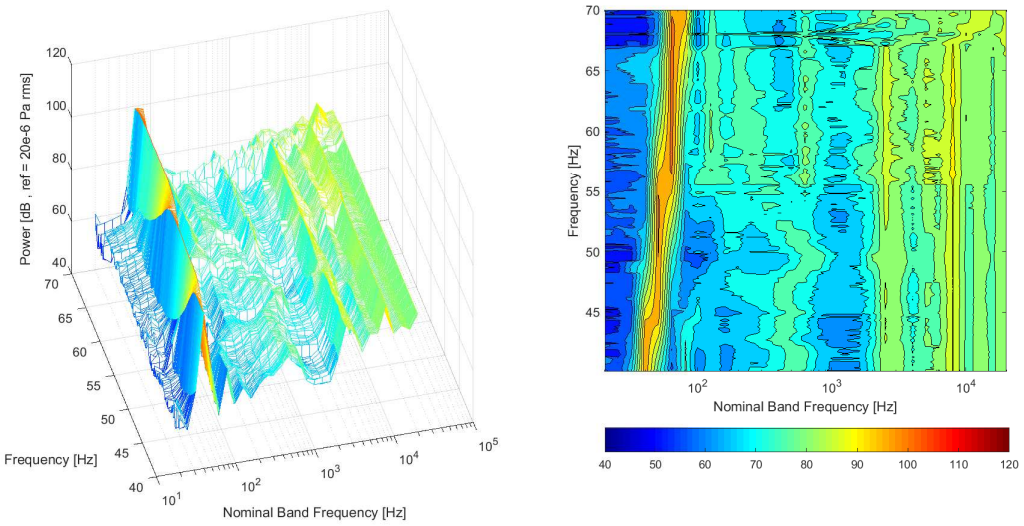

Figure 4.27: Third-octave spectrum of noise (shaker displacement of 0.3mm / 2nd replicate).

4.3.2.1 Varying the particle size

Consider now the cantilever beam treated with the particle impact damper. The influence of two particle sizes in the dynamics of the beam can be assessed by inspecting Figure 4.28. The particle sizes used here are 3mm and 5mm of diameter. In this case, the particle mass was kept constant and particles had enough room to move without hitting the ceiling.

In Figure 4.28, the shaker displacement is 0.4mm. The acceleration level of the untreated beam – the *No Sample* condition – is lower than that encountered for the treated conditions. This should be somehow expected because the mass loading effect provided by the particle impact damper shifts the system's first natural frequency towards lower frequencies. Although higher frequencies were not tested, the flat-like spectrum of the acceleration of the untreated beam suggests that the natural frequency is further than the natural frequency of the treated system.

It is interesting to note that the force levels are reduced when the smaller particle is employed. Lower sound pressure levels are also verified. The fact that smaller particles are desired for better dissipation is in agreement with what has been reported in the literature for harmonic excitation. Third-octave band spectra present a remarkable reduction of noise provided by particles of 3mm. Please compare Figure 4.26 with Figures 4.29 and 4.30. The same trend is also verified for shaker displacement of 0.3mm so it will not be

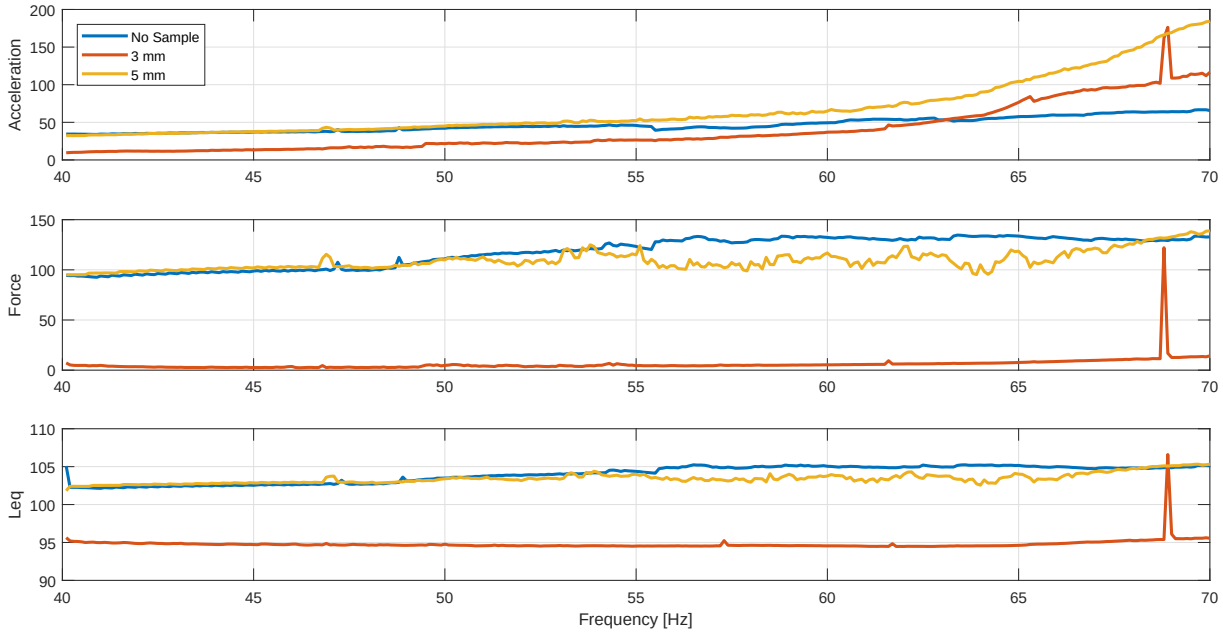

Figure 4.28: Acceleration, force, and sound pressure level for the particle size analysis. Shaker displacement is $0.4mm$.

reported in the following analysis.

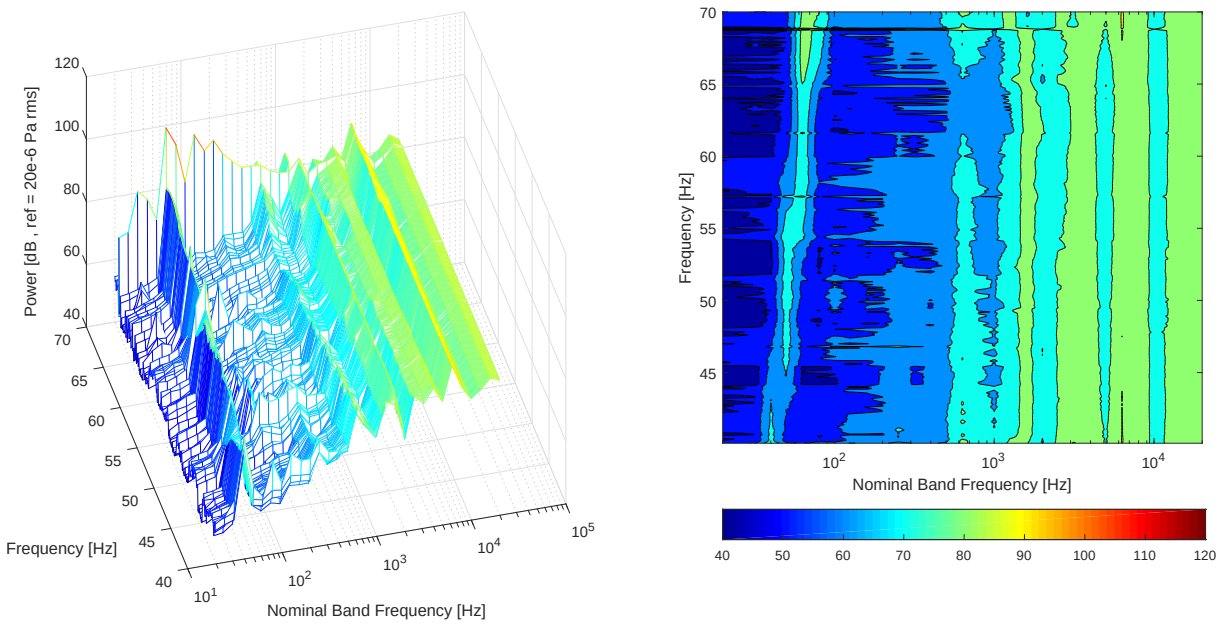

Figure 4.29: Third-octave spectrum of noise for particles with nominal diameter of $3mm$ (shaker displacement of $0.4mm$).

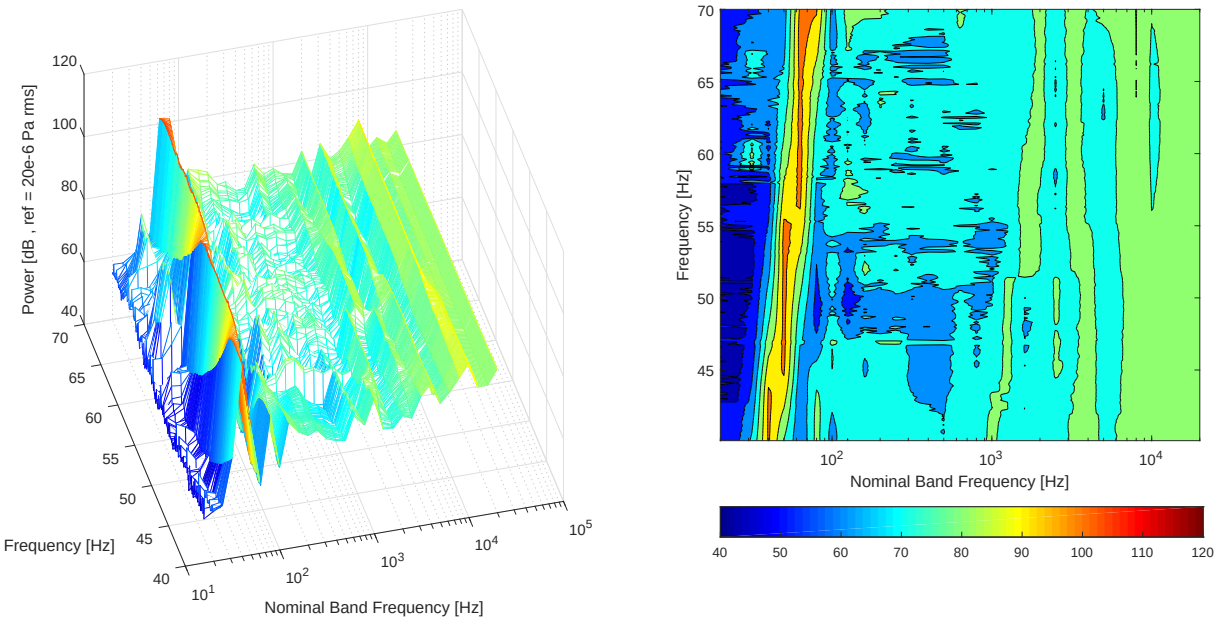

Figure 4.30: Third-octave spectrum of noise for particles with nominal diameter of $5mm$ (shaker displacement of $0.4mm$).

4.3.2.2 Varying the particle mass

Consider now the variation of particle mass. Two particle masses were tested: $26.31g$ and $69.38g$. Particle size was kept constant and particles were prevented from hitting the ceiling by setting an wide gap clearance.

It was verified in Chapter 3 that the dissipation is directly proportional to the particle bed mass, which means that the higher the mass the more energy is dissipated. In Figure 4.31 one can clearly verify that surprisingly the PID with less mass provided a better reduction in the radiated noise. Moreover, the measured force also have diminished considerably.

An explanation for this lies in the amplitude of the impulsive force provided by the impacts. As more particles implies more friction between particles, it is very likely that a better performance was observed for the light PID because the impulsive force were not able set the particles in motion. Hence, it may have impaired the PID's effectiveness.

The third-octave band spectrum depicted in Figures 4.32, and 4.33 provide more insight about the noise reduction provided by the lighter damper (they have to be compared with the undamped beam in Figure 4.26).

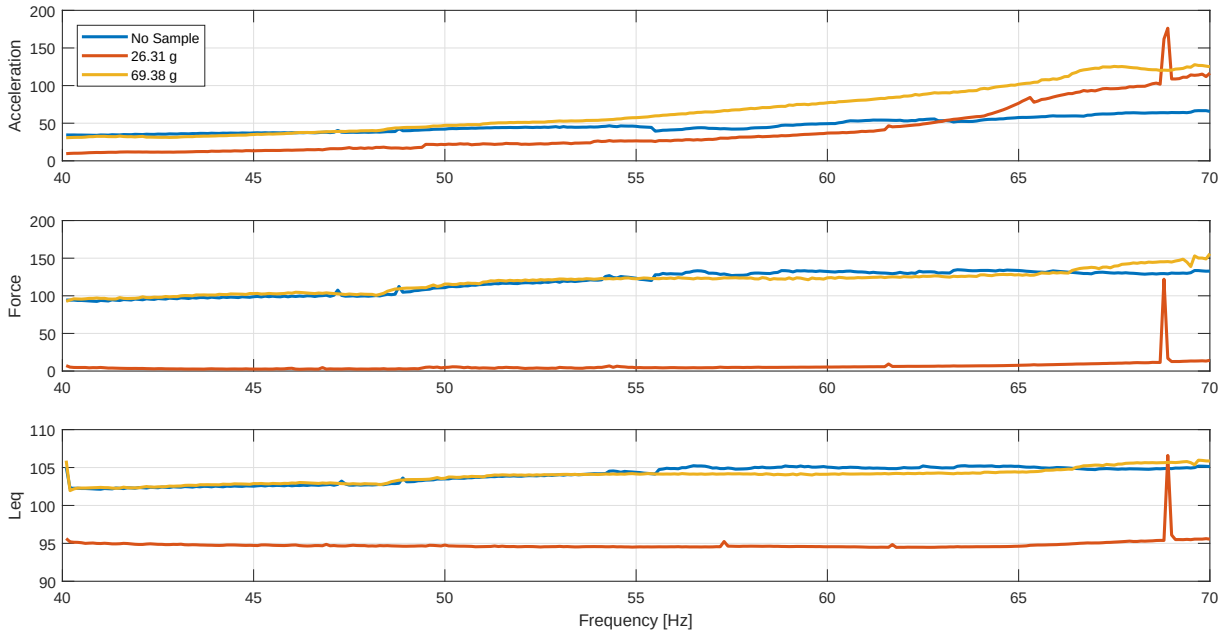

Figure 4.31: Acceleration, force, and sound pressure level for the particle mass analysis. Shaker displacement is $0.4mm$.

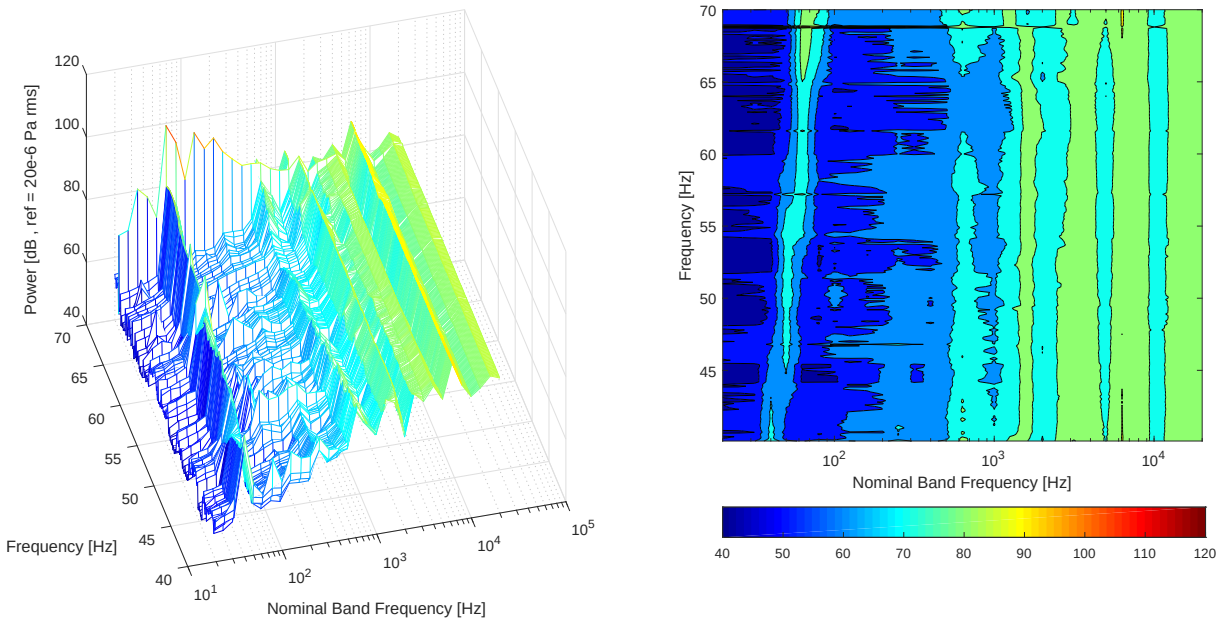

Figure 4.32: Third-octave spectrum of noise for particles mass of $26.31g$ (shaker displacement of $0.4mm$).

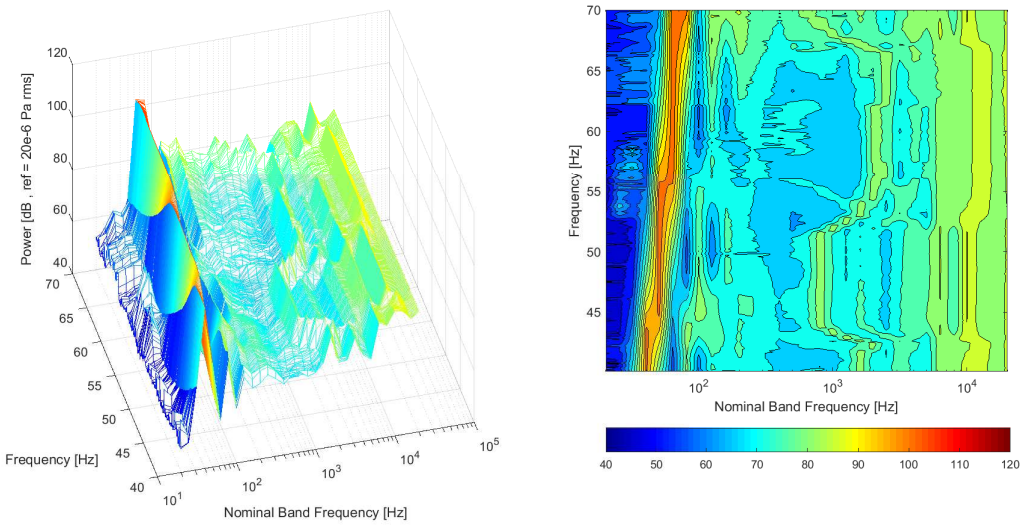

Figure 4.33: Third-octave spectrum of noise for particles mass of 69.38g (shaker displacement of 0.4mm).

4.3.2.3 Varying the gap clearance

Finally, the test conducted to evaluate gap clearance variations are reported next. The last test comprehends the gap clearance's influence by keeping the mass and the particle size constant.

Again, let's analyze what is found when this quantity is varied by looking at Figure 4.34. The gap clearance of 26.5mm allowed the particle bed to move without any contact with cavity's ceiling. On the other hand, in the very narrow gap of 1.5mm, some particles did hit the ceiling. A reproducible tests were not readily possible due to the randomness of the impacts. However, it was observed that did reduce the acceleration amplitudes when compared with the other gap clearance. Force amplitudes and sound pressure levels were not altered with this condition, indicating that, although the vibratory response was attenuated, the noise may not be affected by this parameter.

The third-octave band spectra for the two gap clearances indicate that when the the double impact condition is not achieved, noise at the excitation frequency can be slightly amplified.

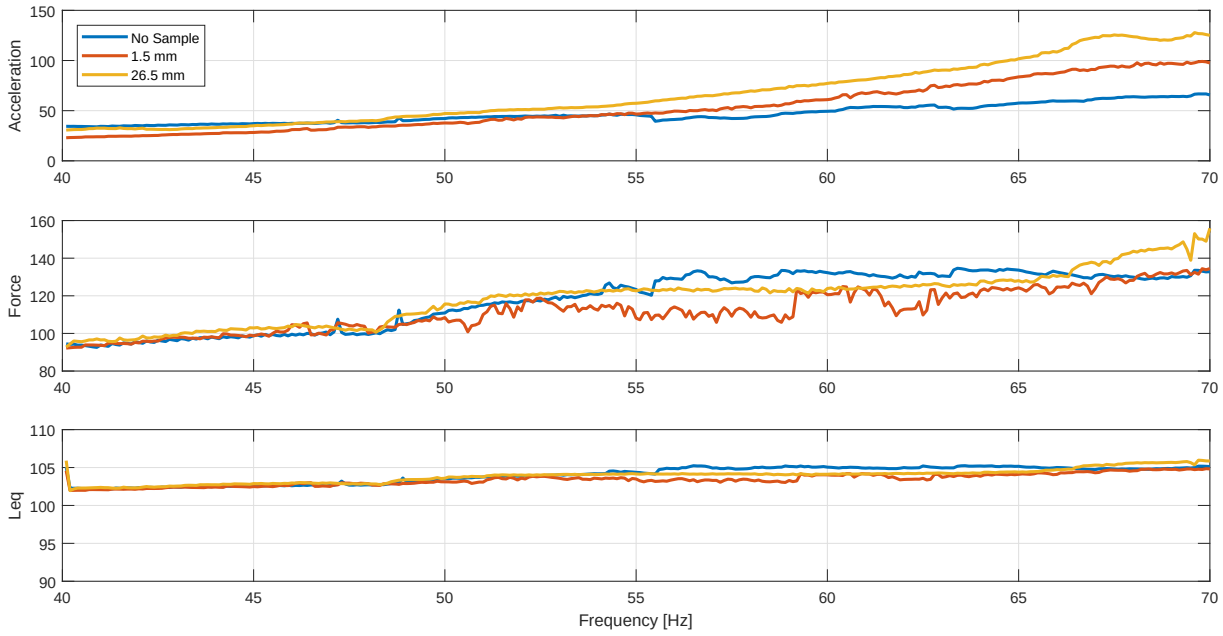

Figure 4.34: Acceleration, force, and sound pressure level for the gap clearance analysis. Shaker displacement is $0.4mm$.

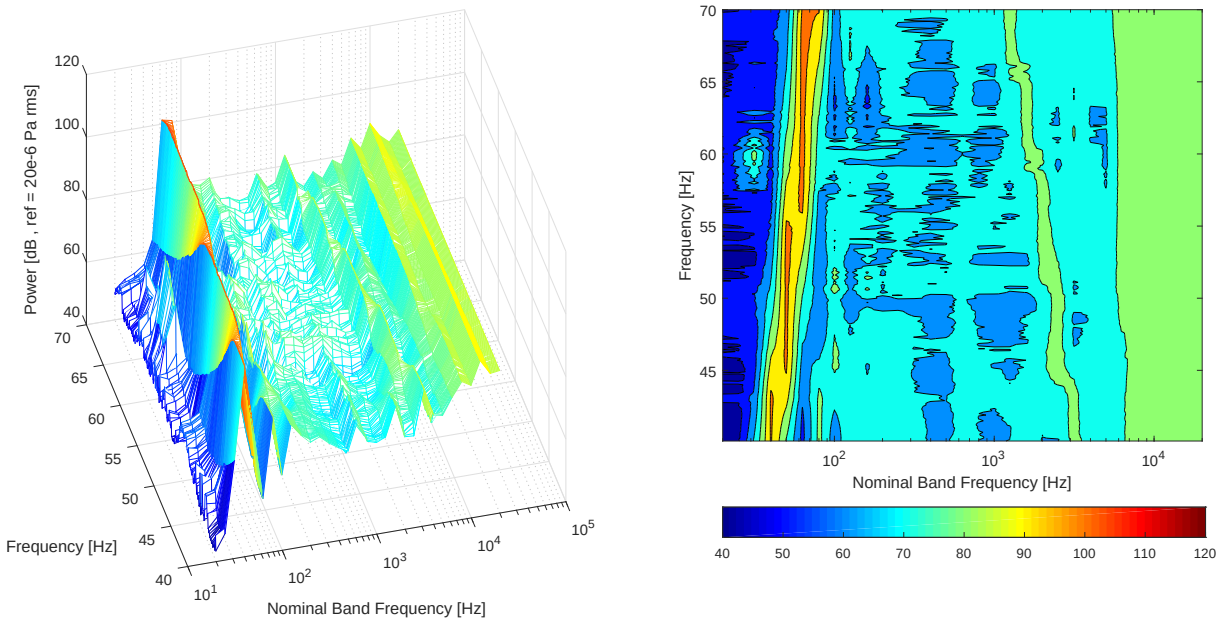

Figure 4.35: Third-octave spectrum of noise for gap clearance (shaker displacement of $0.4mm$).

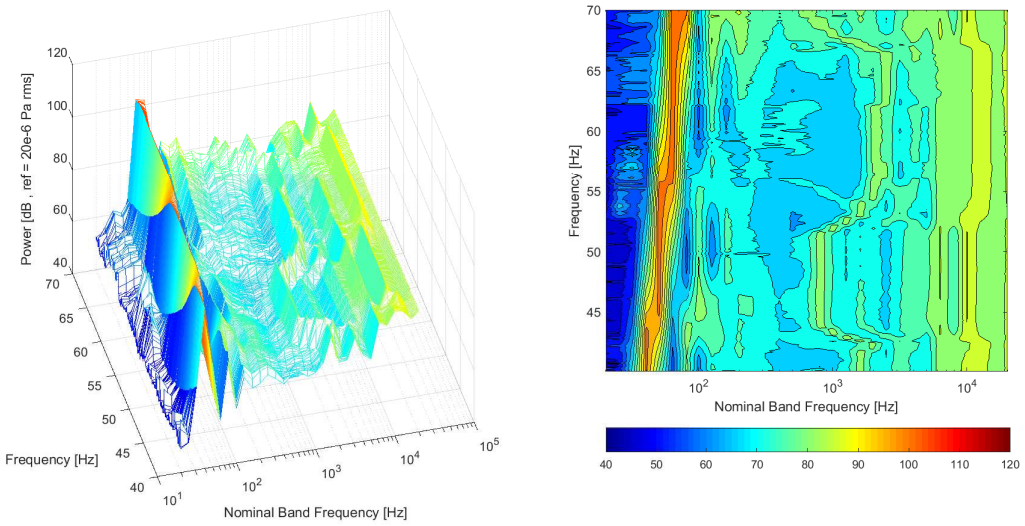

Figure 4.36: Third-octave spectrum of noise for gap clearance (shaker displacement of $0.4mm$).

4.3.3 Comments on the test with cantilever beam

Although the tests described in this section generates some interesting results, for the sake of good science it is good to mention that they may not represent a general trend. More tests should be conducted and, from my point of view, modeling techniques should be employed to determine a general behavior for PIDs under vertical, impact-induced vibration.

That said, the experimental results still can be used as broad rules-of-thumb, useful as initial conditions in a iteration design process.

Experiments conducted here open up new possibilities of application and deep investigation; experimental data provided here can be used to validate future models.

5 Conclusions and final comments

5.1 Overview

The conclusions of the present work are very straightforward. The proposal of the present Thesis was to investigate the behavior of particle impact dampers and to assess their applicability as a passive control method for impact-induced vibration. Moreover, this Thesis contributed to the study of particle impact dampers by comparing two methods employed in the estimation of PID's dissipation. Part of the results were already presented (de Melo *et al.*, 2015).

An experimental work was performed and the list in the following highlights what was observed:

- The results obtained with PIDs of first and second generations are qualitatively similar which indicates that completely different PIDs (in terms of cavity shape, cavity material, geometry, etc.) can demonstrate the same behavior when considering the DPE as the dissipation estimator;
- Regarding the excitation frequency, the DPE curves collapse with respect to the dimensionless acceleration but not the dimensionless displacement;
- When analyzing the gap clearance, the curves are practically equivalent for every frequency analyzed. Exceptions are verified when particles vigorously hit the lid of the cavity. This happens in general for narrow gap clearances. To maximize the dissipation, one should ensure the best combination between the acceleration, the gap clearance and the frequency so that the PID always work under the double impact condition;
- For particle size, bigger particles – $4mm$ and $5mm$ – appeared having a peak dissipation in lower accelerations than particles with diameter of $3mm$. They also dissipated less vibratory energy. The use of bigger particles in real applications may be a concern because this would require bigger cavities, as it is reported that the particle bed should have enough particles to fill more than 4 layers. A scale compromise should be taken into consideration;

- When analyzing different masses, the behavior of DPEs curves diverge from the information found in the literature. DPEs curves show that higher particle mass has lower dissipation than the sample with lower mass;
- Regarding the analysis of the FRFs, the optimal acceleration obtained with DPE was equivalent to the one obtained by the FRF analysis. Optimal acceleration was found but the tests conducted could not determine the existence of an optimal gap clearance. The existence of an optimal gap clearance is related to the interaction of the particle bed with the cavity. Constructive aspects of the acrylic PID impaired the analysis;
- DPE and FRF analysis could be used as complementary dissipation quantifiers;
- PIDs under vertical, impact-induced vibration are as efficient as when they are harmonically excited. Determining the general guidelines to design a PID under impact-induced vibration is still a challenge to be overcome.

5.2 Comments on the experimental procedures

Some experimental aspects of the present work are worth mentioning:

- First, the constructive aspect of a cantilever beam, although simple, represented a challenge. It is not an easy task to prevent one end of the beam from moving. It seems that relative motion between the beam and the fixation structure will always exist, so bolts were used to try to prevent one end of the beam from moving (cantilever beam configuration);
- Deposition of material in the cavity walls were observed, as it was reported by Yang (2003). It happens specially in the early stages of the tests when particles are still coated with lubricant and were not subjected to micro wearing. That is the reason why, between every set of measurements, the cavity was wiped out with a soft fabric to remove this material accumulated on the walls;
- Before every measurement, particles were vigorously shaken for a few seconds so that they could rest randomly at the bottom of the cavity. This procedure was made to ensure that local variations of granular density could not influence the results, specially in terms of the friction each particle is subjected.

Regarding the application of concept, some experimental challenges were faced. First, the removal spray applied on the mold in order to facilitate the removal of the cast from the mold appeared to influence the particles' movement inside the cavity. Eye inspection of particles showed that the spheres ended up coated with the removal fluid. In addition, particles appeared to get stuck on the walls also due to the fluid and due to the inherent sticky feature of the rubber. Improvements in this configuration should take this aspect into consideration.

Thus, when designing an array of vertically-driven PIDs, some constraints are relevant: the ability to transfer momentum to the particles, adaptation to surfaces other than flat ones, assurance the particles hit the ceiling. The resilience of the walls should not impair the momentum transfer.

5.3 Suggestions for future work

The present study is not closed and research spin-offs are suggested in the following:

1. Continuing the analysis of PIDs under impact-induced vibration through the model depicted in Figure 5.1. It is based on the models reported in the literature review.
2. Proposing a model using discrete element method and validate it using experimental data provided in this Thesis.
3. Conducting of a meta-study on particle impact damper. As it was shown here, a myriad of studies under several conditions were already widely reported. A dedicated study to what is found in the literature in terms of PIDs behavior is still of high appealing.
4. Deeper understanding on the physics of granular media. It is of particular interest to understand the correlation between the phase diagram and the dissipation, specially when analyzed from the point of view of the dissipated power efficiency (DPE);
5. Application of optimization techniques using lumped models;
6. Uncertainty analysis of the PID using either discrete element method or other model proposed in the literature;
7. The doctoral period was a time were I could be in touch with several aspects of noise and vibration and also learn new concepts. One in particular called my attention: the acoustic black holes (ABH). ABH is also a passive method employed

to dissipate the vibratory energy. In this concept, wedge of power law profiles are used to attenuate flexural waves in thin plates. In practical applications, strips of viscoelastic material has to be added to the wedge tip in order to dissipate the remaining vibratory energy. Hence, the application of granular material at the tip of wedge as the dissipative element would be worth investigating. The work of Booty *et al.* (2014) compares the effectiveness of particle impact dampers and acoustic black holes in the vibratory response of a plate.

8. Regarding the fabrication of a flexible array of PIDs, it is suggested using a rubber lattice to which is added the rigid cavities as it is illustrated in Figure 5.2. Pads could be designed to meet stiffness targets so that the transmissibility of acceleration between the vibrating structure and the cavity's bottom could be maximized and the PIDs could work in lower base's accelerations.

9. Considering that the double impact condition is more desirable, PIDs with inner bulkheads anchored to the walls – providing several gap clearances inside the same cavity – could also be tested as a design variation. A sketch of this suggestion is in Figure 5.3.

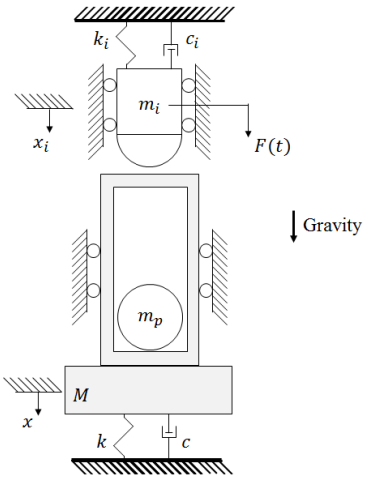

Figure 5.1: Model proposed to study PIDs under impact-induced vibration.

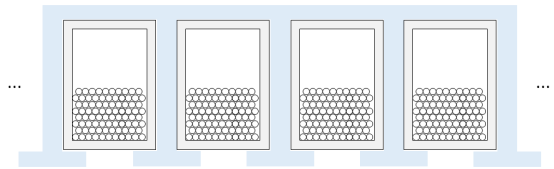

Figure 5.2: Array suggestion

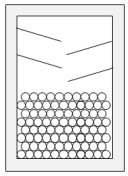

Figure 5.3: PID suggestion

References

AFSHARFARD, A. and FARSHIDIANFAR, A. Design of nonlinear impact dampers based on acoustic and damping behavior. **International Journal of Mechanical Sciences**, v. 65, n. 1, 125–133, 2012.
URL: *http://dx.doi.org/10.1016/j.ijmecsci.2012.09.010*

AHMAD, N.; RANGANATH, R. and GHOSAL, A. Modeling and experimental study of a honeycomb beam filled with damping particles. **Journal of Sound and Vibration**, v. 391, 20–34, 2017.
URL: *http://dx.doi.org/10.1016/j.jsv.2016.11.011*

AREZES, P.M. and MIGUEL, A.S. Hearing protection use in industry: The role of risk perception. **Safety Science**, v. 43, n. 4, 253–267, 2005.

BAI, X.M.; KEER, L.M.; WANG, Q.J. and SNURR, R.Q. Investigation of particle damping mechanism via particle dynamics simulations. **Granular Matter**, v. 11, n. 6, 417–429, 2009.

BANNERMAN, M.N.; KOLLMER, J.E.; SACK, A.; HECKEL, M.; MUELLER, P. and PÖSCHEL, T. Movers and shakers: Granular damping in microgravity. **Physical Review E - Statistical, Nonlinear, and Soft Matter Physics**, v. 84, n. 1, 2011.

BAPAT, C.N. and SANKAR, S. Multiunit impact damper-Re-examined. **Journal of Sound and Vibration**, v. 103, n. 4, 457–469, 1985a.

BAPAT, C.N. and SANKAR, S. Single unit impact damper in free and forced vibration. **Journal of Sound and Vibration**, v. 99, n. 1, 85–94, 1985b.

BEN ROMDHANE, M.; BOUHADDI, N.; TRIGUI, M.; FOLTÊTE, E. and HADDAR, M. The loss factor experimental characterisation of the non-obstructive particles damping approach. **Mechanical Systems and Signal Processing**, v. 38, n. 2, 585–600, 2013.

BLAZEJCZYK-OKOLEWSKA, B. Analysis of an impact damper of vibrations. **Chaos, Solitons and Fractals**, v. 12, n. 11, 1983–1988, 2001.

BOOTY, C.; BOWYER, E.P. and KRYLOV, V.V. Experimental investigation of damping flexural vibrations using granular materials. In **Proceedings of ISMA 2014**

- International Conference on Noise and Vibration Engineering and USD 2014 - International Conference on Uncertainty in Structural Dynamics, pp. 547–558. 2014. ISBN 9789073802919.
URL: *http://www.scopus.com/inward/record.url?eid=2-s2.0-84913606283%7B&%7DpartnerID=tZOtx3y1*

BRAZIL. Perda Auditiva Induzida por Ruído (Pair). Technical report, Ministry of Health, Brasilia, 2006.

CARFAGNI, M.; LENZI, E. and PIERINI, M. The loss factor as a measure of mechanical damping. **SPIE proceedings series**, pp. 580–84, 1998.
URL: *http://sem-proceedings.com/16i/sem.org-IMAC-XVI-16th-Int-161802-The-Loss-Factor-as-Measure-Mechanical-Damping.pdf*

CEMPEL, C. and LOTZ, G. Efficiency of Vibrational Energy Dissipation By Moving Shot. **Journal of Structural Engineering**, v. 119, n. 9, 2642–2652, 1993.

CEMPEL, C. and NATKE, H. Shot impact vibration damper - an equivalent energy approach. **Abhandlungen der Braunschweigischen Wissenschaftlichen Gesellschaft**, v. 41, 87–100, 1989.

CUNDALL, P.A. and STRACK, O.D.L. A discrete numerical model for granular assemblies. **Géotechnique**, v. 29, n. 1, 47–65, 1979.
URL: *http://www.icevirtuallibrary.com/doi/10.1680/geot.1979.29.1.47*

DA ROCHA, Téo Lenquist. **Attenuation of Noise and Vibration Using Piezoelectric Patches and Dissipative Shunt Circuits**. 2014. Doctorate Thesis.

DE MELO, F.M.; BISGAARD, E. and CUNEFARE, K.A. Distributed array of particle impact dampers as a removable noise control treatment in metal fabrication. In **INTER-NOISE and NOISE-CON Congress and Conference Proceedings**, 11. 2015.

DU, Y.; WANG, S.; ZHU, Y.; LI, L. and HAN, G. Performance of a New Fine Particle Impact Damper. **Advances in Acoustics and Vibration**, v. 2008, 1–6, 2008.
URL: *http://www.hindawi.com/journals/aav/2008/140894/*

DUAN, Y. and CHEN, Q. Simulation and experimental investigation on dissipative properties of particle dampers. **Journal of Vibration and Control**, v. 17, n. 5, 777–788, 2010.
URL: *http://jvc.sagepub.com/content/17/5/777.abstract*

DUNCAN, M.R.; WASSGREN, C.R. and KROUSGRILL, C.M. The damping performance of a single particle impact damper. **Journal of Sound and Vibration**, v. 286, n. 1-2, 123–144, 2005.

DUVIGNEAU, F.; KOCH, S.; WOSCHKE, E. and GABBERT, U. An effective vibration reduction concept for automotive applications based on granular-filled cavities. **Journal of Vibration and Control**, , n. July 2015, 2016.
URL: *http://jvc.sagepub.com/cgi/doi/10.1177/1077546316632932*

EAGER, D. and WILLIAMSON, H. Literature review of impact noise reduction in the sheet metal industry. **Acoustics Australia**, v. 24, n. 1, 17–23, 1996.

EMA, S. and MARUI, E. A fundamental study on impact dampers. **International Journal of Machine Tools and Manufacture**, v. 34, n. 3, 407–421, 1994.

ESHUIS, P.; VAN DER WEELE, K.; VAN DER MEER, D.; BOS, R. and LOHSE, D. Phase Diagram of Vertically Shaken Granular Matter. **Physics of Fluids**, v. 19, n. 12, 1–11, 2007.
URL: *http://arxiv.org/abs/physics/0608283%0Ahttp://dx.doi.org/10.1063/1.2815745*

ESHUIS, P.; VAN DER WEELE, K.; VAN DER MEER, D. and LOHSE, D. Granular leidenfrost effect: Experiment and theory of floating particle clusters. **Physical Review Letters**, v. 95, n. 25, 1–4, 2005.

FANG, W. and WICKERT, J. Response of a Periodically Driven Impact Oscillator. **Journal of Sound and Vibration**, v. 170, n. 3, 397–409, 1994.
URL: *http://www.sciencedirect.com/science/article/pii/S0022460X84710704*

FANG, X. and TANG, J. Granular Damping in Forced Vibration: Qualitative and Quantitative Analyses. **Journal of Vibration and Acoustics**, v. 128, n. August 2006, 489, 2006.

FOWLER, B.L.; FLINT, E.M. and OLSON, S.E. Design Methodology for Particle Damping. In **SPIE Conference**, pp. 1–12. 2001.

FRIEND, R.D. and KINRA, V.K. Particle Impact Damping. **Journal of Sound and Vibration**, v. 233, n. 1, 93–118, 2000.
URL: *http://linkinghub.elsevier.com/retrieve/pii/S0022460X99927955*

FULLER, C. and VON FLOTOW, A. Active Control of Sound and Vibration. **IEEE Control Systems**, v. 15, n. 6, 9–19, 1995.

GOMES, Andre Victor Sacone. **Estudo do Acoplamento do Método dos Elementos Finitos e do Método dos Elementos Discretos na Análise de Interação Solo-Estrutura**. 2014. p. 160. Master's dissertation. University of Campinas.

HAKIMI, B.; RAHNAVARD, A. and HONARBAKHSH, T. Seismic design of structures using friction damper bracings. In **13th World Conference on Earthquake Engineering, Paper 3446**, p. 9. 2004.
URL: *http://www.iitk.ac.in/nicee/wcee/article/13_3446.pdf*

HEAVER, C.; GOONETILLEKE, K.S.; FERGUSON, H. and SHIRALKAR, S. Hand-arm vibration syndrome: a common occupational hazard in industrialized countries. **Journal of Hand Surgery (European Volume)**, v. 36, n. 5, 354–363, 2011.
URL: *http://0-jhs.sagepub.com.innopac.up.ac.za/content/36/5/354.full*

HECKEL, M.; SACK, A.; KOLLMER, J.E. and PÖSCHEL, T. Granular dampers for the reduction of vibrations of an oscillatory saw. **Physica A: Statistical Mechanics and its Applications**, v. 391, n. 19, 4442–4447, 2012.
URL: *http://dx.doi.org/10.1016/j.physa.2012.04.007*

ITANKAR, J. and SUJATHA, C. Experimental studies on particle damping cantilever beams. In **20th International Congress on Sound and Vibration**, pp. 1–8. 2013.

KEMBER, S.A. and BABITSKY, V.I. Excitation of vibro-impact systems by periodic impulses. **Journal of Sound and Vibration**, v. 227, n. 2, 427–447, 1999.

KOCAK, K. and CUNEFARE, K.A. Analytical Modeling of a Single Hybrid Particle Impact Damper Under Periodic Impulse Excitation. In **INTER-NOISE and NOISE-CON Congress and Conference Proceedings**, p. 7. 2016.

KOCH, S.; DUVIGNEAU, F.; ORSZULIK, R.; GABBERT, U. and WOSCHKE, E. Partial filling of a honeycomb structure by granular materials for vibration and noise reduction. **Journal of Sound and Vibration**, v. 393, 30–40, 2017.
URL: *http://dx.doi.org/10.1016/j.jsv.2016.11.024*

KUHL, W. and KAISER, H. Absorption of structure-borne sound in building materials without and with sand-filled cavities. **Acta Acustica united with Acustica**, , n. 4, 179–188.

KURAM, E. and OZCELIK, B. **Modern Mechanical Engineering**. JANUARY. 2014. ISBN 978-3-642-45175-1.
URL: *http://link.springer.com/10.1007/978-3-642-45176-8*

LEE, K.H.; LEE, Y.J.; KIM, M.N.; CHO, J.H. and LEE, S.H. A research for efficiency of hearing protection device using a small acoustic filter. In **World Congress on Medical Physics and Biomedical Engineering 2006, Vol 14, Pts 1-6**, v. 14, pp. 868–870. 2007. ISBN 978-3-540-36839-7.

LENZI, Arcanjo. **The use of damping material in industrial machines**. 1985. p. PhD Thesis. Doctorate Thesis.

LI, K. and DARBY, A.P. Experiments on the Effect of an Impact Damper on a Multiple-Degree-of-Freedom System. **Journal of Vibration and Control**, v. 12, n. 5, 445–464, 2006.
URL: *http://jvc.sagepub.com/content/12/5/445.abstract*

LI, S. and LI, X. The effects of distributed masses on acoustic radiation behavior of plates. **Applied Acoustics**, v. 69, n. 3, 272–279, 2008.

LI, S. and TANG, J. On Vibration Suppression and Energy Dissipation using Tuned Mass Particle Damper. **Journal of Vibration and Acoustics**, v. 139, n. February, 1–9, 2017.

LINDQVIST, E.A. Noise attenuation in factories. **Applied Acoustics**, v. 16, n. 3, 183–214, 1983.

LIU, W.; TOMLINSON, G.R. and RONGONG, J.A. The dynamic characterisation of disk geometry particle dampers. **Journal of Sound and Vibration**, v. 280, n. 3-5, 849–861, 2005.

LU, Z. An Experimental Investigation into the Use of Buffered Particle Dampers. **15th World Conference on Earthquake Engineering (15WCEE)**, 2012.

LU, Z.; WANG, Z.; MASRI, S.F. and LU, X. Particle impact dampers: Past, present, and future. **Structural Control and Health Monitoring**, , n. May, 1–25, 2017.

MAIA, N.M.M. **Theoretical and Experimental Modal Analysis**. Research Studies Pre; 1st edition, 1997. ISBN 0863802087.

MARHADI, K.S. and KINRA, V.K. Particle impact damping: Effect of mass ratio, material, and shape. **Journal of Sound and Vibration**, v. 283, n. 1-2, 433–448, 2005.

NELSON, D.; NELSON, R.; CONCHA-BARRIENTOS, M. and FINGERHUT, M. The global burden of occupational noise-induced hearing loss. **American journal of industrial medicine**, v. 48, n. 6, 446–458, 2005.
URL: *http://onlinelibrary.wiley.com/doi/10.1002/ajim.20223/abstract*

OLSON, S.E. An analytical particle damping model. **Journal of Sound and Vibration**, v. 264, n. 5, 1155–1166, 2003.

O'SULLIVAN, C. **Particulate Discrete Element Modelling**. 2011. ISBN 9780415343046.

PALL, A. and PALL, R. Friction-Dampers for Seismic Control of Buildings "A Canadian Experience". In **Eleventh World Conference on Earthquake Engineering, Paper 497**, p. 8. 1996.

PANOSSIAN, H.V. Structural Damping Enhancement Via Non-Obstructive Particle Damping Technique. **Journal of Vibration and Acoustics**, v. 114, 101–105, 1992.

PAPALOU, A. and MASRI, S.F. Response of Impact Dampers With Granular Materials Under Random Excitation. **Earthquake Engineering & Structural Dynamics**, v. 25, n. 3, 253–267, 1996.
URL: *http://doi.wiley.com/10.1002/(SICI)1096-9845(199603)25:3%3C253::AID-EQE553%3E3.0.CO;2-4*

PAPALOU, A. and MASRI, S.F. An Experimental Investigation of Particle Dampers Under Harmonic Excitation. **Journal of Vibration and Control**, v. 4, n. 4, 361–379, 1998.
URL: *http://jvc.sagepub.com/cgi/doi/10.1177/107754639800400402*

PAPALOU, A. and STREPELIAS, E. Effectiveness of particle dampers in reducing monuments' response under dynamic loads. **Mechanics of Advanced Materials and Structures**, v. 23, n. 2, 128–135, 2016.

PARK, W.H. Mass-Spring-Damper Response to Repetitive Impact. **Journal of Engineering for Industry**, , n. November, 587–596, 1967.

RAJU, S.G.; ROGNESS, O.; PERSSON, M.; BAIN, J. and RILEY, D. Vibration from a riveting hammer causes severe nerve damage in the rat tail model. **Muscle and Nerve**, v. 44, n. 5, 795–804, 2011.

RAMACHANDRAN, S. and LESIEUTRE, G.A. Dynamics and Performance of a Harmonically Excited Vertical Impact Damper. **Journal of Vibration and Acoustics**, v. 130, n. 2, 21008, 2008.
URL: *http://dx.doi.org/10.1115/1.2827364*

RONGONG, J.A. and TOMLINSON, G.R. Amplitude dependent behaviour in the application of particle dampers to vibrating structures. In **Collection of Technical Papers - AIAA/ASME/ASCE/AHS/ASC Structures, Structural Dynamics and Materials Conference**, v. 10, pp. 6433–6441. 2005.
URL: *http://www.scopus.com/inward/record.url?eid=2-s2.0-28844450284&partnerID=tZOtx3y1*

SAEKI, M. Impact Damping With Granular Materials in a Horizontally Vibrating System. **Journal of Sound and Vibration**, v. 251, n. 1, 153–161, 2002.
URL: *http://linkinghub.elsevier.com/retrieve/pii/S0022460X01939859*

SAEKI, M. Analytical study of multi-particle damping. **Journal of Sound and Vibration**, v. 281, n. 3-5, 1133–1144, 2005.

SAEKI, M.; MIZOGUCHI, T. and BITOH, M. Particle damping: Noise characteristics and large-scale simulation. **Journal of Vibration and Control**, , n. November 2016, 107754631771634, 2017.
URL: *http://journals.sagepub.com/doi/10.1177/1077546317716345*

SANCHEZ, M.; CARLEVARO, C.M. and PUGNALONI, L.A. Effect of particle shape and fragmentation on the response of particle dampers. **Journal of Vibration and Control**, v. 20, n. 12, 1846–1854, 2013.
URL: *http://jvc.sagepub.com/content/20/12/1846.abstract*

SÁNCHEZ, M.; ROSENTHAL, G. and PUGNALONI, L.A. Universal response of optimal granular damping devices. **Journal of Sound and Vibration**, v. 331, n. 20, 4389–4394, 2012.

SEMERCIGIL, S.E.; LAMMERS, D. and YING, Z. A new tuned vibration absorber for wide-band excitations. **Journal of Sound and Vibration**, v. 156, n. 3, 445–459, 1992.

SEMERCIGIL, S.E.; POPPLEWELL, N. and TYC, R. Impact Damping of Random Vibrations. **Journal of Sound and Vibration**, v. 121, n. 1, 178–184, 1988.

SHAH, B.M.; PILLET, D.; BAI, X.M.; KEER, L.M.; JANE WANG, Q. and SNURR, R.Q. Construction and characterization of a particle-based thrust damping system. **Journal of Sound and Vibration**, v. 326, n. 3-5, 489–502, 2009.
URL: *http://dx.doi.org/10.1016/j.jsv.2009.06.007*

SHAW, S.W. and HOLMES, P.J. A periodically forced piecewise linear oscillator. **Journal of Sound and Vibration**, v. 90, n. 1, 129–155, 1983.

STEFFEN JR, V.; RADE, D.A. and INMAN, D.J. Using passive techniques for vibration damping in mechanical systems. **Journal of the Brazilian Society of Mechanical Sciences**, v. 22, 411–421, 00 2000.

VERMA, S. and LI, W. Measurement of Vibrations and Radiated Acoustic Noise of Electrical Machines. **Electrical Machines and Systems, 2003. ICEMS 2003. Sixth International Conference on**, v. 2, 861–866 vol.2, 2003.

WONG, C.X.; DANIEL, M.C. and RONGONG, J.A. Prediction of the amplitude dependent behaviour of particle dampers. In **Collection of Technical Papers - AIAA/ASME/ASCE/AHS/ASC Structures, Structural Dynamics and Materials Conference**, April, pp. 1–16. 2007. ISBN 1563478927.

WONG, C.X.; SPENCER, A.B. and RONGONG, J.A. Effects of Enclosure Geometry on Particle Damping Performance. In **Collection of Technical Papers - AIAA/ASME/ASCE/AHS/ASC Structures, Structural Dynamics and Materials Conference**, May, pp. 1–16. 2009. ISBN 9781563479731.

WONG, W. The Effects of Distributed Mass Loading on Plate Vibration Behavior. **Journal of Sound and Vibration**, v. 252, n. 3, 577–583, 2002.
URL: *http://linkinghub.elsevier.com/retrieve/pii/S0022460X01939471*

WU, C.; WANG, D.; YANG, R. and LEI, X. Acoustic radiation response prediction of thin-walled box with particle dampers using multiphase flow theory of gas-particle. **Inter noise**, pp. 1–8, 2014.

WU, C.J.; LIAO, W.H. and WANG, M.Y. Modeling of Granular Particle Damping Using Multiphase Flow Theory of Gas-Particle. **Journal of Vibration and Acoustics**, v. 126, n. 2, 196–201, 2004.

XIAO, W.; HUANG, Y.; JIANG, H.; LIN, H. and LI, J. Energy dissipation mechanism and experiment of particle dampers for gear transmission under centrifugal loads. **Particuology**, 2016.
URL: *http://linkinghub.elsevier.com/retrieve/pii/S1674200116000432*

XU, Z.; CHAN, K. and LIAO, W. An empirical method for particle damping design. **Shock and Vibration**, v. 11, n. 5-6, 647–664, 2004a.

XU, Z.; WANG, M.Y. and CHEN, T. A particle damper for vibration and noise reduction. **Journal of Sound and Vibration**, v. 270, n. 4-5, 1033–1040, 2004b.
URL: *http://linkinghub.elsevier.com/retrieve/pii/S0022460X03005030*

YANG, M. Y. **Development of master design curves for Particle Impact Dampers**. 2003. p. 242. Doctorate Thesis.

YANG, M.Y.; LESIEUTRE, G.A.; HAMBRIC, S.A. and KOOPMANN, G.H. Development of a design curve for particle impact dampers. In **Proceedings of SPIE**, v. 5386, p. 450. 2004.
URL: *http://link.aip.org/link/?PSISDG/5386/450/1*

YIN, Z.; SU, F. and ZHANG, H. Investigation of the energy dissipation of different rheology behaviors in a non-obstructive particle damper. **Powder Technology**, v. 321, 270–275, 2017.
URL: *http://dx.doi.org/10.1016/j.powtec.2017.07.090*

ZHANG, K.; CHEN, T.; WANG, X. and FANG, J. Motion mode of the optimal damping particle in particle dampers. **Journal of Mechanical Science and Technology**, v. 30, n. 4, 1527–1531, 2016a.

ZHANG, K.; CHEN, T.; WANG, X. and FANG, J. Rheology behavior and optimal damping effect of granular particles in a non-obstructive particle damper. **Journal of Sound and Vibration**, v. 364, 30–43, 2016b.
URL: *http://dx.doi.org/10.1016/j.jsv.2015.11.006*

ZIMMERMAN, J.J.; RILEY, D.A. and BAIN, J.L.W. Riveting Hammer Vibration and Nerve Damage. In **Proceedings of the 25th Annual Wisconsin Space Conference**, pp. 1–10. 2015.

Appendix A - Vita

Fábio Menegatti de Melo

A.1 Education

BSc., *Mechanical Engineering*, University of Campinas / Brazil, 2010

MSc., *Mechanical Engineering*, *Area of Solid Mechanics and Mechanical Design*, University of Campinas, 2013

PhD., *Mechanical Engineering*, *Area of Solid Mechanics and Mechanical Design*, University of Campinas, 2018

- Visiting Scholar at Georgia Institute of Technology - Georgia Tech (Atlanta / USA) from March to October, 2015.

A.2 Related publications

1. Melo, F.; Bisgaard, E.; Cunefare, K. *Distributed array of particle impact dampers as a removable noise control treatment in metal fabrication.* In: INTER.NOISE 2015, San Francisco, 2015.

2. Melo, F.; Dias Jr., M.; Cunefare, K. *Discussion on "Rheology behavior and optimal damping effect of granular particles in a non-obstructive particle damper" [J. Sound Vib. 364 (2016) 30-43].* Submitted to Journal of Sound and Vibration in November 13th, 2017. Revision submitted in March 27th, 2018.